Abstract

Laboratory and Field Investigations of Stable Water Isotopes in Ecosystems

Kyounghee Kim
May 2011

This dissertation project aimed to improve understanding of plant water relations, with an emphasis on the use of stable water isotopes. This study attempted to integrate gas exchange theories of stable water isotopes into the models of hydrologic processes by measuring fine time resolution vapor isotope ratios including both laboratory and ecosystem levels of analysis. This dissertation focuses on three research areas: (1) isotopic enrichment at the evaporating surfaces, (2) the effects of dew on isotopic equilibrium of leaf water with vapor, and (3) the dynamics of ecosystem water pools in a mixed temperate forest in Ontario, Canada.

An evaporation flux chamber was developed to make continuous measurements of $H_2{}^{18}O$ and HDO in vapor. My results revealed that surface enrichment due to the kinetic effect was substantial and likely to be stronger at a high evaporation rate. My results suggested that the surface enrichment could exist in natural environments under conditions of suppressed natural mixing in evaporating water bodies. The estimate of surface enrichment was insensitive to the consideration of evaporative surface cooling.

A fumigated plant chamber was developed to investigate the effect of dew on leaf water isotope ratios. My results showed that the exchanges of $H_2{}^{18}O$ and HDO between leaf water and the air continued in the darkness via incomplete stomatal closure. The estimates of the leaf conductance at wet foliage following the isotopic mass balance

method fell in the ranges of the nighttime stomatal conductance reported in the literature. Of the species used in the study, the C_4 stomatal conductance was lower than the C_3 conductance.

Continuous measurements of evapotranspiration flux isotope ratios were made in a mixed temperate forest over a full growing season of 2009. Disequilibrium between vapor and precipitation isotope ratios was observed, peaking in dry periods. The isotopic steady state assumption turned out to be invalid in the site and the xylem of the overstory species was coupled with soil water collected at 50 cm depth. The vertical profiles of soil water isotope ratios revealed the dynamics of soil water, resulting from infiltration and mixing of newer precipitation with existing soil water.

Laboratory and Field Investigations of Stable Water Isotopes in Ecosystems

A Dissertation
Presented to the Faculty of the Graduate School
of
Yale University
in Candidacy for the Degree of
Doctor of Philosophy

By
Kyounghee Kim

Yale School of Forestry and Environmental Studies
New Haven, Connecticut

Dissertation Director: Xuhui Lee
May, 2011

Table of Contents

List of Figures

List of Tables

List of Photos

List of Symbols

Variables	Description
α_K	Kinetic fractionation factor (>1)
α_{eq}	Equilibrium fractionation factor (>1)
ε_K	Isotopic kinetic fractionation (‰)
ε_{eq}	Isotopic equilibrium fractionation (‰)
δ	Isotopic composition of sample water relative to a standard of known composition (‰)
δD	Isotopic composition of D/H
$\delta^{18}O$	Isotopic composition of $^{18}O/^{16}O$
δ_B	Isotopic composition of bubbler vapor
δ_{ET}	Isotopic composition of evapotranspiration flux
δ_{ET5}	5-day running average of δ_{ET}
δ_F	Isotopic composition of net flux of fumigation chamber
δ_G	Isotopic composition of groundwater
δ_d	Isotopic composition of dew water
δ_P	Isotopic composition of precipitation
$\delta_{P\text{-}W}$	5-day weighted average of δ_P
δ_X	Isotopic composition of xylem sap
δ_S	Isotopic composition of soil water
δ_E	Isotopic composition of evaporation flux
δ_W	Isotopic composition of liquid water body
ΔL_{NSS}	Leaf water isotopic enrichment at a non-steady state mode
δ_L	Isotopic composition of liquid (Chap. 2) or leaf water (Chap. 3 and 4)
$\delta_{L,e}$	Isotopic composition of surface water undergoing evaporation
$\delta_{L,b}$	Isotopic composition of bulk water
$\delta_{L,SS}$	Isotopic composition of leaf water at steady state
$\Delta\delta_L$	Leaf water isotopic enrichment over xylem
δ_O	Isotopic composition error associated with the instrument nonlinearity
δ_V	Isotopic composition of chamber vapor (Chap. 2 and 3) or ambient vapor (Chap. 4)
δ_T	Isotopic composition of transpiration flux
c	Mixing ratio of water vapor
e_a	Vapor pressure of air (kPa)
e_S	Saturation vapor pressure (kPa)
g_S	Stomatal conductance (mol $m^{-2}s^{-1}$)
h	Humidity
f	Fractional contribution of dew water in leaf water
n	Aerodynamic parameter
m	Mass of water (mol)
p_a	Atmospheric pressure (101.3 kPa)

ρ_s	Saturation vapor density (mol m^{-3})
r	Diffusion resistance
τ	Isotopic turnover time of leaf water (hr)
t	Time
ω_i	Mole fraction of water vapor in the intercellular space (mol mol^{-1})
x	Volume mixing ratio of water vapor
C_3	C_3 photosynthetic mode
C_4	C_4 photosynthetic mode
D	Molecular diffusivity in air
E	Evaporation flux (mol $m^{-2}s^{-1}$)
F	Net fumigation chamber flux (mol $m^{-2}s^{-1}$)
F_d	Dew flux (mol $m^{-2}s^{-1}$)
F_L	Leaf flux (mol $m^{-2}s^{-1}$)
Q	Flow rate (m^3 s^{-1})
S	Surface area of the evaporation container (Chap. 2) or leaf (Chap. 3; m^2)
T_a	Temperature of air (°C)
T_B	Temperature of bubbler (°C)
T_S	Surface temperature of water (°C)
T_W	Bulk water temperature (°C)
W	Leaf water content (mol m^{-2})
superscript i	Minor isotopes of water (^{18}O or Deuterium)

Acknowledgement

First, I would like to thank to my advisor, Prof. Xuhui Lee. I cannot even imagine that I would be able to make this work possible without his support. At the moment that I had accepted the admission offer from Yale, a professor who knew him said he was a mentor more than an advisor. And it did not take much time to confirm that it was true. During the past six years, he has been a figure of such a big tree during my years in the program. He has been always there so that I could find an answer whenever I needed; needless to say, he was in active support of me with full of ideas and foremost patience.

I wish to express sincere appreciation to two committees, Prof. Graeme Berlyn and Prof. Ronald Smith. They have always welcomed me who randomly showed up with countless questions and problems in great need of help. Graeme has provided me almost unlimited access to the resources of his lab and the Greeley greenhouse. Ron has actually given me an idea about the water evaporation experiment and he has allowed me to utilize all the resources in his lab for the water extraction. In particular, I want to stress my qualifying exam. At the moment of written prospectus submission, I knew a weakness in the theoretical component that needed to be strengthened further which I was unable to make it due to the limited time given for the work. After the submission, I received two questions as the written exam that I had to complete within two weeks. Once I found the questions, I quickly understood that my committees gave me one more chance to teach myself that theory through the written exam because the questions were directly related to the point that I was unable to complete in the prospectus. To answer the questions, I had to get through tough computations regarding the kinetic theories but the two weeks was full of the joy of learning, surprisingly. I have to agree that it was the first time in my

academic years that I enjoyed an exam as a process of teaching myself not an exam for exam's sake.

I would like to thank current and former lab colleagues for their infinite support and generosity. I am thankful to have made unforgettable colleagues out of Yale whom I met during the multiple field deployments, especially in Minnesota and in Guelph, Canada.

I would like to send a big hug to my beloved friends whom I met in Yale but now in everywhere in U.S. and the world. I feel that words cannot even express my love for life-time friends in Korea, who provided moral support for the past years as well as fed me during my home trip to Seoul.

I want to thank my parents, Jungsook Cho and Dongkyu Kim, and my brother Yeehwan Kim, for their support, love, and patience to their daughter/sister who becomes easily less considerate during the state of deep concentration on a certain task.

엄마, 아빠 고맙습니다.

As a final remark, I would like to state that it has been a great honor to have been a member of the wonderful institution, Yale, which opened a new world for me. Through my time at Yale, I have beheld the pleasure of being intellectual and learned the weight of responsibility of being educated that have grown me up both professionally and personally.

Chapter 1. Introduction

1.1 Introduction

This chapter briefly outlines the significance of plants in hydrologic processes, the implications of dew water input on plants water relations, and the advantages of stable water isotopes in studying the dynamics of plant water uses. A knowledge gap between theories and observations in the isotopic enrichment is briefly discussed. The importance of leaf water contents and some uncertainties of nocturnal stomatal behavior are briefly considered as determinants of leaf water isotope ratios. The power of continuous measurements of vapor isotopes is given. The chapter ends with an overview of the dissertation studies.

Plants assume a significant role in the hydrologic processes in terrestrial ecosystems. Evapotranspiration (ET) is one of the important sources of atmospheric water vapor and energy flux from terrestrial ecosystems: approximately 70% of the precipitation which falls on the continents returns back to the atmosphere through ET processes (Shiklomanov and Sokolov, 1983). Long term ET measurements are credible indicators to recognize the intensity of the water cycle (Huntington, 2006). In vegetative areas, water vapor transfer is mainly driven by transpiration rather than evaporation (Dawson *et al*., 2002) so that deeper understanding of the dynamics of plants water uses is necessary in order to account for ET processes. However, conventional methods have been limited in quantifying total fluxes of ET above vegetation surfaces (Baldocchi *et al*., 1988; Monteith, 1965).

Identification of possible plant water sources is a fundamental step in understanding and constructing the dynamics of hydrologic processes in ecosystems. It is crucial to fully understand the dynamics of water uses by plants, especially under conditions of climate changes that the hydrologic cycle will experience in the future (IAEA, 2001). Spatial and

temporal variations of water concentration in soil are a crucial factor in determining plant diversity. Combining multiple water sources is a common strategy in plants aimed to secure the supply of water. Though the effect of commonly known water pools, e.g. groundwater, stream water and precipitation has been established, the consequence of additional water input to plant water requirement has not been fully understood.

Water input by nighttime dew formation is equivalent to 11% of the annual precipitation in the desert valleys of the western US (Malek *et al*., 1999) and the frequency of dew occurrence over a growing season is approximately 85% in an soybean field in Minnesota (Welp *et al*., 2008). Impact of dew in the regional water budget becomes significant in dry climatic regions, restoring leaf water at night in Mediterranean (Munne-Bosch and Alegre, 1999). These observations provide evidence that the nocturnal phase of water movement is substantially high, which is supposedly driven by incomplete stomatal closure during nighttime, considering a reported threshold of cuticular conductance (Caird *et al*., 2007). Dew formation can alter the $H_2{}^{18}O$ and HDO isotopic compositions of leaf water (Welp *et al*., 2008; Wen *et al*., In review).

1.2 Water isotopologues in the study of plant water relations

1.2.1. Uses of water isotopologues

Stable isotopes allow us to trace water movement in the forest hydrologic cycle and to identify plant source water. The source water of trees can be determined by comparing the isotope composition of xylem sap (δ_X) to soil water (δ_S) and other possible water sources such as groundwater, rain, or stream water (Dawson and Ehleringer, 1991; Walker and

Richardson, 1991; Stratton *et al*., 2000; Yakir and Sternberg, 2000). Soil water is the complex mixture and redistribution of rain events and the accompanying isotopic fractionation during evaporation (Zimmerman *et al*., 1967), resulting in unique depth profiles of isotopic composition of soil water. Many studies have established that δ_S at the surface is highly enriched compared to deep soil water (Allison *et al*., 1983; Barnes and Allison, 1983; Mathieu and Bariac, 1996; Melayah *et al*., 1996). Root uptake and xylem transport do not cause isotopic fractionation, so that measurements of δ_X can provide unique information on the origin of source water (Dawson and Ehleringer, 1991).

In recent years, there are increasing efforts to combine stable isotope methods and micrometeorological flux measurements in order to investigate atmosphere-vegetation water exchange. The isotopic compositions of soil evaporation from forest floor and transpiration are not identical. If the isotope analysis combines with the net flux measurement, they allow us to distinguish gross flux components from the net flux (Yakir and Wang, 1996; Yakir and Sternberg, 2000; Lai *et al*., 2006). This method requires obtaining the isotopic information of ecosystem water pools, with an exceptional need for leaf water isotope ratios. Indeed, understanding of leaf water enrichment governed by diffusive kinetic effect through stomata lies in an analogy to isotopic enrichment at evaporating surfaces.

1.2.2. Enrichment theory

Gas exchanges at the evaporating surface include both upward and downward fluxes of water molecules whose rate is determined by vapor pressure deficit at the liquid-vapor interface. At saturation, liquid water is in equilibrium with vapor at the liquid-air interface,

so that the isotopic composition of evaporation (δ_E) is a function of temperature at the water surface. Even though the net flux of major isotopes ($H_2{}^{16}O$) is zero, the flux of minor isotopologues apparently exists at saturation if the concentration gradient of minor isotopes between two phases is presented. At sub-saturation, in addition to the equilibrium effect, the kinetic effect is involved as a one of the driving forces in determining δ_E. This results in the isotopic enrichment at the evaporating surface due to the preferential diffusion of lighter isotopes across the boundary layer. Consequently, measurements of δ_E reveal the surface enrichment against the bulk water created at the evaporating surfaces.

Isotopic enrichment of leaf water can be estimated with a modification of the evaporation enrichment model proposed by Craig and Gordon (Craig and Gordon, 1965). They first proposed an explanation for the isotopic composition of the evaporated vapor (δ_E), molar fraction of minor isotopes to major isotope species in evaporating vapor, and liquid water body (δ_W). Their model was adopted to predict leaf water enrichment during transpiration, assuming transpiration isotope ratios are identical to those of the source of leaf water, a condition called isotopic steady-state. This model was later modified to isotopic enrichment at leaf water. The modified Craig-Gordon model did not concur with bulk leaf water measurements, especially at nighttime (Cernusak *et al*., 2002; Dongmann *et al*., 1974; Farquhar and Cernusak, 2005; Flanagan and Ehleringer, 1991; Flanagan *et al*., 1993) because the model oversimplified the dynamics of leaf water by assuming static conditions of stomatal behaviors.

A non-steady state assumption has improved the prediction of leaf water isotope ratios, indicating the significance of leaf water contents and stomatal conductance. Dongmann *et al* (1974) has demonstrated that isotopic enrichment of a leaf in the non-steady state

(ΔL_{NSS}) can be estimated by leaf water turnover time, conductance, relative humidity with the time step changes of ΔL_{NSS} at time (t) and (t-1). $\Delta L_{NSS}(t)$ and $\Delta L_{NSS}(t\text{-}1)$ are estimated from the steady state model. Farquhar and Lloyd (1993) plugged back-diffusion of enriched water molecules at the evaporating site in leaves into the Dongmann's model. In order to explain isotopic heterogeneity of leaf water at a given time step, Farquhar and Lloyd model acknowledged leaf water contents and stomatal conductance as major constraints in controlling leaf water enrichment. Implications of dew formation and nocturnal stomatal behavior on the leaf water enrichment have not been understood. Consequently, new experimental studies place a greater emphasis on mechanisms by which dew effects take place and on investigation of the extent to which they modulate leaf water isotopes.

1.3 Relationship between leaf water content (LWC) and the isotopic enrichment of leaf water

Leaf water status is associated with the isotopic enrichment of leaf water in two possible ways: regulating transpiration and affecting leaf water turnover time. Leaf water status physiologically regulates transpiration by controlling stomatal closure. Stomatal behaviors are governed by completed physiological responses to the surrounding environment. The major mechanisms of such regulation are mediated by releasing abscisic acid (ABA), potassium ion channels, and the concentration of soluble sugars at a cellular level. Along with soil water status and atmospheric variables (Gallego *et al*., 1994; Millar *et al*., 1971; Saranga *et al*., 1991; Smart and Barrs, 1973), it can influence transpiration (Jones, 1978) and stomatal conductance (Saliendra *et al*., 1995). Increasing leaf temperature due to leaf

water stress (Millar *et al*., 1971) may potentially affect the isotopic enrichment of leaf water.

Limited observations suggested that leaf water content (LWC) may play a significant role in the temporal variations in δ_L. For example, according to the measurements from an intensive campaign conducted in a soybean field in the summer of 2006, LWC was closely related to leaf water enrichments (Figures 1.1 and 1.2). Comparing the top and bottom leaves, the trends of LWC were the inverse of the trends of the isotopic composition of leaf water. The diurnal variation of LWC of the top leaves was smaller than the one of the bottom leaves. In case of δ_L, however, the top leaves had slightly larger diurnal variation than that of the bottom leaves. Further investigation is required to understand the relationship between LWC and δ_L.

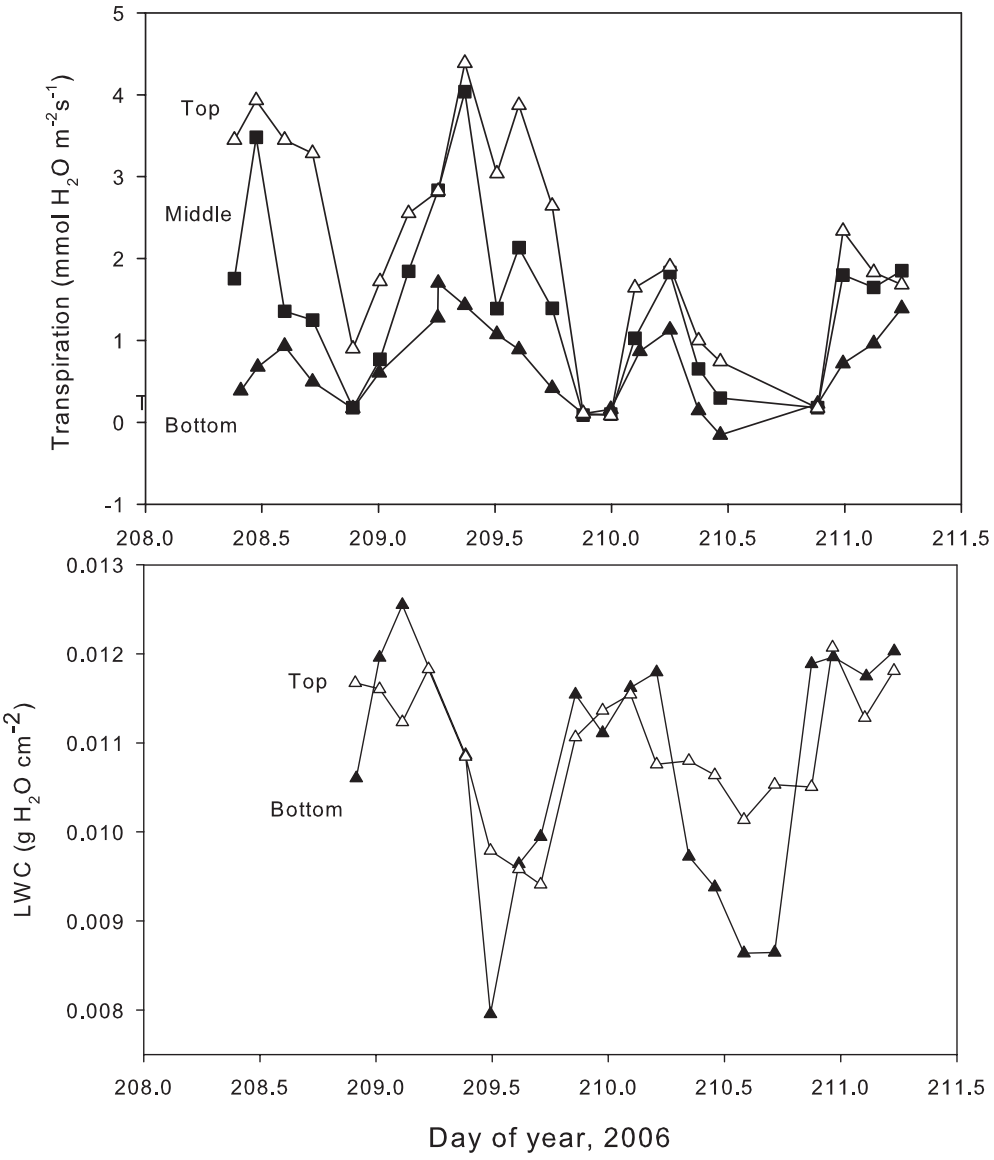

Figure 1.1. Diurnal variation of the measured transpiration rate (top) and leaf water content (bottom) in the intensive campaign, DOY 208 – 211 (July 27 – 30), 2006 in a soybean field, MN. First four measurements for LWC (bottom) were conducted including both top and bottom leaves.

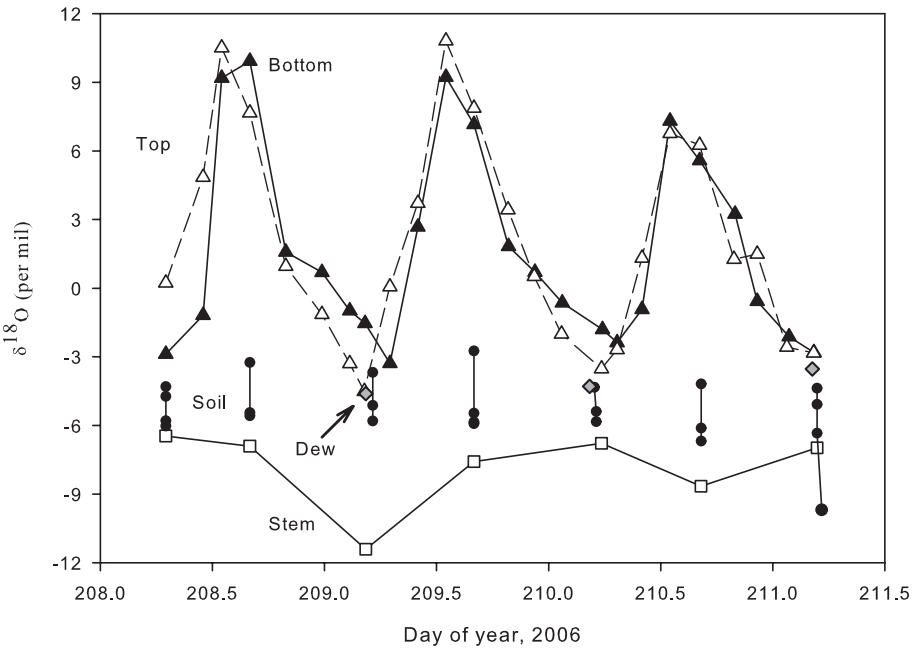

Figure 1.2. The isotope composition of top leaves (open triangles), bottom leaves (closed triangles), soil (closed dots) from 0, 5, 10 cm depth and 20 cm depth (7 measurements in 3 days), stem (open squares), and dew (shaded diamonds), soybean field, MN.

1.4 Nocturnal stomatal behaviors under dew formation

Dew formed at leaf surfaces may be in exchange with leaf water through two possible pathways: partially open stomata and cuticular permeability. At high humidity, foliar uptake is possible because equilibrium between intercellular space and leaf boundary layer can be achieved. This foliar uptake may be a key to understand the enrichment of leaf water less than predicted by existing models.

There are two possible pathways suggested for water uptake by leaves: via cuticles and via stomata. Very few studies were conducted to investigate the permeability of water through leaf cuticles and a threshold cuticular conductance of 0.02 mol $m^{-2}s^{-1}$ is considered to be a background leaf conductance (Caird *et al*., 2007). It is found that the properties of cuticular waxes determine the permeability (Fernandez and Ebert, 2005; Schonherr, 2000). Temperature is not correlated with penetration, but high humidity likely enhances the cuticular penetration of water at night (Schonherr, 2001).

Two hypotheses have been proposed to explain dew penetration via stomata: imperfect stomatal closure and the form of water at the time of penetration. There is growing evidence that plant stomata remain partially open at night, including measurements of both nocturnal sap flow and diurnal leaf water isotopes (Dawson *et al*., 2007; Welp *et al*., 2008). With partially closed stomata, stomatal penetration of water has been shown to only happen by gaseous diffusion due to the combination of stomata geometry and the surface tension of water (Schonherr and Bukovac, 1972). The authors described stomatal pores as a conical capillary with a small wall angle. Solutes having surface tension greater than the leaf surface tension (i.e. water) cannot penetrate through stomata of such physical structure. Other than direct infiltration, however, the presence of water at leaf

surfaces would form thin water films (Burkhardt and Eiden, 1994). Water films that are very thin (less than 100nm) and overlaying the entire leaf surface evenly on both the abaxial and adaxial sides of the leaf are able to extend into stomata and to reach thermodynamic equilibrium. The validity of the water film hypothesis has been tested experimentally (Eichert and Burkhardt, 2001; Eichert *et al*., 1998).

1.5 Measurements of vapor isotope ratios at high time resolution

As the demand for isotopic analysis is increasing in various ecosystem water vapor and carbon cycle studies, technical challenges are becoming more evident with the existing methodologies and instrumentation (Bowling *et al*., 2003b). The majority of the existing methods rely on trapping air in a flask and then analyzing it using mass spectrometry in the laboratory. However, collecting gaseous samples for isotopic analysis is labor intensive, which results in low sampling frequency and becomes an obstacle in vapor isotope investigation. Also, mass spectrometry analysis requires preparation (i.e. equilibrating water samples over one day), making it impossible to obtain real time measurements.

Continuous measurements of vapor isotope ratios provide unique insights into gas exchanges processes between ecosystem surfaces and the atmosphere. Use of direct measurements of evaporation over water surface makes it possible to investigate evapotranspiration flux partitioning (Yakir and Wang, 1996), surface enrichment at the evaporating surfaces (Welp *et al*., 2008) and kinetic discrimination of carbon and water isotopologues at the canopy scale (Lee *et al*., 2009).

In this dissertation, a tunable diode laser analyzer (TDL analyzer, TGA100, Campbell Scientific, Inc., Logan, UT, USA) was extensively used to measure continuous vapor isotope ratios. The TDL analyzer was originally designed for micrometeorological trace gas fluxes measurements (Edwards *et al*., 2003). Recently, the TDL analyzer was adapted to measure the isoflux of $^{12}C^{18}OO$ and $^{13}CO_2$ (Bowling *et al*., 2003a; Griffis *et al*., 2004; Griffis *et al*., 2005; Pataki *et al*., 2006) and HDO and $H_2{}^{18}O$ (Lee *et al*., 2005; Welp *et al*., 2008; Wen *et al*., 2008).

A detailed discussion about TDL analyzer can be found in Bowling *et al*. (2003b) and a modified version of its technical and operational descriptions for the water vapor are provided by Lee *et al*. (2005). Briefly, the TDL analyzer technology builds on the fact that each isotope has a specific absorptivity of infrared radiation at a certain wavelength so that it is possible to measure the concentration of target isotopes of interest. The wavelength of the laser, which is controlled simultaneously by both temperature and current, is tuned to an absorption line of a particular molecule of interest (TGA manual, Campbell Scientific, 2004). In the proposed experiment, absorption lines of $H_2{}^{16}O$ and $H_2{}^{18}O$ are chosen at 1500.546 cm^{-1} and 1501.188 cm^{-1}, respectively (Lee *et al*., 2005). Based on the flux gradient method, two air samples from different heights and calibration zero gas (ultra purified nitrogen) for zero offset are pulled into the TDL analyzer. In the described experiment, inlet and outlet air samples of a dynamic chamber were measured by comparison with the known isotopic composition of the reference gas (see Section. 2.3.1. in the evaporation chamber experiment).

1.6 Overview of study

This dissertation project has both laboratory and ecosystem levels of analysis and attempts to integrate gas exchange theories of stable water isotopes into hydrologic processes by measuring vapor isotope ratios continuously. The main goal of the project is to improve the methodology used in isotopic-based studies of hydrological processes on multiple scales, from the single leaves to ecosystems and to provide reliable measurements of the water dynamic for terrestrial ecosystems. This study appears to be the first of its kind in that isotopic measurement of evaporation was made continuously at a high resolution in a controlled environment. To improve theoretical understanding of the kinetic effects, these measurements of evaporation isotope ratios were used in order to quantify surface enrichment of water at various types of evaporating conditions. Furthermore, the isotopic mass balance approach was provided for the first time to estimate stomatal conductance at wet foliage. To quantify the nocturnal stomatal behaviors, fluxes of minor isotopologues were measured at saturation in a fumigation plant chamber, when net fluxes of major isotopologues vanished. To investigate the temporal dynamic of forest water uses, observation of whole-canopy evapotranspiration isotope ratios was made at a high time resolution over a growing season in a mixed forest, Ontario, Canada.

Detailed methodologies and further literature review can be found in Chapter 2 – 4 of this dissertation. Chapter 2 and 3 are presented in the form of manuscripts published in or, at the time of writing, under peer review by journals. Chapter 2 presents a laboratory study regarding isotopic enrichment of surface water during evaporation. Chapter 3 describes the effects of dew on isotopic equilibrium of leaf water with vapor and the estimation of

stomatal conductance using the fluxes of minor isotopologues at a wet surface. Chapter 4 presents the field observations of ecosystem water pools conducted in the Borden forest, Ontario, Canada during the summer of 2009. Chapter 5 summarizes the main conclusions and overall implications of this work. The appendices report two pilot studies: direct measurements of predawn leaf water potential under dew formation and a comparison of three water content measurements with spectral reflectance measurements.

1.7 References

Allison, G.B., Barnes, C.J. and Hughes, M.W., 1983. The distribution of deuterium and ^{18}O in dry soils: 2. Experimental. Journal of Hydrology, 64: 377-397.

Baldocchi, D.D., Hicks, B.B. and Meyers, T.P., 1988. Measuring Biosphere-Atmosphere Exchanges of Biologically Related Gases with Micrometeorological Methods. Ecology, 69(5): 1331-1340.

Barnes, C.J. and Allison, G.B., 1983. The distribution of deuterium and 18O in dry soils: 1. Theory. Journal of Hydrology, 60: 141-156.

Bowling, D.R., Pataki, D.E. and Ehleringer, J.R., 2003a. Critical evaluation of micrometeorological methods for measuring ecosystem-atmosphere isotopic exchange of CO2. Agricultural and Forest Meteorology, 116(3-4): 159-179.

Bowling, D.R., Sargent, S.D., Tanner, B.D. and Ehleringer, J.R., 2003b. Tunable diode laser absorption spectroscopy for stable isotope studies of ecosystem-atmosphere CO2 exchange. Agricultural and Forest Meteorology, 118(1-2): 1-19.

Burkhardt, J. and Eiden, R., 1994. Thin Water Films on Coniferous Needles. Atmospheric Environment, 28(12): 2001-2011.

Caird, M.A., Richards, J.H. and Donovan, L.A., 2007. Nighttime stomatal conductance and transpiration in C-3 and C-4 plants. Plant Physiology, 143(1): 4-10.

Campbell Scientific, I., 2004. TGA100 trace gas analyzer user and reference manual.

Cernusak, L.A., Pate, J.S. and Farquhar, G.D., 2002. Diurnal variation in the stable isotope composition of water and dry matter in fruiting Lupinus angustifolius under field conditions. Plant Cell and Environment, 25(7): 893-907.

Craig, H. and Gordon, L.I., 1965. Deuterium and oxygen 18 variations in the ocean and the marine atmosphere. In: E. Tongiorgi (Editor), Stable Isotopes in Oceanographic Studies and Paleotemperatures, Lischi & Figli, Pisa, Italy, pp. 9-130.

Dawson, T.E., Burgess, S.S.O., Tu, K.P., Oliveira, R.S., Santiago, L.S., Fisher, J.B., Simonin, K.A. and Ambrose, A.R. 2007. Nighttime transpiration in woody plants from contrasting ecosystems. Tree Physiology, 27(4): 561-575.

Dawson, T.E. and Ehleringer, J.R., 1991. Streamside trees that do not use stream water. Nature, 350: 335-337.

Dawson, T.E., Mambelli, S., Plamboeck, A.H., Templer, P.H. and Tu, K.P., 2002. Stable isotopes in plant ecology. Annual Review of Ecology and Systematics, 33: 507-559.

Dongmann, G., Nurnberg, H.W., Forstel, H. and Wagener, K., 1974. Enrichment of $H_2{}^{18}O$ in Leaves of Transpiring Plants. Radiation and Environmental Biophysics, 11(1): 41-52.

Edwards, G. C., G. W. Thurtell, G. E. Kidd, G. M. Dias, and C. Wagner−Riddle (2003), A diode laser based gas monitor suitable for measurementof trace gas exchange using micrometeorological techniques, Agric. For.Meteorol., 115, 71–89, doi:10.1016/S0168-1923(02)00166-1.

Eichert, T. and Burkhardt, J., 2001. Quantification of stomatal uptake of ionic solutes using a new model system. Journal of Experimental Botany, 52(357): 771-781.

Eichert, T., Goldbach, H.E. and Burkhardt, J., 1998. Evidence for the uptake of large anions through stomatal pores. Botanica Acta, 111(6): 461-466.

Farquhar, G.D. and Cernusak, L.A., 2005. On the isotopic composition of leaf water in the non-steady state. Functional Plant Biology, 32(4): 293-303.

Farquhar, G.D. and Lloyd, J., 1993. Carbon and oxygen isotope effects in the exchange of carbon dioxide between terrestrial plants and the atmosphere, Stable isotopes and plant carbon–water relations. Academic Press, San Diego, pp. 47–70.

Fernandez, V. and Ebert, G., 2005. Foliar iron fertilization: A critical review. Journal of Plant Nutrition, 28(12): 2113-2124.

Flanagan, L.B. and Ehleringer, J.R., 1991. Effects of Mild Water-Stress and Diurnal Changes in Temperature and Humidity on the Stable Oxygen and Hydrogen Isotopic Composition of Leaf Water in Cornus-Stolonifera L. Plant Physiology, 97(1): 298-305.
Flanagan, L.B., Marshall, J.D. and Ehleringer, J.R., 1993. Photosynthetic Gas-Exchange and the Stable-Isotope Composition of Leaf Water - Comparison of a Xylem-Tapping Mistletoe and Its Host. Plant Cell and Environment, 16(6): 623-631.
Gallego, H.A., Rico, M., Moreno, G. and Regina, I.S., 1994. Leaf Water Potential and Stomatal Conductance in Quercus-Pyrenaica Willd Forest - Vertical Gradients and Response to Environmental-Factors. Tree Physiology, 14(7-9): 1039-1047.
Griffis, T.J., Baker, J.M., Sargent, S.D., Tanner, B.D. and Zhang, J., 2004. Measuring field-scale isotopic CO2 fluxes with tunable diode laser absorption spectroscopy and micrometeorological techniques. Agricultural and Forest Meteorology, 124(1-2): 15-29.
Griffis, T.J., Baker, J.M. and Zhang, J., 2005. Seasonal dynamics and partitioning of isotopic CO2 exchange in C-3/C-4 managed ecosystem. Agricultural and Forest Meteorology, 132(1-2): 1-19.
Huntington, T.G., 2006. Evidence for intensification of the global water cycle: Review and synthesis. Journal of Hydrology, 319(1-4): 83-95.
IAEA (International Atomic Energy Agency). 2001. Annual report 2001. http://www.iaea.org/Publications/Reports/Anrep2001/marine_environment.pdf
Jones, H.G., 1978. Modeling Diurnal Trends of Leaf Water Potential in Transpiring Wheat. Journal of Applied Ecology, 15(2): 613-626.
Lai, C.T., Ehleringer, J.R., Bond, B.J. and U, K.T.P., 2006. Contributions of evaporation, isotopic non-steady state transpiration and atmospheric mixing on the delta O-18 of water vapour in Pacific Northwest coniferous forests. Plant Cell and Environment, 29(1): 77-94.
Lee, X., Griffis, T.J., Baker, J.M., Billmark, K.A., Kim, K., and Welp, L.R. 2009. Canopy-scale kinetic fractionation of atmospheric carbon dioxide and water vapor isotopes. Global Biogeochemical Cycles, 23: GB1002, doi:10.1029/2008GB003331.
Lee, X.H., Sargent, S., Smith, R. and Tanner, B., 2005. In situ measurement of the water vapor O-18/O-16 isotope ratio for atmospheric and ecological applications. Journal of Atmospheric and Oceanic Technology, 22(5): 555-565.
Malek, E., McCurdy, G. and Giles, B., 1999. Dew contribution to the annual water balances in semi-arid desert valleys. Journal of Arid Environments, 42(2): 71-80.
Mathieu, R. and Bariac, T., 1996. A numerical model for the simulation of stable isotope profiles in drying soils. Journal of geophysical research, 101(D7): 12685-12696.
Melayah, A., Bruckler, L. and Bariac, T., 1996. Modeling the transport of water stable isotopes in unsaturated soils under natural conditions: 1. Theory. Water resources research, 32(7): 2047-2054.
Millar, A.A., Jensen, R.E., Bauer, A. and Norum, E.B., 1971. Influence of Atmospheric and Soil Environmental Parameters on Diurnal Fluctuations of Leaf Water Status of Barley. Agricultural Meteorology, 8(2): 93-105.
Monteith, J.L., 1965. Evaporation and environment. Symposia of the Society for Experimental Biology, 19: 205-234.
Munne-Bosch, S. and Alegre, L., 1999. Role of dew on the recovery of water-stressed Melissa officinalis L-plants. Journal of Plant Physiology, 154(5-6): 759-766.
Pataki, D.E., Bowling, D.R., Ehleringer, J.R. and Zobitz, J.M., 2006. High resolution atmospheric monitoring of urban carbon dioxide sources. Geophysical Research Letters, 33(3): -.
Saliendra, N.Z., Sperry, J.S. and Comstock, J.P., 1995. Influence of Leaf Water Status on Stomatal Response to Humidity, Hydraulic Conductance, and Soil Drought in Betula-Occidentalis. Planta, 196(2): 357-366.
Saranga, Y., Rudich, J. and Marani, A., 1991. The Relations between Leaf Water Potential of Cotton Plants and Environmental and Plant Factors. Field Crops Research, 28(1-2): 39-46.

Schonherr, J., 2000. Calcium chloride penetrates plant cuticles via aqueous pores. Planta, 212(1): 112-118.
Schonherr, J., 2001. Cuticular penetration of calcium salts: effects of humidity, anions, and adjuvants. Journal of Plant Nutrition and Soil Science-Zeitschrift Fur Pflanzenernahrung Und Bodenkunde, 164(2): 225-231.
Schonherr, J. and Bukovac, M.J., 1972. Penetration of Stomata by Liquids - Dependence on Surface-Tension, Wettability, and Stomatal Morphology. Plant Physiology, 49(5): 813-819.
Shiklomanov, A. and Sokolov, A.A., 1983. Methodological basis of world water balance investigation and computation. In: A. Van der Beken and A. Herrmann (Editors), New Approaches in Water Balance Computations. IAHS Publication, pp. 77-92.
Smart, R.E. and Barrs, H.D., 1973. Effect of Environment and Irrigation Interval on Leaf Water Potential of 4 Horticultural Species. Agricultural Meteorology, 12(3): 337-346.
Stratton, L.C., Goldstein, G. and Meinzer, F.C. 2000. Temporal and spatial partitionaing of water resources among eight woody species in a Hawaiian dry forest. Oecologia, 124:309-317.
Walker, C.D. and Richardson, S.B. 1991. The use of stable isotopes of water in characterizing the source of water in vegetation. Chemical Georology, 94(2): 145-158.
Welp, L.R., Lee, X., Kim, K., Griffis, T.J., Billmark, K., Baker, J.M. 2008. $\delta^{18}O$ of water vapour, evapotranspiration and the sites of leaf water evaporation in a soybean canopy. Plant Cell and Environment, 31(9): 1214-1228.
Wen, X.F., Lee, X., Sun, X.M., Wang, J.L., Li, S.G. and Yu, G.R. In review. Dew water isotopic ratios and their relations to ecosystem water pools and fluxes in a cropland and a grassland in China.
Wen, X.F., Sun, X.M., Zhang, S.C., Yu, G.R., Sargent, S.D. and Lee, X. 2008. Continuous measurement of water vapor D/H and O-18/O-16 isotope ratios in the atmosphere. Journal of Hydrology, 349(3-4): 489-500.
Yakir, D. and Wang, X.F., 1996. Fluxes of CO2 and water between terrestrial vegetation and the atmosphere estimated from isotope measurements. Nature, 380(6574): 515-517.
Zimmerman, U., Ehhalt, D. and Munnich, K.O. (Editors), 1967. Soil water movement and evapotranspiration: changes in the isotopic composition of the water. Isotopes in hydrology. Int. At. Energy Agency, Vienna, 567-584 pp.

Chapter 2. [1]Isotopic enrichment of liquid water during evaporation from water surfaces

[1]Manuscript published as Kim, K. and Lee, X. 2011. Isotopic enrichment of liquid water during evaporation from water surfaces. *Journal of Hydrology*, doi:10.1016/j.jhydrol.2011.01.008

Abstract

The predictions of isotopic composition of evaporation (δ_E) from a water body are often made with the Craig-Gordon model on the assumption that the isotopic composition of water surface undergoing evaporation ($\delta_{L,e}$) is the same as that of the bulk water ($\delta_{L.b}$). The validity of this well-mixed assumption is not known due to the lack of the δ_E measurements. In this study, a tunable diode laser (TDL) analyzer was deployed to make fine time-resolution measurements of $H_2{}^{18}O$ and HDO in vapor in a developed flux chamber. The results show that the surface enrichment was substantial: on average, the surface water was 7.5 – 8.9‰ more enriched in ^{18}O and 12.6 – 16.5‰ in D than the bulk water, the exact value depending on the choice of the kinetic fractionation factor for evaporation. Also I reported greater uncertainties of D than that of ^{18}O in the estimation of surface enrichment; the measured ^{18}O surface enrichment was statistically different from zero but the D enrichment was not. The kinetic effect appeared stronger under conditions of higher evaporation. In addition to leaf water, I suggest that the surface enrichment should also exist in lakes and evaporation pans although it is likely lower than the estimated enrichment values. The well-mixed assumption may have also affected previous effects of determining the $^{18}O/^{16}O$ and D/H diffusivity ratios in air.

2.1 Introduction

Isotopic fractionation effects determine the isotopic compositions of both the evaporating vapor and the residual water by discriminating heavier isotopes in the process of phase changes of water. Understanding these fractionation effects is a necessary step in many isotope studies. The isotope tracers provide us a means to understand the dynamics of hydrologic processes (Gat *et al*., 1994). The meteoric water exerts an imprint on plant source water, which can be used to reveal water relations (Dawson and Ehleringer, 1991). The ecosystem-scale water flux can be partitioned into its component fluxes using the isotope tracers (Lee *et al*., 2007; Williams *et al*., 2004). Furthermore, the oxygen isotope of water is tightly associated with that of atmospheric CO_2, offering an opportunity to constrain the atmospheric carbon budget using the knowledge of discrimination processes associated with plant photosynthesis and soil respiration (Ciais *et al*., 1995; Farquhar *et al*., 1993).

The evaporative enrichment at the water surface is created by the accumulation of the heavier isotopes, in part, due to the kinetic effect. This effect arises from the different molecular diffusion rate between the heavier HDO and $H_2{}^{18}O$ molecules and the lighter $H_2{}^{16}O$ molecules at the air-liquid interface. Craig and Gordon (1965; hereafter referred to as the C-G model) first proposed an isotopic evaporation model for open water surfaces. The model characterizes the isotopic kinetic fractionation effect as being controlled by turbulent and laminar boundary layers above the isotopically equilibrated air-water interface. Conceptually, in the laminar layer, isotopic fractionation is governed by molecular diffusion, while no fractionation occurs under fully turbulent conditions in the turbulent layer. Applying this principle to evaporation from a soil surface, Zimmermann

et al. (1967) suggested that turbulent mixing is minimal and molecular diffusion represents dominant process above the evaporating front in the soil pores. Allison *et al*. (1983) found this diffusion-controlled fractionation effect increases with the depth of the evaporating front. In contrast to soil water, evaporation from a leaf surface is governed by kinetic fractionation effects in both stomata and the boundary layer of the leaf (Farquhar *et al*., 1989). Many studies have confirmed the necessity of accounting for the boundary layer diffusion in determining the leaf isotopic exchange (Barbour *et al*., 2007; Cernusak *et al*., 2002; Ogee *et al*., 2007).

Application of the C-G model to quantifying the evaporative enrichment is difficult due to theoretical and technical limitations. During the phase change of water, the heavier isotopes accumulated at the water surface diffuse downwards to the liquid reservoir and the lighter isotopes move upwards by advection. The thickness of the advection-diffusion layer at the liquid surface controls the degree of evaporative enrichment at the surface (He and Smith, 1999). This thickness is, however, not amenable to direct observation. In the studies of plant-atmosphere vapor isotope exchange, questions exist about the role of turbulent transport in the kinetic fractionation. The exponent n in the kinetic factor ε_K formula (section 2.2.2) can vary from zero in fully turbulent diffusion to 1 in fully molecular diffusion. In spite of the expected turbulent diffusion in the canopy boundary layer, global modeling studies deploy ε_K with an effective n value greater than 0.9 (Hoffmann *et al*., 2004), which is larger than the kinetic factor for open water evaporation whose n value is typically around 0.5. In leaf-scale studies, ε_K is mostly controlled by diffusive fractionation through the stomata. This ε_K gives good agreement between the C-G model prediction and the measurement of leaf water enrichment only if

humidity and vapor isotope contents are measured very close to the leaf boundary layer (Xiao *et al*., 2010).

Recent advances in laser spectroscopy make it possible to obtain high temporal resolution measurements of the isotopic compositions of atmospheric vapor (δ_V) and the evaporated water (δ_E). These measurements provide new constraints on the kinetic effects and surface enrichment during evaporation. Several laboratory experiments have been conducted on isotopic evaporation (Cappa *et al*., 2003; Craig *et al*., 1963; Merlivat, 1978; Rozanski and Chmura, 2006; Stewart, 1975) but none of them has used continuous measurement of δ_E. The advantage of the continuous and simultaneous measurement of δ_E and δ_V is that it allows us to determine the evolution of evaporative enrichment of the surface water as evaporation progresses, which in turn can be used to quantify the kinetic fractionation effects experimentally.

The temperature at the evaporating surface controls both the equilibrium fractionation factor (ε_{eq}) and relative humidity (h) (Gat and Bowser, 1991; Kumar and Nachiappan, 1999; Lloyd, 1966). Cappa *et al*. (2003) proposed that a significant degree of cooling exists at the surface of the evaporating water, which can affect the accuracy of water isotope predictions. They argued that it is the surface temperature, T_S, not that of the bulk water temperature, T_W, that drives the isotopic exchange between the surface and the air aloft. A similar argument can be made for the stratification of the isotopic composition in the water: δ_E is dependent upon the isotopic composition at the evaporating surface ($\delta_{L,e}$), not directly on that of the bulk water ($\delta_{L,b}$). Cappa *et al*. (2003) made the implicit assumption that $\delta_{L,b}$ is identical to $\delta_{L,e}$. But in reality, I expect these two parameters to be

different although to our best knowledge no published studies have quantified the difference between $\delta_{L,b}$ and $\delta_{L,e}$. Obviously $\delta_{L,e}$ is the more appropriate parameter than $\delta_{L,b}$ for quantifying the isotopic exchange during evaporation. According to Welp *et al*., (2008), $\delta_{L,e}$ can be backed out of the C-G model from the observed δ_E.

In this study, a tunable diode laser (TDL) analyzer was deployed to make fine time-resolution measurements of $H_2{}^{18}O$ and HDO in vapor in a home-made flux chamber. Flux chambers have been widely used for measuring gaseous emissions to the atmosphere at various types of surfaces. Using continuous measurement of the isotopic composition of evaporation (δ_E), this study aims to improve our understanding of fractionation during evaporation and to quantify the isotopic enrichment at the evaporating surface.

2.2 Theory

2.2.1. Predictions of evaporative enrichment

The isotopic composition of evaporation (δ_E) is described by Craig and Gordon (1965) as

$$\delta_E = \frac{\alpha_{eq}^{-1}\delta_{L,e} - h\delta_V - \varepsilon_{eq} - (1-h)\varepsilon_K}{(1-h) + 10^{-3}(1-h)\varepsilon_K} \tag{2.1}$$

where h is the relative humidity calculated with the measured vapor pressure inside the chamber in reference to the temperature of the evaporating surface (T_S), δ_V and $\delta_{L,e}$ are the isotope ratios of the vapor in the air aloft and the liquid water at the surface undergoing evaporation, respectively, ε_K is the kinetic fractionation factor in per mil, α_{eq} (>1) is a temperature-dependent fractionation factor (Majoube, 1971), and

$$\varepsilon_{eq} = \left(1 - \frac{1}{\alpha_{eq}}\right) \times 1000 \tag{2.2}$$

The reader should be aware that $\delta_{L,e}$ is generally heavier than $\delta_{L,b}$, the isotope ratio of the bulk water. The difference, $\delta_{L,e}$ - $\delta_{L,b}$, a measure of evaporative enrichment, is the focus of the experimental investigation.

Eq. (2.1) is a simplified version of the original Craig-Gordon model. In the original model, the surface isotope value is higher than the value of the bulk water by an unspecified amount. Although modeling studies have been reported on the enrichment process (He and Smith, 1999), I am not aware of experimental investigations that attempt to quantify the enrichment.

If δ_E is known, Eq. 2.1 can be solved for $\delta_{L,e}$ as

$$\delta_{L,e} = \alpha_{eq}\left[(1-h)\left(\delta_E + 10^{-3}\varepsilon_K\delta_E + \varepsilon_K\right) + h\delta_V\right] + 10^3\left(\alpha_{eq} \quad 1\right) \tag{2.3}$$

One difficulty in applying Eq. 2.3 stems from uncertainties in T_S and ε_K, two variables that are not measured directly. The determination of ε_K requires the characterization of the degree of molecular and turbulent diffusion. Cappa *et al*. (2003) and Lee *et al*. (2009) show that it can be written in the general form of

$$\varepsilon_K = n\left(1 - \frac{D_i}{D}\right) \times 10^3 \tag{2.4}$$

where D is the molecular diffusivity in air, subscript i denotes the minor water isotopic species ($H_2{}^{18}O$ or HDO) and n is an aerodynamic parameter that appears as the exponent in the following relationship (Stewart, 1975),

$$\frac{r_i}{r} = \left(\frac{D}{D_i}\right)^n \tag{2.5}$$

In Eq. 2.5, r and r_i are diffusion resistances to the major and minor isotope species, respectively. The diffusivity ratios are 0.9691 ($^{18}O/^{16}O$) and 0.9839 (D/H) (Cappa *et al*., 2003). The evaporating dishes used in the present study are small objects immersed in air slowly circulated by a fan inside a chamber (see below), so it is reasonable to assume a laminar boundary layer value of n = 0.67 (Barnes and Allison, 1983; Mathieu and Bariac, 1996).

I used two methods to determine $\delta_{L,e}$. The first method, described in the next subsection, is that of Cappa *et al*. (2003) that solves n and T_S from the measured changes in the $^{18}O/^{16}O$ and D/H of the bulk water during the evaporation experiment. In the second method, I assumed a value of 0.67 for n and approximate T_S by T_W.

2.2.2. Determination of T_S and n from the isotopic composition of evaporating water

Cappa *et al*. (2003) pointed out that the water surface undergoing evaporation should be cooler than the bulk water. They proposed an experimental method that allows simultaneous determination of T_S and n from the $^{18}O/^{16}O$ and D/H ratios measured at the beginning and the end of the evaporation experiment. A brief summary of their method is provided here. Mass conservation requires that

$$\frac{dR_{L,b}}{dt} = \frac{E}{m}(R_{L,b} - R_E) \tag{2.6}$$

where m is the mass of water, t is time, and $R = c_i / c$, is the molar ratio, c_i and c are the mixing ratio of the minor and major isotopologue, respectively. Subscripts L and E denote bulk liquid and evaporation, respectively. The molar ratios can be converted to the delta-notation, as $\delta = (R_L / R_{VSMOW} - 1) \times 10^3$, where R_{VSMOW} is the VSMOW standard for water. Assuming $\delta_L = \delta_{L,e}$ and combining with Eq. 2.1, I obtain the solution of Eq. 2.6 as

$$\left(\delta_L - \frac{b}{a-1}\right) = \left(\delta_{L,0} - \frac{b}{a-1}\right)\left(\frac{m}{m_0}\right)^{(a-1)} \tag{2.7}$$

where subscript 0 denotes values at $t = 0$, and

$$a = \frac{1}{\alpha_{eq}(1-h)(1+10^{-3}\varepsilon_K)}$$

$$b = \frac{h\delta_V + 10^3(1-\alpha_{eq}^{-1}) + (1-h)\varepsilon_K}{(1-h)(1+10^{-3}\varepsilon_K)} \tag{2.8}$$

In Eq. 2.7, δ_L, $\delta_{L,0}$, m and m_0 are taken from the measurement, and T_S, which determines α_{eq} (Majoube, 1971), and n, which determines ε_K in Eq. 2.4, are unknowns. Since Eq. 2.7 can be written for both ^{18}O and D, I have a closed system in which the two unknowns are constrained by two independent equations. The solution of T_S and n was achieved numerically for every evaporation experiment. The reader is reminded that this procedure does not require the measurement of δ_E. For the purpose of consistency with Cappa *et al.* (2003), the diffusivity ratios of 0.9691 ($^{18}O/^{16}O$) and 0.9839 (D/H) were used in Eq. 2.4.

2.3 Experimental Methods

2.3.1. Evaporation chamber

The evaporation experiments were conducted with a dynamic chamber. A TDL analyzer was used to measure the mixing ratios of the three isotopic species, HDO, $H_2{}^{18}O$ and $H_2{}^{16}O$ in water vapor at the inlet and outlet airstreams of the chamber (Figure 2.1). The chamber was a glass cylinder dome placed, without airtight seal, on a high density polyethylene (HDPE) plate. Glass and HDPE were chosen as the chamber materials in order to minimize the problem of water vapor sticking to the chamber walls (Lee *et al*., 2005). The water absorption of HDPE is 0.02-0.06% and no absorption or swelling of glass is reported when it is exposed to water (Avallone and Baumeister, 1996; NACE International, 2002). The sampling tubing was made of Synflex composite material (Dekabon Type 1300, 1/4 in OD × 0.040 in wall, Dekoron, Aurora, Ohio, USA). A fan was installed on the bottom plate and pointed upward to circulate air inside the chamber, so the possibility of humidity buildup near the evaporation source should be minimal. Because the chamber was not air-tight, the pressure inside was atmospheric. Once a pump was turned on, room air bled into the chamber, at a flow rate of 15 L min^{-1}, all around through the bottom edge of the glass dome in contact with the HDPE plate. The resident time of chamber air was 2.3 min. Simultaneously air was drawn, through a tube perforated with small holes and looped around the bottom of the dome, into the TDL analyzer for analysis of the inlet moisture mixing ratio and isotope ratio. Air inside the chamber (chamber outlet air) was drawn from a perforated tube standing vertically in the chamber. The difference in humidity between the inlet and outlet was about 3% and 5% of relative humidity, respectively, relative to T_S for the heated and unheated experiments

shown in Table 2.1. A small evaporating container was placed in the middle of the bottom plate. The temperatures of the water and air inside the chamber were measured with two thermocouples. The inlet humidity was not actively controlled. The air handling system of the laboratory was quite stable. The inlet water vapor molar mixing ratio varied by less than 1 mmol/mol peak-to-peak or its relative humidity h varied by less than 0.04 peak-to-peak during each evaporation experiment.

Another important component of the experimental system was the TDL analyzer (TGA 100 Campbell scientific Inc., Logan, UT, USA). Details of the system have been discussed elsewhere (Lee *et al*., 2007; Lee *et al*., 2005; Welp *et al*., 2008; Wen *et al*., 2008). Briefly, the TGA manifold was operated with five intakes. The intake assignments were span 1 (S1; intake 1), span 2 (S2; intake 2), chamber outlet (intake 3) and inlet (intake 4), and dry air (intake 5). The chamber inlet and outlet air were brought into the TGA manifold through a gradient interface system (GI) inside which two buffer volumes served to dampen fluctuations in the humidity and isotope ratios. S1 and S2 were calibration air generated by a homemade device (called dripper) that generated water vapor of known isotopic composition. The calibration was made in every manifold switching cycle which was three minute long. Dry air served as a reference zero gas. Flow through the manifold inlets was controlled at 0.25 L min^{-1} by heated critical orifices.

The experiments were performed under heated and unheated setup using four types of containers. In the heated experiments, heating was provided by two lamps of 250 and 120 W installed outside the chamber. The average evaporation rate of the heated experiments was 73% higher than that of the unheated experiments (Table 2.1). The kinetic

fractionation effects may be associated with surface roughness. Four types of containers were used: a 10-ml beaker (area 4 cm^2, depth 3.3 cm), a 30-ml beaker (area 8 cm^2, depth 5.6 cm), a glass cup (area 13.2 cm^2, depth 7.7 cm) and a petri-dish (area 20.6 cm^2, depth 1.8 cm). The surface dimensions of these containers are similar to that of a typical broad leaf of a plant. A specific experimental goal was to find out if the different geometry of the evaporation containers may alter the surface boundary layer enough to cause detectable differences in the kinetic factor.

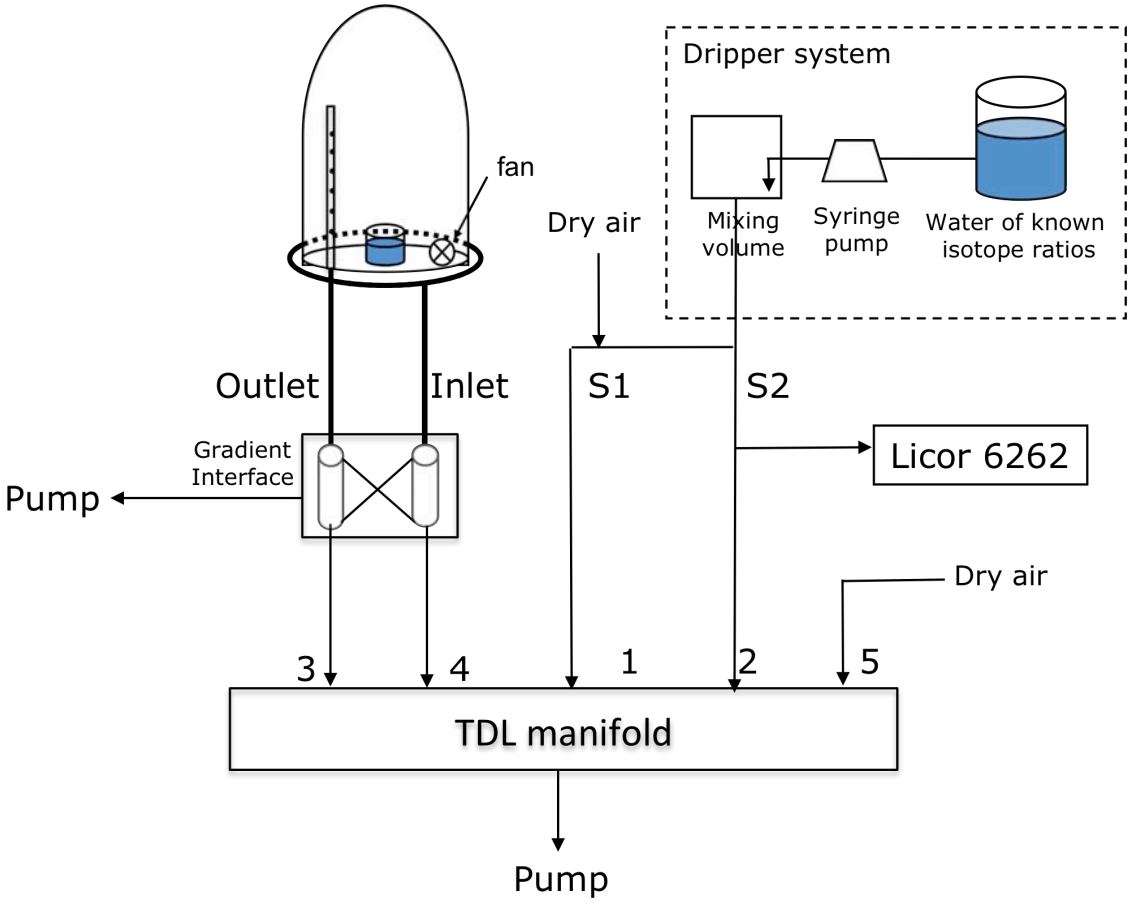

Figure 2.1. Schematic diagram of the evaporation chamber and the TDL system for water vapor isotopes. The numbers represent the five intakes to the TDL manifold.

2.3.2. Determination of the evaporation flux and vapor and flux isotope ratios

The evaporation flux (E) was determined from the measured water vapor mixing ratios of the inlet (c_i) and outlet (c_o) of the chamber air and the chamber flow rate (Q), as

$$E = Q\,(C_O - C_i) / S \tag{2.9}$$

where S is the surface area of the evaporation container.

This flux was integrated with time over the duration of the experiment and was compared with the total water loss measured with a precision balance.

The isotope ratio of water vapor at the inlet and outlet air was computed from the mixing ratio measurements and calibrated against the two span values according to Lee *et al*. (2005) and Wen *et al*. (2008). The molar $^{18}O/^{16}O$ and D/H ratio of the chamber evaporation flux (R_E) was given by

$$R_E = R_d \times \frac{x_2 - x_1}{x_2' - x_1'} \times \frac{x_3' - x_4'}{x_3 - x_4} \tag{2.10}$$

where R_d is the molar ratio of the dripper calibration water ($^{18}O/^{16}O$ of -15.7‰ and D/H of -120.9‰), subscripts denote the TDL inlet assignments (Figure 2.1), and x and x' denote uncalibrated volume mixing ratios of the major and minor species, respectively (Lee *et al*., 2007). The molar ratio R_E was converted to the delta notation. The isotope ratios in this study were reported relative to VSMOW.

One source of measurement error was related to the nonlinear response of the TDL analyzer to ambient humidity. In a linear system whose gain factor of each of the

isotopologues is linear with its mixing ratio, the measured molar ratio of the span vapor should be a constant or independent of the mixing ratio. This turns out not to be case with this analyzer. According to Wen *et al*. (2008), nonlinearity can be minimized via periodic adjustment of a nonlinearity parameter of the instrument. In this study, the nonlinearity error in δ_E was corrected, *a posteriori*, on the basis of mass conservation. Let δ_O be the error associated with the instrument nonlinearity, δ_E be the measured isotopic composition of evaporation, and δ_L be the isotopic composition of the liquid water. Mass conservation requires

$$\frac{d\delta_L}{dt} = \frac{E}{m}\left[\delta_L - \left(\delta_E + \delta_O\right)\right] \tag{2.11}$$

where E is evaporation rate and m is mass of liquid water. This equation was integrated over time to the end of the experiment. The correction δ_O was found by matching the predicted δ_L with the measured value at the end of the experiment. The average correction was 1.6 (±2.6)‰ (^{18}O) and 38.1 (±13.6)‰ (D). The data presented below have been corrected.

Local snow water with low isotope ratios (^{18}O/^{16}O = -13.5‰ and D/H = -88.9‰) was used for all the evaporation experiments. The weight of the initial water and the remaining water at the end of the experiment were measured, and the remaining water was sampled for the isotope analysis. Water isotopic analyses were carried out on a Thermo Finnigan DeltaPlus XP with Gas Bench, Thermo Finnigan MAT 253 with a H-device and a Thermo Finnigan DeltaPlus XP with TC/EA at the Yale Isotope Laboratory.

2.3.3. Measurements of transpiration flux isotope ratios

The chamber performance was further examined by measuring $^{18}O/^{16}O$ and D/H of plant transpiration (δ_T). A cotton seedling grown in hydroponic solution was first exposed to full sunlight in the ambient environment for 5 h and then placed in the chamber for 40 hr. The pot containing the root and the hydroponic solution was sealed so that only transpired water was detected. The photosynthetically active photon flux density was very low at 15 μmol $m^{-2}s^{-1}$ during the experiment, resulting in a low transpiration rate of 0.45 mmol m^{-2} (leaf area) s^{-1}. The low transpiration rate was compensated by a total leaf area (0.03 m^2) much bigger than the surface area of the evaporation containers so that the humidity difference between the chamber inlet and outlet was comparable to those found in the evaporation experiments. The transpiration experiment provided an independent evaluation of the accuracy and precision of the δ_E measurement.

2.4 Results

Recently, Sturm and Knohl (2009) pointed out a potential problem arising from the use of Synflex tubing in the isotope measurements of water vapor. They observed that a long retention time existed when their analyzer intake was switched after a step change from a sample gas to a calibration gas. The delay is particularly noticeable in the D/H response. Synflex tubing was also used in the present study. Figure 2.2 presents the measured vapor $^{18}O/^{16}O$ and D/H ratio time series, averaged over 16 switching cycles, in response to switching from the chamber inlet to the calibration span 1 during an unheated experiment (Evapo 5). Both isotope ratios responded rapidly to the step change, attaining the target values 2 s after the transition. The rapid response may have been a result of low pressure

(150-500 mb) in the tube. The low pressure was generated by a critical orifice at the tube inlet which regulated the flow through the tube and by the small orifices of the manifold.

Figure 2.3 compares the cumulative evaporation estimated with the TDL mixing ratios (Eq. 2.9) against the total water loss during the experiment. The evaporation derived from the chamber measurement was in excellent agreement with the measured water loss except for Evapo 6. The reason is not clear as to why Eq. 2.9 underestimated the water loss during Evapo 6. This experiment was excluded from the analysis of surface water enrichment. Figure 2.3 indicates that the developed chamber system was in general reliable.

The results of the plant transpiration measurement can be used to quantify the performance of the chamber system for measuring δ_E. Figure 2.4 presents the time evolution of the measured $^{18}O/^{16}O$ and D/H of the transpiration water (δ_T). Also shown is the isotope compositions of the plant source water (δ_X). The average transpiration rate and the turnover time of leaf water were 0.45 mmol $m^{-2}s^{-1}$ (on the leaf area basis) and 6.1 h, respectively. The reader is reminded that because the plant had been exposed to full sunlight, the isotopic contents of its leaf water must have been highly enriched over the source water. The δ_T measurement indicates that transpiration was not in steady-state for the first 13 h of the experiment. The transition time was much longer than other observations in which the isotopic steady state is achieved in less than 2 h under controlled environment conditions (Flanagan *et al*., 1991; Yakir *et al*., 1994). The long transition time was not surprising given the extremely low transpiration rate in the dark conditions. After 13 h of the elapsed time, δ_T became stabilized, with average values of

1.8‰ and 20.8‰ lighter than $^{18}O/^{16}O$ and D/H of the source water, respectively. This bias occurred due to the nonlinearity of the TDL analyzer (Lee *et al*., 2005). The biases fall in the ranges found with the mass balance approach described in Section 2.3.2. Excluding the first 13 h of the observation, the standard deviation of the hourly δ_T was 1.4 and 21.7‰ for $^{18}O/^{16}O$ and D/H, respectively. This can be viewed as the precision of the δ_E measurement. Relative to the precisions of the vapor isotope ratios, the precision of the flux D/H ratio was much worse than the precision of the flux $^{18}O/^{16}O$ ratio. The precision of the $^{18}O/^{16}O$ ratio was comparable to that reported by Lee *et al*. (2007).

Figure 2.5 presents an example of the time evolution of the hourly δ_E and δ_V in one of the unheated experiments (Evapo 5). The δ_E predictions (dots) were made with the C-G model using the measured delta value of the bulk water ($\delta_{L,b}$, crosses) at the beginning and end of the experiment. Both the evaporation flux and the bulk water were steadily enriched in ^{18}O and D with time during the experiment. The measured δ_E disagreed with the predicted δ_E. In general, the C-G predictions of $^{18}O/^{16}O$ of the evaporation flux underestimated δ_E while the C-G predictions of D/H showed inconsistent tendency. The discrepancy between the predictions and the observations appeared larger at the end than at the beginning of the experiment.

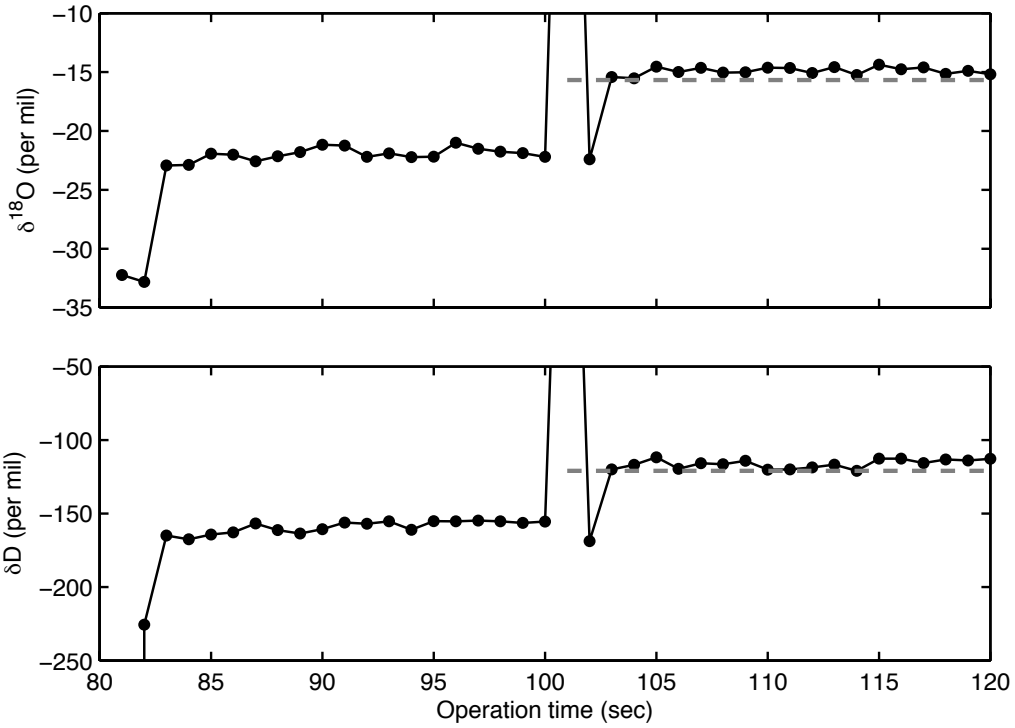

Figure 2.2. Response of the TDL to step changes from the inlet air sample (81 - 100 s) to span 1 calibration (101 - 120 s) in 180 s measurement cycles. Dashed lines are the known values of the span calibration, -15.7 and -120.9‰ for $^{18}O/^{16}O$ and D/H, respectively.

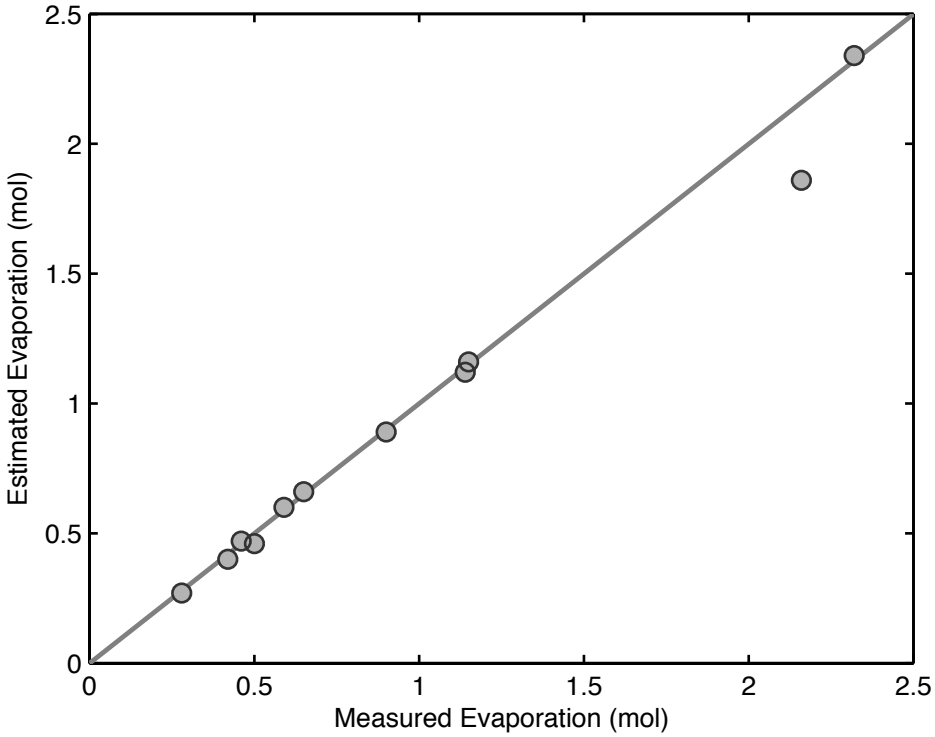

Figure 2.3. Relationship between the measured water loss ($m - m_0$) and cumulative evaporations estimated with the TDL mixing ratios according to Eq. 2.9. The line represents a 1:1 relationship. The outlier represents Evapo 6 which was excluded from further analyses.

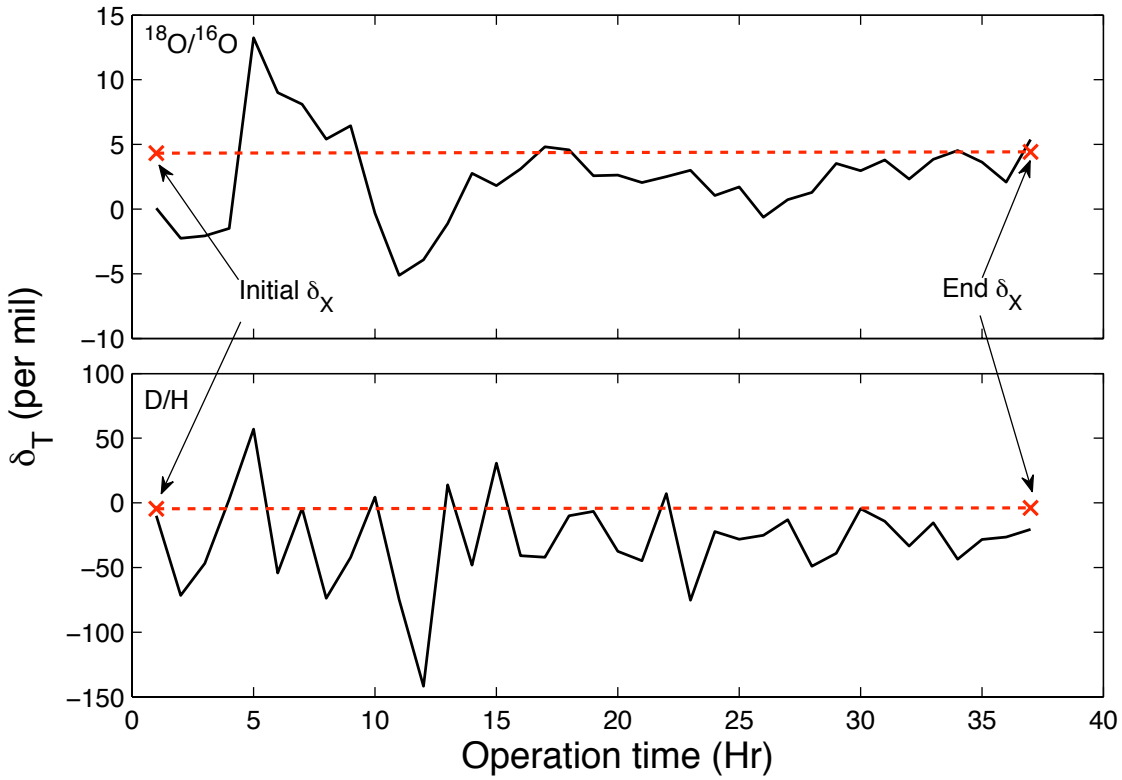

Figure 2.4. The isotopic compositions of transpiration. The source water $^{18}O/^{16}O$ and D/H represented by the crosses were 4.3 and -4.5‰ at the beginning and 4.4 and -3.9‰ at the end of the experiment, respectively. Excluding the first 13 h under non-steady state, the variations suggest an uncertainty (one standard deviation) of the hourly flux isotope ratio measurement on the order of 1.8 and 21‰ for $^{18}O/^{16}O$ and D/H, respectively.

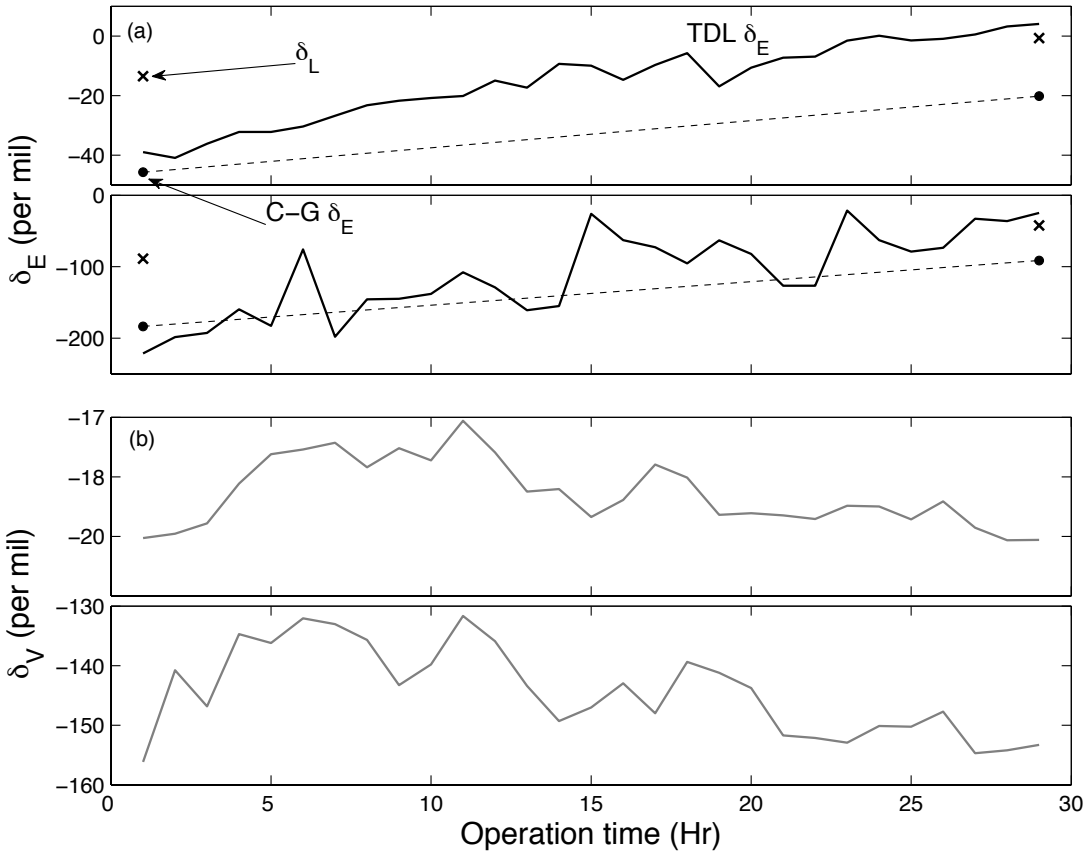

Figure 2.5. Hourly means of the evaporation isotope ratios (a) and vapor isotopic compositions of chamber air (b) in the one of unheated experiments (Evapo 5). The C-G model predictions of δ_E (dots) were made with the measured bulk water isotope ratios ($\delta_{L,b}$) and bulk water temperature (T_W) and the n value of 0.67. The uncertainty (one standard deviation) of the hourly δ_V measurement was about 0.1‰ for $^{18}O/^{16}O$ and 1‰ for D/H (Lee *et al*. 2005; Wen *et al*. 2008), and that of the hourly δ_E was 1.8‰ for $^{18}O/^{16}O$ and 21‰ for D/H (Figure 2.4).

Table 2.1 summarizes the experimental conditions. In a total of 11 experiments, 4 were performed with heating and the rest without heating. Heating produced a much higher evaporation flux ranging from 0.01 to 0.0276 mol $m^{-2}s^{-1}$ than without heating (0.005 to 0.0081 mol m^{-2} s^{-1}). For comparison, Blanken *et al*. (2000) reported a typical midday evaporation rate, ranging from 0.00167 to 0.0034 mol $m^{-2}s^{-1}$ from a boreal lake in the summer. The fraction of residual water at the end of experiment, m/m_0, varied depending on operation duration, heating setup, and container type. The relative humidity inside the chamber in reference to T_S ranged between 0.40 and 0.59 depending on the experimental conditions. A large difference in the aerodynamic parameter *n* occurred between the two experimental settings. The same container was used for the first three heated experiments (Evapo 2-4). No solution of *n* in the range 0-1 could be found for Evapo 2, 4 and 8. The solutions found for Evapo 3 were used for analysis of Evapo 2 and 4 and those for Evapo 5 were used for Evapo 8 on the assumption that the same container would cause identical influence of turbulence on the diffusion characteristics to generate the same T_S and *n* values. In the heated set-up, the *n* values varied from 0.89 to 0.94. That the *n* value was close to the molecular value suggests that molecular diffusion dominated isotopic fractionation under conditions of high evaporation. I suggest that this was because turbulence was suppressed in the stably stratified interfacial surface boundary layer above the water surface. The strong evaporative cooling caused the surface temperature of the water to be on the average 9.9°C lower than air temperature in the chamber in the heated setup. In the unheated set-up, the mean *n* value was 0.55, indicating that turbulent diffusion was stronger at the lower evaporation rates. The average surface temperature of the unheated evaporation experiments was 0.8°C higher than the bulk water temperature

and 1.2°C lower than air temperature in the chamber. The *n* variation among the unheated experiments was quite small, implying that the boundary layer condition above the evaporating surface was insensitive to the shape of the container. The *n* value was uncorrelated with the evaporation rate.

The estimated evaporating surface temperature (T_S) was similar between the heated and unheated set-up even though the measured bulk water temperature (T_W) was quite different. The mean T_S value (standard deviation) was 21.3°C (± 2.2) for the heated setup and 21.4°C (± 1.4) for the unheated setup. With respect to evaporative cooling, the heated setup had the surface that was consistently cooler than the bulk water with the maximum temperature difference of 11.8°C during Evapo 4. No consistent pattern was observed in the unheated setup. Evapo 9 and 10 produced slight cooling while during Evapo 1, 5, 7 and 8, some warming was observed. The physically unrealistic warming of the evaporative surface could be related to measurement errors and errors arising from the well-mixed assumption in the solution of *n* and T_S.

Table 2.1. Summary of experimental conditions. The aerodynamic parameter n and surface water temperature (T_S) were determined with the isotope mass balance method described in the text. Relative humidity (*h, both outlet and inlet streams were* normalized to T_S) and evaporation flux were averages of the whole experiment. Bulk water temperature (T_W) is the first 3 hour average of thermocouple measurements.

	Container	m/m_0	T_W (°C)	n	T_S (°C)	*Outlet h*	Inlet *h*	Evaporation flux (mol $m^{-2}s^{-1}$)
Heated								
Evapo 2	10ml beaker	0.29	33.8	0.94	23.0	0.45	0.42	2.48×10^{-2}
Evapo 3	10ml beaker	0.22	33.1	0.94	22.4	0.45	0.40	2.44×10^{-2}
Evapo 4	10ml beaker	0.07	33.4	0.94	21.6	0.46	0.42	2.29×10^{-2}
Evapo 11	Glass cup	0.59	26.7	0.89	18.0	0.59	0.52	1.02×10^{-3}
Unheated								
Evapo 1	10ml beaker	0.54	20.3	0.54	21.1	0.45	0.43	8.11×10^{-3}
Evapo 5	Petri-dish	0.26	19.5	0.49	22.7	0.42	0.38	5.22×10^{-3}
Evapo 6	Glass cup	0.23	20.3	0.52	20.3	0.48	0.45	3.97×10^{-3}
Evapo 7	Glass cup	0.17	21.0	0.55	21.4	0.45	0.42	4.43×10^{-3}
Evapo 8	Petri-dish	0.19	19.8	0.49	23.8	0.40	0.37	5.53×10^{-3}
Evapo 9	30ml beaker	0.58	21.7	0.51	20.1	0.49	0.46	6.77×10^{-3}
Evapo 10	Glass cup	0.78	21.0	0.67	20.1	0.50	0.46	5.09×10^{-3}

Table 2.2 summarizes the $^{18}O/^{16}O$ and D/H values of the bulk ($\delta_{L,b}$) and the surface water ($\delta_{L,e}$). Here $\delta_{L,e}$ was determined with Eq. 2.3 using the n and T_S values listed in Table 2.1. The initial $\delta_{L,b}$ was identical as water of the same isotope ratios was used in all the experiments. At the beginning of these experiments, the mean surface enrichment ($\delta_{L,e}$-$\delta_{L,b}$) values (standard deviation in parentheses) are 12.4 (5.3) and 31.1 (35.7)‰ for the heated and 4.0 (2.3) and -12.4 (37.9)‰ for the unheated setup for $^{18}O/^{16}O$ and D/H, respectively. At the end of the experiments, the mean values are 8.7 (5.2) and 22.4 (30.0)‰ for the heated and 8.7 (3.8) and 18.6 (33.1)‰ for the unheated setup for $^{18}O/^{16}O$ and D/H, respectively. The average value of all the data (heated and unheated, beginning and end) was 8.0‰ (standard deviation 4.8‰) for $^{18}O/^{16}O$ and 12.6‰ (36.2) for D/H. The mean $^{18}O/^{16}O$ enrichment was significantly different form zero ($p < 0.001$) but the mean D/H enrichment was not ($p = 0.14$). Because of the large uncertainties found in D/H, the analysis of surface enrichment for $^{18}O/^{16}O$ should be more reliable than that of D/H.

The more variable D/H enrichment estimates than the $^{18}O/^{16}O$ values were related partly to the fact that the precision for the D/H flux ratio measurement was much lower than for the $^{18}O/^{16}O$ flux ratio (Figure 2.5). Other researchers have also reported uncertainties in D/H previously in the case of leaf water enrichment (Cernusak *et al.*, 2002; Roden and Ehleringer, 1999). Roden *et al.* (2000) suggested in their sensitivity analysis of the C-G leaf water model that errors in the model predictions can be magnified as the difference in D/H between the vapor and the source water increases. The D/H difference between the liquid and the vapor was on average 52.0‰ at the beginning and became larger

(101.2‰) at the end of the experiments. This seems to explain why the D/H enrichment estimates were more scattered at the end than at the beginning of the experiment.

To ensure that the enrichment results in Table 2.2 are not an artifact of the well-mixed assumption (section 2.5.4), I did another set of calculations using the *n* value of 0.67 for the kinetic factor (Eq. 2.3) and evaluating relative humidity (*h*) and the equilibrium factor at the measured bulk water temperature. As stated previously, the *n* value of 0.67 is frequently used for assessing the fractionation during diffusion through the laminar boundary layer of a small object (Farquhar and Lloyd, 1993). When these values were deployed in the C-G model, only small changes in the surface enrichment were detected for either type of the experimental setups (Table 2.3). At the end of evaporation, the mean surface enrichment in ^{18}O changed to 12.1 and 9.1‰ from 8.7 and 8.7‰ and the enrichment in D changed to 31.4 and 16.1‰ from 22.4 and 18.6‰ for the heated and unheated setups, respectively. The average enrichment of all the data (heated and unheated at the beginning and end of the experiments) was 8.9‰ (standard deviation 4.1‰, significantly different from zero at $p < 0.001$) for $^{18}O/^{16}O$ and 13.1‰ for D/H (standard deviation 35.7‰, $p = 0.12$). The enrichment estimates are insensitive to the choice of the Cappa method or the commonly accepted *n* value.

Table 2.2. The isotopic compositions (‰) of the bulk water ($\delta_{L,b}$) and the evaporating surface water at the beginning and the end of experiment. Here , $\delta_{L,e}$ was estimated from the hourly measurements of δ_E using n and T_S shown in Table 2.1. Typical measurement precision was 0.1 (^{18}O) and 1‰ (D) for $\delta_{L,b}$ and 0.9 (^{18}O) and 11‰ (D) for $\delta_{L,e}$.

$^{18}O/^{16}O$	$\delta_{L,b}$		$\delta_{L,e}$	
	Initial	End	Initial	End
Heated				
Evapo 2	-13.5	5.5	-2.1	19.3
Evapo 3		9.1	2.6	19.9
Evapo 4		19.9	3.3	28.8
Evapo 11		-3.8	-8.2	-2.3
Unheated				
Evapo 1	-13.5	-2.3	-7.5	9.5
Evapo 5		-0.7	-13.4	12.1
Evapo 6		4.8	n/a	n/a
Evapo 7		6.5	-8.4	15.0
Evapo 8		2.0	-10.9	12.3
Evapo 9		-5.2	-7.8	-2.3
Evapo 10		-7.4	-9.1	-1.6
D/H	$\delta_{L,b}$		$\delta_{L,e}$	
	Initial	End	Initial	End
Heated				
Evapo 2	-88.9	-33.8	-30.0	-15.2
Evapo 3		-23	-44.0	39.5
Evapo 4		12.7	-46.8	2.6
Evapo 11		-63.6	-110.2	-45.0
Unheated				

Evapo 1	-88.9	-48.3	-119.2	-51.4
Evapo 5		-42.3	-110.8	10.8
Evapo 6		-24.5	n/a	n/a
Evapo 7		-19	-57.9	27.0
Evapo 8		-5.2	-157.7	10.6
Evapo 9		-63.9	-60.2	-29.9
Evapo 10		-72.5	-101.7	-106.9

Table 2.3. The isotopic compositions (‰) of water at the evaporating surface. The measured bulk water temperature and the n value of 0.67 were used for the $\delta_{L,e}$ estimations. The same data is also plotted in Figure 2.6b. Typical measurement precision was 0.9 (^{18}O) and 11‰ (D).

	$^{18}O/^{16}O$		D/H	
	Initial	End	Initial	End
Heated				
Evapo 2	-6.9	19.6	-30.8	-17.7
Evapo 3	-1.3	21.5	-53.0	56.5
Evapo 4	0.6	35.3	-59.6	5.7
Evapo 11	-5.0	2.6	-128.2	-26.5
Unheated				
Evapo 1	-5.4	11.1	-115.0	-49.6
Evapo 5	-10.2	11.6	-101.3	1.1
Evapo 6	n/a	n/a	n/a	n/a
Evapo 7	-6.4	16.6	-56.7	26.6
Evapo 8	-8.1	11.5	-139.6	3.3
Evapo 9	-4.8	1.2	-59.1	-25.1
Evapo 10	-12.3	-4.5	-105.7	-110.7

The δD-δ^{18}O slope analysis in Figure 2.6 reveals that evaporation caused a fractionation effect at the evaporating surface than in the bulk water. The slope of the δD-δ^{18}O relationship reflects the difference in kinetic fractionation between D and ^{18}O of the residual water after evaporation has occurred. A stronger kinetic effect shifts the slope further from the slope of 8 in which is the GMWL slope resulting from the isotopic equilibrium between the precipitation and the vapor (Gat, 1996). The δD-δ^{18}O slope for $\delta_{L,b}$ is 3.0 at the end of the experiments. The δD-δ^{18}O slope for $\delta_{L,e}$ at the end of experiments was predicted in the range of between 1.5 and 3.8 (mean slope of 2.6 at the 95% confidence intervals) in Figure 2.6b.

Figure 2.7 shows the evolution of δ_E, measured during Evapo 5 (Figure 2.5), in the δD-δ^{18}O plot. The best fit of the data gives a linear regression with a slope of 3.6, similar to the slope shown in Figure 2.6a for the bulk water.

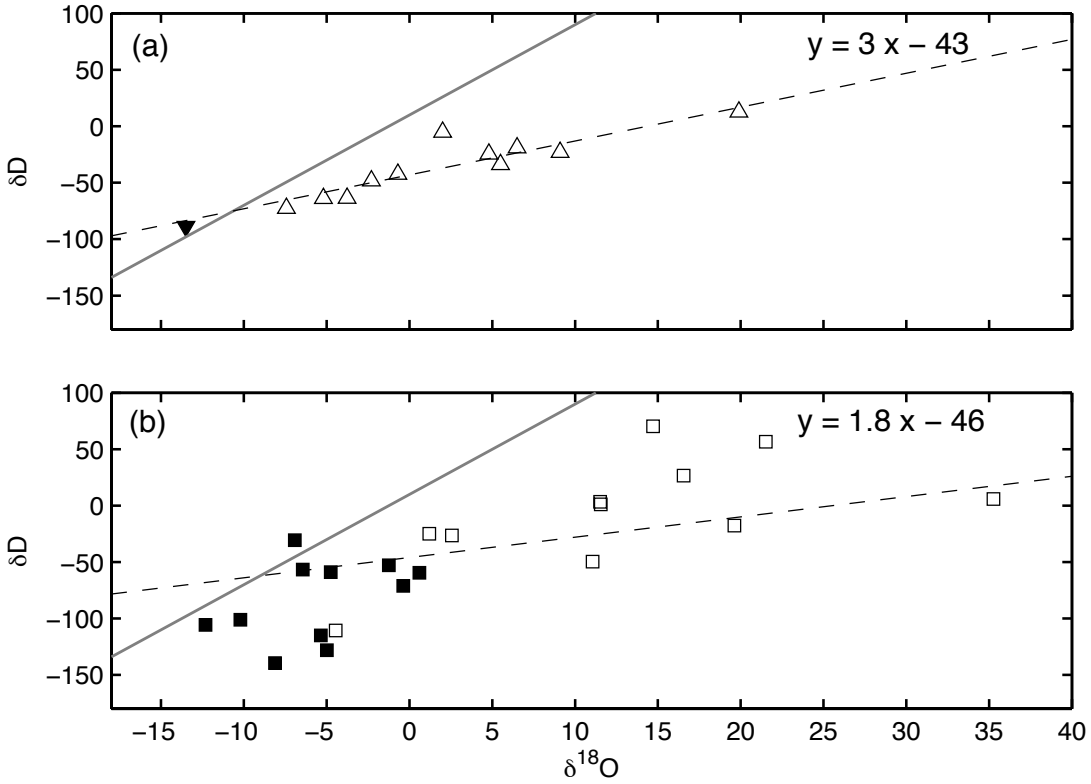

Figure 2.6. δD-δ^{18}O relationships for the evaporating water reservoirs:(a) isotope ratios of the bulk water ($\delta_{L,b}$), and (b) at the evaporating sites ($\delta_{L,e}$). $\delta_{L,e}$ was estimated with the C-G model with the n value of 0.67 and the measured T_W. Closed and open symbols represent isotope ratios at the beginning and the end of the evaporation experiment, respectively. Dashed lines are the best-fit of the open symbols, with the regression equation of (a) δD= 3.0 (±1.2) $\delta^{18}O$ – 43 (±10) and (b) δD = 2.6 (± 2.4) $\delta^{18}O$ – 47 (±40) with parameter ranges given at the 95% confidence level. Dotted lines in (b) are the 95% confidence intervals. Solid lines are GMWL. The same data is given in Table 2.3.

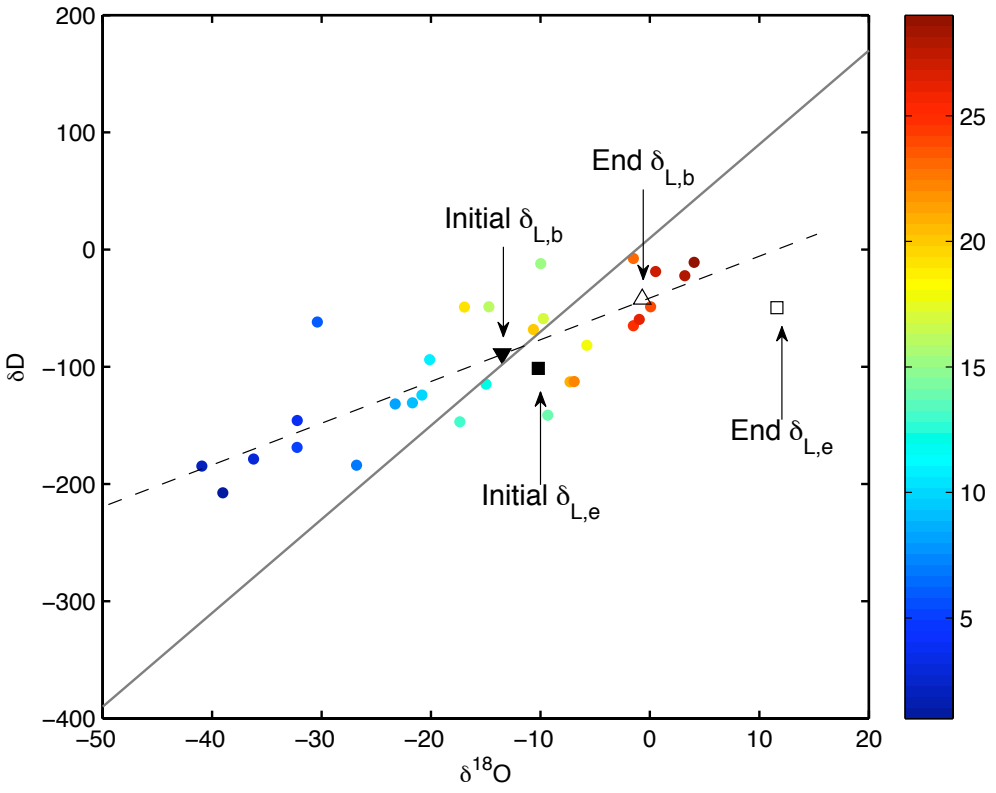

Figure 2.7. Evolutions of isotopic composition of the evaporation flux (δ_E) over the course of Evapo 5. The diagonal solid line is the GMWL. The color bar shows the time evolution of the experiment (hour). The dashed line is the linear regression of δ_E. Also shown are the C-G model calculation of the surface water isotope compositions ($\delta_{L,e}$), made with n = 0.67 the measured T_W, and the compositions of the bulk water. Additional information on this experiment is given in Figure 2.5. See Figure 2.5 for δ_L symbols.

2.5 Discussion

2.5.1. The role of molecular and turbulent diffusion

The overall kinetic effect on evaporation depends on the relative roles of molecular and turbulent diffusion. Three limits of n value are known: non-fractionating, fully turbulent diffusion (n = 0), diffusion through the laminar boundary layer of a small object (n = 0.67) and pure molecular diffusion (n = 1) (Craig and Gordon, 1965). In leaf scale observations, n ranges from 0.48 to unity depending on leaf morphology (Buhay *et al.*, 1996). According to wind tunnel studies, n should be equal to 0.67 if the motion in the leaf boundary layer is laminar and 0.50 if it is turbulent (Monteith and Unsworth, 1990). In the process of soil evaporation, diffusion through the soil pore space is a molecular process and n should be close to unity (Allison *et al*., 1983). At the ecosystem-scale, the gaseous exchange pathway consists of both molecular diffusion through the stomatal opening and turbulent diffusion through the canopy air space and the atmospheric surface layer, and as a consequence the effective n value can be very small (Lee *et al*., 2009). The estimated n values were closer to the molecular limit at high rates of evaporation and the limit of turbulent leaf boundary layer at low rates of evaporation. In comparison, Cappa *et al*. (2003) reported the n values in the range of 0.32-0.39 at evaporation rates similar to those in the unheated experiments. These exceptionally low n values may be an indication that turbulent diffusion played a large role in their chamber experiment.

2.5.2. Isotopic enrichment at the evaporating sites

The results show that the predictions of δ_E with the C-G model (Eq. 2.1) were lower than the δ_E observations if the bulk water isotope ratios were used in the model calculations. The disagreement can only be explained by the surface being more enriched in ^{18}O and D than the bulk water. The disagreement existed at the very beginning of the evaporation experiment (Figure 2.5a), indicating the development of the vertical gradient in the water ^{18}O and D compositions was a nearly instant process.

The enrichment in ^{18}O and D during evaporation has been extensively studied through the examination of leaf water. Numerous studies have used the C-G model to predict the isotopic compositions of the water at the evaporating sites within the leaf at steady state (Allison *et al*., 1985; Barnard *et al*., 2007; Flanagan and Ehleringer, 1991; Seibt *et al*., 2006). The predicted values are generally higher than that of the bulk leaf water. A Péclet effect model has been used to describe the isotopic mixing of the xylem water flow and the back diffusion from the evaporation sites in the leaf (Farquhar and Cernusak, 2005; Farquhar and Lloyd, 1993; Ripullone *et al*., 2008; Wang *et al*., 1998). This isotopic gradient developed within the leaf bears some resemblance to this experimental situations. Unlike leaf transpiration where the leaf water is continuously refilled by the inflow of the xylem water, this system was a closed one in that there was no continuous supply of water with constant isotopic compositions to the evaporating reservoir. In a closed system, I expect a stronger back-diffusion than in an open system, imposing a constraint on the magnitude of the isotopic gradient between the surface and the bulk water.

Even though the dimension of the evaporation source was small, the underlying processes can shed some light on evaporation from water bodies such as rivers, lakes and evaporation pans (Gibson *et al*., 1999) in natural conditions. Running the C-G model in the inverse mode (Eq. 2.3), I estimated that the gradients between the surface and the bulk water were 8.0 and 12.6‰ for $^{18}O/^{16}O$ and D/H, respectively (Table 2.2). These enrichment values are likely to represent the upper limit of natural water bodies undergoing evaporation. In ocean waters, wave breaking, which occurs at scales greater than the thickness of the interfacial layer undergoing evaporation, should act to smear the isotopic gradient. It is also known that the diffusion process in river and lake waters is more efficient than molecular diffusion (Csanady, 1963), further inhibiting the development of the isotopic gradient at the surface. Indeed, recent isotopic studies of marine vapor do not show evidence for such large enrichment of surface water (Uemura *et al*., 2010; Uemura *et al*., 2008). Nevertheless, this research raises the possibility that the calculations of the isotopic compositions of the water vapor at the source region may have been biased low in previously published studies because the bulk water isotopic content was used to drive the C-G model (Terwilliger and DeNiro, 1995; Yadav, 1997; Yi *et al*., 2008). Horita *et al*. (2008) also pointed out in their review that the degree of surface cooling suggested by Cappa *et al*. (2003) must also produce surface enrichment. The advection-diffusion model of He and Smith (1999) shows that in the limit of high evaporation rates, evaporation from a water body should approach a "batch" process analogous to leaf transpiration. In this process, the evaporated water has an identical isotopic composition as the bulk water and the water surface undergoing evaporation must be enriched over the bulk water to sustain this isotopic steady state.

2.5.3. Isotopic fractionation indicated by the δD-δ^{18}O slope

Numerous studies have examined the δD-δ^{18}O slope of environmental water. In the studies of atmospheric transport, the δD-δ^{18}O slope of precipitation provides insights into the mixing of the vapor generated locally with the water transported from the remote source region (Gat *et al*., 1994; Gat *et al*., 2003; Gibson, 2002). In the process of leaf transpiration, the δD-δ^{18}O slope is a measure of the mixture of the un-fractionated xylem water with the fractionated leaf water at the evaporative sites (Allison *et al*., 1985; Cernusak *et al*., 2002; Flanagan *et al*., 1991; Pendall *et al*., 2005; Roden and Ehleringer, 1999). The majority of the studies on the leaf water enrichment reported the slope value in the range from 3 to 5. In dry soils, the slope of the soil water is less than 3 due to the dominance of molecular diffusion through the soil layers (Allison *et al*., 1983; Tang and Feng, 2001).

In the present study, the δD-δ^{18}O slope for the bulk water, $\delta_{L,b}$ (Figure 2.6a) was 3.0 (±1.2, 95% confidence interval) close to the low end of the values reported for the bulk leaf water in the literature. The slope of for $\delta_{L,e}$ at the end of the experiments (Figure 2.6b) was 2.6 (± 2.4, 95% confidence interval), falling in the ranges reported by previous studies conducted on evaporating water bodies (Allison *et al*., 1985; Craig and Gordon, 1965; Gat *et al*., 2007). In a model calculation with the assumption of no vertical isotopic gradient, Gat (1971) reported a modeled slope value of 2.3 for an evaporating reservoir. The estimated slope for the surface water was closer to those found for extremely dry soil and for leaves of water-stressed plants. For example, a slope of 2 was reported for soil water in Sahara (Dincer *et al*., 1974 in Gibson *et al*., 2008). Gat *et al*. (2007) reported the slope of 2.1 to 2.8 for the leaf water of desert plants sampled in

midday hours. Allison *et al*. (1985) reported a slope of 1.3 to 2.4 for water of pine needles at various height collected in water-stressed and non-stressed seasons, respectively, and a slope of 1.5 for annual pigweed and sunflower plants under controlled greenhouse conditions. Presumably when the plants are in drought stress, the stomatal resistance should be much higher than the aerodynamic resistance and as result the kinetic fractionation is dominated by molecular diffusion (Lee *et al*., 2009). The small slope for δD-δ^{18}O suggests that the kinetic fractionation of evaporation from isolated water bodies may be stronger than previously thought, although the large range of the slope parameter in Fig 6b prevents us from drawing a firm conclusion.

2.5.4. A closure problem

The application of the C-G model (Eq. 2.1) for predicting the isotopic composition of evaporation requires three parameters that are not directly observable. They are the temperature of the evaporating surface (T_S), the aerodynamic parameter n, and the isotopic composition of the water at the surface ($\delta_{L,e}$). However, there are only two mass conservation equations (Eq. 2.7), one for each of the two isotopic species (^{18}O and D). Mathematically, I have a closure problem because there are more unknowns than the number of equations to constrain them. To solve for T_S and n, Cappa *et al*. (2003) made the implicit assumption that $\delta_{L,e} = \delta_{L,b}$. The same closure or well-mixed assumption was tacitly adopted in this study. How this assumption affects the T_S and n estimates is not known. The estimates of the surface enrichment ($\delta_{L,e} - \delta_{L,b}$) seem robust because they are

not sensitive to the choice of n or the temperature at which the equilibrium fractionation was evaluated (Tables 2.2 and 2.3).

The molecular diffusivity ratios determined by Merlivat (1978a; 0.9727 for $^{18}O/^{16}O$ and 0.9757 for D/H) have been widely used because they were obtained from carefully conducted experiments (Horita *et al*., 2008). Cappa *et al* (2003) proposed the values of 0.9691 and 0.9839 for $^{18}O/^{16}O$ and D/H, respectively, based on a set of chamber evaporation experiments similar to this expeirment and with the surface cooling accounted for. Some of the differences between Cappa's and Merlivat's values may have been caused by the well-mixed assumption noted above. In a more recent study, Luz *et al*. (2009) stirred the water undergoing evaporation, creating a true well-mixed condition. By doing so they arrived at estimates of these diffusivity ratios in close agreement with Merlivat's values.

2.5.5. Uncertainty in the determination of evaporative enrichment

Three sources of uncertainty can affect the enrichment calculations in this study. First, the input variables on the right of Eq. 2.3 were influenced by measurement noises. Of these δ_E carried the largest uncertainties (1.4‰ for $^{18}O/^{16}O$ and 21.7‰ for D/H). The errors in $\delta_{L,e}$ caused by the δ_E uncertainties were reduced by half to 0.7‰ for $^{18}O/^{16}O$ and 11‰ for D/H because relative humidity h was about 0.5 (Table 2.1). The combined uncertainties in $\delta_{L,e}$ due to errors in h (0.02) and the vapor isotope ratios (0.1-0.2‰ for $^{18}O/^{16}O$ and 1‰ for D/H) were less than 0.2‰ for $^{18}O/^{16}O$ and 1‰ for D/H. The error propagation accounted for about 20% of the observed variability in surface enrichment

(Tables 2.2 and 2.3). The remaining variability in the observed enrichment values was associated with changes in experimental conditions.

The second source of uncertainty is related to nonlinearity errors. Unlike the first source of uncertainties which was random, these errors were systematic. The overall accuracy of the $\delta_{L,e}$ calculations were improved by the nonlinearity corrections because they were made to each experiment on the basis of mass balance principle. Without these corrections to δ_E, the ^{18}O and D surface enrichments would be reduced by an average of 0.8‰ and 19‰, respectively.

Third, uncertainties in the Craig-Gordon model parameters (water temperature and aerodynamic parameter n) can affect the enrichment calculations. The Cappa method was circular because the n and T_S values derived from the well-mixed assumption were used to estimate a nonzero surface enrichment which violated the assumption. Fortunately, calculations without this assumption yielded similar surface enrichment values (Table 2.3). If the Merlivat's diffusivity ratios were used in Eq. 2.3, the calculated $\delta_{L,e} - \delta_{L,b}$ would increase to 16.5‰ for D and decrease to 7.5‰ for ^{18}O, as compared to the estimates shown in Table 2.2. In this sensitivity analysis, the aerodynamic parameter n had taken the value of 0.67 and the equilibrium fractionation factor had been evaluated at the bulk water temperature T_W. The new ^{18}O enrichment value was still significantly different from zero (p <0.001). When the n value of 1 for pure molecular diffusion was used (Luz *et al*. 2009), the mean enrichment values became 13.0 and 20.0‰ for ^{18}O (p <0.001) and D (p < 0.05), respectively. Only by using an extremely low value of n of 0.25 did both enrichment values become insignificant (0.4‰ for ^{18}O, p > 0.5; 10.4‰, p > 0.2). Such a low n value may occur in highly turbulent conditions in the field (Horita *et*

al. 2008; Lee *et al*. 2009) but was extremely unlikely in the low flow, smooth wall situations of this experiment. Accordingly, the best estimates of the surface enrichment were in the range 7.5 – 8.9‰ for ^{18}O and 12.6 – 16.5‰ for D.

2.6 Conclusions

The results show, not surprisingly, that the isotope ratios of evaporation (δ_E) and the residual water ($\delta_{L,b}$) were progressively enriched with time during the evaporation experiments. The C-G model was unable to predict δ_E if $\delta_{L,b}$ was used in the model. This was because the heavier isotopes accumulated at the evaporating surface. Using the C-G model in the inverse mode, I found that the surface enrichment was 7.5 – 8.9‰ more enriched in ^{18}O and 12.6 – 16.5‰ in D than the bulk water. The enrichment was statistically different from zero for $^{18}O/^{16}O$ ($p < 0.001$) but not for D/H ($p = 0.14$). It is not known how accurately these estimates represent the fractionation process in the real world. The surface enrichment observed in the synthetic laboratory environment can be considered a research hypothesis worth testing in future field experiments.

The slopes of δD-$\delta^{18}O$ relations for the surface and the bulk water were close to the values reported for the leaf water of desert plants and water in dry soils. The small slope for δD-$\delta^{18}O$ suggests that the kinetic fractionation of evaporation from isolated water bodies may be stronger than previously thought, although the large uncertainties in the measurement of D/H of evaporation prevented us from drawing a firm conclusion.

The aerodynamic parameter (n) estimated with the Cappa method was in the range of 0.89 to 0.94 for the heated experiments, indicating that kinetic fractionation was

dominated by molecular diffusion. In the unheated experiments, the n values were less than that of the heated setup, falling in the range of 0.49 to 0.67, suggesting the existence of turbulent diffusion.

A closure or well-mixed assumption, that $\delta_{L,e} = \delta_{L,b}$ was made in the determination of n and the surface temperature. However, the estimates of $\delta_{L,e}$ were insensitive to this assumption, the choice of the molecular diffusivity ratios, or the consideration of surface cooling. The same well-mixed assumption was made by Cappa *et al* (2003) their determination of the $^{18}O/^{16}O$ and D/H molecular diffusivity ratios using an evaporation apparatus similar to ours.

Acknowledgments

This work was supported by the U. S. National Science Foundation through grants DEB-0514904 and ATM-0914473 and by a Yale University Fellowship (to Kyounghee Kim).

2.7 References

Allison, G.B., Barnes, C.J. and Hughes, M.W., 1983. The distribution of deuterium and 18O in dry soils 2. Experimental. Journal of Hydrology, 64(1-4): 377-397.

Allison, G.B., Gat, J.R. and Leaney, F.W.J., 1985. The relationship between deuterium and oxygen-18 delta values in leaf water. Chemical Geology, 58(1-2): 145-156.

Avallone, E.A. and Baumeister, T., III, 1996. Marks' Standard Handbook for Mechanical Engineers (10th Edition). McGraw-Hill.

Barbour, M.M. *et al*., 2007. A new measurement technique reveals temporal variation in delta O-18 of leaf-respired CO2. Plant Cell and Environment, 30(4): 456-468.

Barnard, R.L. *et al*., 2007. Evaporative enrichment and time lags between delta O-18 of leaf water and organic pools in a pine stand. Plant Cell and Environment, 30(5): 539-550.

Barnes, C.J. and Allison, G.B., 1983. The distribution of deuterium and O-18 in dry soils. 1. Theory. Journal of Hydrology, 60(1-4): 141-156.

Blanken, P.D. *et al*., 2000. Eddy covariance measurements of evaporation from Great Slave Lake, Northwest Territories, Canada. Water Resources Research, 36(4): 1069-1077.

Buhay, W.M., Edwards, T.W.D. and Aravena, R., 1996. Evaluating kinetic fractionation factors used for ecologic and paleoclimatic reconstructions from oxygen and hydrogen isotope ratios in plant water and cellulose. Geochimica Et Cosmochimica Acta, 60(12): 2209-2218.

Cappa, C.D., Hendricks, M.B., DePaolo, D.J. and Cohen, R.C., 2003. Isotopic fractionation of water during evaporation. Journal of Geophysical Research-Atmosphere, 108(D16): 4525, doi:10.1029/2003JD003597.

Cernusak, L.A., Pate, J.S. and Farquhar, G.D., 2002. Diurnal variation in the stable isotope composition of water and dry matter in fruiting Lupinus angustifolius under field conditions. Plant Cell and Environment, 25(7): 893-907.

Ciais, P., Tans, P.P., White, J.W.C., Troiler, M. and Grancey, R.J.1995. Partitioning of ocean and land uptake of CO2 as inferred by ä13C measurements from the NOAA climate monitoring and diagnostics laboratory global air sampling network. Journal of Geophysical Research-Atmospheres, 100(D3): 5051-5070.

Craig, H. and Gordon, L.I., 1965. Deuterium and oxygen 18 variations in the ocean and the marine atmosphere. In: E. Tongiorgi (Editor), Stable Isotopes in Oceanographic Studies and Paleotemperatures, Lischi & Figli, Pisa, Italy, pp. 9-130.

Craig, H., Gordon, L.I. and Horibe, Y., 1963. Isotopic exchange effects in the evaporation of water, 1.Low-temperature experimental results. Journal of Geophysical Research, 68(17): 5079-5087.

Csanady, G.T., 1963. Turbulent diffusion in Lake Huron. Journal of Fluid Mechanics, 17(3): 360-384.

Dawson, T.E. and Ehleringer, J.R., 1991. Streamside trees that do not use stream water. Nature, 350(6316): 335-337.

Dincer, T., Mugrin, A.A. and Zimmermann, U., 1974. Study of the infiltration and recharge through the sand dunes in arid zones with special reference to the stable isotopes and thermonuclear tritium. Journal of Hydrology, 23(1-2): 79-109.

Farquhar, G.D. and Cernusak, L.A., 2005. On the isotopic composition of leaf water in the non-steady state. Functional Plant Biology, 32(4): 293-303.

Farquhar, G.D., Hubick, K.T., Condon, A.G. and Richards, R.A., 1989. Carbon isotope discrimination and water-use efficiency. In: P.W. Rundel, J.R. Ehleringer and K.A. Nagy (Editors), Stable Isotopes in Ecological Research. Springer-Verlag, New York, pp. 21-46.

Farquhar, G.D. and Lloyd, J., 1993. Carbon and oxygen isotope effects in the exchange of carbon dioxide between terrestrial plants and the atmosphere, Stable isotopes and plant carbon–water relations. Academic Press, San Diego, pp. 47–70.

Farquhar, G.D., Lloyd, J., Taylor, J.A., Flanagan, L.B., Syvertsen, J.P., Hubick, K.T., Wong, S.C. and Ehleringer, J.R. 1993. Vegetation effects on the isotope composition of oxygen in atmospheric CO2. Nature, 363(6428): 439-443.

Flanagan, L.B., Comstock, J.P. and Ehleringer, J.R., 1991. Comparison of Modeled and Observed Environmental Influences on the Stable Oxygen and Hydrogen Isotope Composition of Leaf Water in Phaseolus vulgaris L. . Plant Physiology, 96(2): 588-596.

Flanagan, L.B. and Ehleringer, J.R., 1991. Effects of Mild Water Stress and Diurnal Changes in Temperature and Humidity on the Stable Oxygen and Hydrogen Isotopic Composition of Leaf Water in Cornus stolonifera L. Plant Physiology, 97(1): 298-305.

Gat, J.R., 1971. Comments on the stable isotope method in regional groundwater investigations. Water Resources Research, 7(4): 980-993.

Gat, J.R., 1996. Oxygen and hydrogen isotopes in the hydrologic cycle. Annual Review of Earth and Planetary Sciences, 24: 225-262.

Gat, J.R. and Bowser, C.J., 1991. Heavy isotope enrichment in coupled evaporative systems. In: J. Taylor, H.P., J.R. O'Neil and I.R. Kaplan (Editors), Stable Isotope Geochemistry: A Tribute to Samuel Epstein, Special publication No.3. The Geochemical Society, pp. 159-168.

Gat, J.R., Bowser, C.J. and Kendall, C., 1994. The contribution of evaporation from the Great-lakes to the continental atmosphere - estimate based on stable-isotope data. Geophysical Research Letters, 21(7): 557-560.

Gat, J.R. *et al*., 2003. Isotope composition of air moisture over the Mediterranean Sea: an index of the air-sea interaction pattern. Tellus Series B-Chemical and Physical Meteorology, 55(5): 953-965.

Gat, J.R., Yakir, D., Goodfriend, G., Fritz., P., Trimborn, P., Lipp, J., Gev, I., Adar, E. and Waisel, Y. 2007. Stable isotope composition of water in desert plants. Plant and Soil, 298(1-2): 31-45.

Gibson, J.J., 2002. Short-term evaporation and water budget comparisons in shallow Arctic lakes using non-steady isotope mass balance. Journal of Hydrology, 264(1-4): 242-261.

Gibson, J.J., Edwards, T.W.D. and Prowse, T.D., 1999. Pan-derived isotopic composition of atmospheric water vapour and its variability in northern Canada. Journal of Hydrology, 217(1-2): 55-74.

He, H. and Smith, R.B., 1999. An advective-diffusive isotopic evaporation-condensation model. Journal of Geophysical Research-Atmospheres, 104(D15): 18619-18630.

Hoffmann, G., Cuntz, M., Weber, C., Ciais, P., Friedlingstein, P., Heimann, M., Jouzel, J., Kaduk, J., Maier-Reimer, E., Seibt, U. and Six, K.D. 2004. A model of the Earth's Dole effect. Global Biogeochemical Cycles, 18(1) GB1008, doi:10.1029/2003GB002059.

Horita, J., Rozanski, K. and Cohen, S., 2008. Isotope effects in the evaporation of water: a status report of the Craig-Gordon model, International Workshop on the Isotope Effects in Evaportation. Taylor & Francis Ltd, Pisa, ITALY, pp. 23-49.

Kumar, B. and Nachiappan, R.P., 1999. On the sensitivity of Craig and Gordon model for the estimation of the isotopic composition of lake evaporates. Water Resources Research, 35(5): 1689-1691.

Lee, X., Griffis, T.J., Baker, J.M., Billmark, K.A., Kim, K., and Welp, L.R. 2009. Canopy-scale kinetic fractionation of atmospheric carbon dioxide and water vapor isotopes. Global Biogeochemical Cycles, 23: GB1002, doi:10.1029/2008GB003331.

Lee, X., Kim, K. and Smith, R., 2007. Temporal variations of the O-18/O-16 signal of the whole-canopy transpiration in a temperate forest. Global Biogeochemical Cycles, 21(3): GB3013, doi:10.1029/2006GB002871.

Lee, X., Sargent, S., Smith, R. and Tanner, B., 2005. In situ measurement of the water vapor O-18/O-16 isotope ratio for atmospheric and ecological applications. (vol 22, pg 555, 2005). Journal of Atmospheric and Oceanic Technology, 22(8): 1305-1305.

Lloyd, R.M., 1966. Oxygen isotope enrichment of sea water by evaporation. Geochimica Et Cosmochimica Acta, 30(8): 801-814.

Majoube, M., 1971. Oxygen-18 and deuterium fractionation between water and steam. Journal de Chimie Physique et de Physico-Chimie Biologique, 68(10): 1423-1436.

Mathieu, R. and Bariac, T., 1996. A numerical model for the simulation of stable isotope profiles in drying soils. Journal of Geophysical Research-Atmospheres, 101(D7): 12685-12696.

Merlivat, L., 1978. Molecular diffusivities of H2 16O, HD16O, and H2 18O in gases. Journal of Chemical Physics, 69(6): 2864-2871.

Monteith, J.L. and Unsworth, M.H., 1990. Principles of environmental physics. Chapman and Hall, New York.

NACE International, T.C.S., 2002. Corrosion Survey Database (COR•SUR). NACE International.

Ogee, J., Cuntz, M., Peylin, P. and Bariac, T., 2007. Non-steady-state, non-uniform transpiration rate and leaf anatomy effects on the progressive stable isotope enrichment of leaf water along monocot leaves. Plant Cell and Environment, 30(4): 367-387.

Pendall, E., Williams, D.G. and Leavitt, S.W., 2005. Comparison of measured and modeled variations in pinon pine leaf water isotopic enrichment across a summer moisture gradient. Oecologia, 145(4): 605-618.

Ripullone, F., Matsuo, N., Stuart-Willianms, H., Wong, S.C., Borghetti, M., Tani, M. and Farquhar, G. 2008. Environmental effects on oxygen isotope enrichment of leaf water in cotton leaves. Plant Physiology, 146(2): 729-736.

Roden, J.S. and Ehleringer, J.R., 1999. Observations of hydrogen and oxygen isotopes in leaf water confirm the Craig-Gordon model under wide-ranging environmental conditions. Plant Physiology, 120(4): 1165-1173.

Roden, J.S., Lin, G.G. and Ehleringer, J.R., 2000. A mechanistic model for interpretation of hydrogen and oxygen isotope ratios in tree-ring cellulose. Geochimica Et Cosmochimica Acta, 64(1): 21-35.

Rozanski, K. and Chmura, L., 2006. Isotope effects accompanying evaporation of water from leaky containers, International Workshop on the Isotope Effects in Evaportation, Pisa, ITALY, pp. 51-59.

Seibt, U., Wingate, L., Berry, J.A. and Lloyd, J., 2006. Non-steady state effects in diurnal O-18 discrimination by Picea sitchensis branches in the field. Plant Cell and Environment, 29(5): 928-939.

Stewart, M.K., 1975. Stable isotope fractionation due to evaporation and isotopic exchange of falling waterdrops: Applications to atmospheric processes and evaporation of lakes. Journal of Geophysical Research, 80(9): 1133-1146.

Sturm, P. and Knohl, A., 2009. Water vapor ä2H and ä18O measurements using off-axis integrated cavity output spectroscopy. Atmos. Meas. Tech. Discuss., 2(4): 2055-2085.

Tang, K.L. and Feng, X.H., 2001. The effect of soil hydrology on the oxygen and hydrogen isotopic compositions of plants' source water. Earth and Planetary Science Letters, 185(3-4): 355-367.

Terwilliger, V.J. and DeNiro, M.J., 1995. Hydrogen isotope fractionation in wood-producing avocado seedlings: Biological constraints to paleoclimatic interpretations of delta D values in tree ring cellulose. Geochimica Et Cosmochimica Acta, 59(24): 5199-5207.

Uemura, R., Barkan, E., Abe, O. and Luz, B., 2010. Triple isotope composition of oxygen in atmospheric water vapor. Geophysical Research Letters, Vol. 37, L04402, doi:10.1029/2009GL041960.

Uemura, R., Matsui, Y., Yoshimura, K., Motoyama, H. and Yoshida, N., 2008. Evidence of deuterium excess in water vapor as an indicator of ocean surface conditions. Journal of Geophysical Research-Atmospheres, 113. D19114, doi:10.1029/2008JD010209.

Wang, X.F., Yakir, D. and Avishai, M., 1998. Non-climatic variations in the oxygen isotopic compositions of plants. Global Change Biology, 4(8): 835-849.

Welp, L.R., Lee, X., Kim, K., Griffis, T.J., Billmark, K., Baker, J.M. 2008. d18O of water vapour, evapotranspiration and the sites of leaf water evaporation in a soybean canopy. Plant Cell and Environment, 31(9): 1214-1228.

Wen, X.F., SUn, X.M., Zhang, S.C., Yu, G.R., Sargent, S.D. and Lee, X., 2008. Continuous measurement of water vapor D/H and O-18/O-16 isotope ratios in the atmosphere. Journal of Hydrology, 349(3-4): 489-500.

Williams, D.G. *et al*., 2004. Evapotranspiration components determined by stable isotope, sap flow and eddy covariance techniques. Agricultural and Forest Meteorology, 125(3-4): 241-258.

Xiao, W. *et al*., 2010. A modeling investigation of canopy-air oxygen isotopic exchange of water vapor and carbon dioxide in a soybean field. Journal of Geophysical Research-Biogeosciences, 115. G01004, doi:10.1029/2009JG001163.

Yadav, D.N., 1997. Oxygen isotope study of evaporating brines in Sambhar Lake, Rajasthan (India). Chemical Geology, 138(1-2): 109-118.

Yakir, D., Berry, J.A., Giles, L. and Osmond, C.B., 1994. Isotopic heterogeneity of water in transpiring leaves: identification of the component that controls the ä18O of atmospheric O2 and CO2. Plant Cell and Environment, 17(1): 73-80.

Yi, Y., Brock, B.E., Falcone, M.D., Wolfe, B.B. and Edwards, T.W.D., 2008. A coupled isotope tracer method to characterize input water to lakes. Journal of Hydrology, 350(1-2): 1-13.

Zimmermann, U., Ehhalt, D. and Munnich, K.O., 1967. Soil-water movement and evapotranspiration; changes in the isotopic composition of the water, Proc. Symp. Isotopes in Hydrology. IAEA, Vienna, pp. 567-584.

Chapter 3. [2] Transition of stable isotope ratios of leaf water under simulated dew formation

[2] Under review by *Plant Cell and Environment*

Abstract

Dew formation, a common meteorological phenomenon, is expected to intensify in the future. Dew can influence the $H_2{}^{18}O$ and HDO isotopic compositions of leaf water (δ_L), but the phenomenon has been neglected in many experimental and modeling studies. In this study, the dew effect on δ_L was investigated with a dark plant chamber in which dew formation was introduced. The $H_2{}^{18}O$ and HDO compositions of water vapor, dew water and leaf water of five species (including C_3 and C_4) were measured for up to 48 h of dew exposure. This study shows that the exchanges of $H_2{}^{18}O$ and HDO in leaf water with the air continued in the darkness when the net $H_2{}^{16}O$ flux was zero. Our estimates of the leaf conductance using the isotopic mass balance method ranged from 0.035 to 0.087 mol $m^{-2}s^{-1}$, in broad agreement of the nighttime stomatal conductance reported in the literature. In this experiments, the conductance of the C_4 species was 0.04 ± 0.01 mol $m^{-2}s^{-1}$ and that of the C_3 plants was 0.10 ± 0.04 mol $m^{-2}s^{-1}$. At the end of 48 h dew exposure, 89 (±0.04) and 100 (±0.05) % of the leaf water came from dew according to the ^{18}O and D tracer, respectively.

3.1 Introduction

Dew formation is a common meteorological phenomenon in tropical and temperate climatic zones. Dew water can be an important hydrological input in some ecosystems. In a mid-latitude grassland ecosystem in the Netherlands, the amount of dew formation is about 4.5% of the mean annual precipitation and the frequency of dew nights is 70% (Jacobs *et al*., 2006). The frequency of dew occurrence is 84% over a growing season in an agricultural field in the Midwest of US (Welp *et al*., 2008). The long duration of dew presence, up to 14.5 h at the leaf surface of montane and subalpine plants in the central Rocky Mountains (Brewer and Smith, 1997) and up to 22 h in the lower shaded canopy in tropical montane forests of Indonesia (Dietz *et al*., 2007), have been reported. In arid and semiarid regions, the role of dew formation in the regional water budget becomes more significant than in humid climatic regions. Dew relieves water stress by restoring 72% of leaf water at night in Mediterranean evergreen shrubs under constant water stress (Munne-Bosch *et al*., 1999). Water input by nighttime dew formation is equivalent to 11% of the annual precipitation in the desert valleys of the western US (Malek *et al*., 1999).

Dew formation also has important implications for studies of gas exchanges between the atmosphere and terrestrial ecosystems. The formation of dew is the result of radiation energy exchange between the cold plant surface and the atmosphere (Pitacco *et al*., 1992). Considering the dew flux in the energy balance budget provides a critical improvement to eddy covariance measurements which tend to overestimate evaporation component measurements made in the early morning hours (Sauer *et al*., 2007). Dew formation is highly effective in coating the leaf surface with liquid water (Burkhardt and Eiden, 1994).

The blockage of the stomata openings can alter the efficiency of diffusion of gases. The initiation of transpiration can be delayed in the early morning immediately after heavy dewfall (Pitacco *et al*., 1992). In the presence of dew water, the photosynthetic CO_2 uptake is decreased (Brewer and Smith, 1997) due to 10,000 times slower CO_2 diffusion in water than in air (Weast, 1977), except in cases of water-stressed plants where direct dew absorption can possibly improve photosynthesis (Munne-Bosch and Alegre, 1999). From the experimental perspective, in the presence of dew water, it is nearly impossible to directly measure the leaf gas exchange of water vapor (Feild *et al*., 1998).

Dew formation can alter the $H_2{}^{18}O$ and HDO isotopic compositions of leaf water. In a study conducted in a soybean field, Welp *et al*. (2008) found that in the early morning the $^{18}O/^{16}O$ isotope ratio of leaf water in the upper canopy, which was covered with dew water, is in approximate equilibrium with water vapor, while the leaf water in the lower canopy, which remained dew-free, is more positive than the isotopic equilibrium value. Their results suggest that the leaf stomata are not fully closed at night and may continue to exchange the minor isotopologues with the atmosphere even though there is no net water flux of the major isotope species. This process can be explained only by gaseous diffusion, not by dew water penetration through the stomatal openings, because of the strong capillary force created by the stomatal geometry as well as the surface tension of liquid water (Schonher and Bukovac, 1972). There is growing evidence that plant stomata remain partially open at night (Barbour and Buckley, 2007; Caird *et al*., 2007b; Easlon and Richards, 2009; Ludwig *et al*., 2006; Snyder *et al*., 2003). A question of interest to us is whether plants can take up a significant amount of atmospheric vapor via the stomatal pathway in high humidity conditions.

The occurrence of dew also impacts the leaf-air exchanges of the ^{18}O-CO_2 isotope. The oxygen isotope in CO_2 is exchanged with the ^{18}O-H_2O of leaf water by the enzyme reaction of carbonic anhydrase in leaves (Francey and Tans, 1987). The dew alternation of ^{18}O-H_2O in leaf water, in turn, affects the ^{18}O-CO_2, which diffuses through open stomata back to the atmosphere without being assimilated (Cernusak *et al*., 2002; Farquhar and Lloyd, 1993; Farquhar *et al*., 1993). The retro-diffusion of ^{18}O-CO_2 is often assumed to be a half to two-thirds of CO_2 originally diffused into the leaf intercellular spaces (Ciais *et al*., 1997; Francey and Tans, 1987), however, possible underestimation of the retro-diffusion has been discussed (Cernusak *et al*., 2004; Seibt *et al*., 2007). There may be time delayed effects in the morning hours, influencing the ^{18}O-CO_2 that diffuses out of the stomata during photosynthesis. The dew alternation should be taken into account in predictions of global mean leaf water isotope ratios, which vary in a wide range of 0.4 to 6.5‰ (Ciais *et al*., 1997; Farquhar *et al*., 1993; West *et al*., 2008).

In this study, I performed laboratory dew simulation experiments in order to examine the isotopic exchanges of leaf water with the vapor in the surrounding saturated air. I made continuous measurements of vapor isotope ratios in a dark plant chamber where saturation was maintained for up to 48 h by feeding with a vapor stream of known isotope ratios. In these experiment, the plants source water (or xylem water, δ_X) was isotopically much more enriched than the vapor feed, creating two unambiguous end members. This is in contrast to field conditions where the two end members are often isotopically indistinguishable (Welp *et al*., 2008; Wen *et al*., 2011 manuscript in review). The artificially long dew exposure permitted the determination of the transient and steady-state behaviors of δ_L.

This study examines three hypotheses: (1) dew coating on the leaf surface enhances the leaf-air isotopic exchange of water; (2) the exchange of the minor isotopologues between the leaf and the surrounding air persists under the condition of no net flux of the major species; (3) C_4 species are less likely to exchange water isotopologues in the leaf with the vapor even at very high humidity.

3.2 Materials and Methods

3.2.1. Dew simulation experiment

An opaque polyethylene container (diameter: 0.5 m; height: 0.7 m; volume: 121 L) was used as the plant chamber. The chamber top was closed with a lid that did not form an airtight seal so air could continuously flow out of the chamber (Figure 3.1). In this setup, the air pressure inside the chamber was identical to the ambient atmospheric pressure. A layer of foam insulation outside the chamber stabilized the temperature inside, minimizing temperature fluctuations to less than 1ºC during each dew experiment. Two fans were installed inside the chamber to promote mixing.

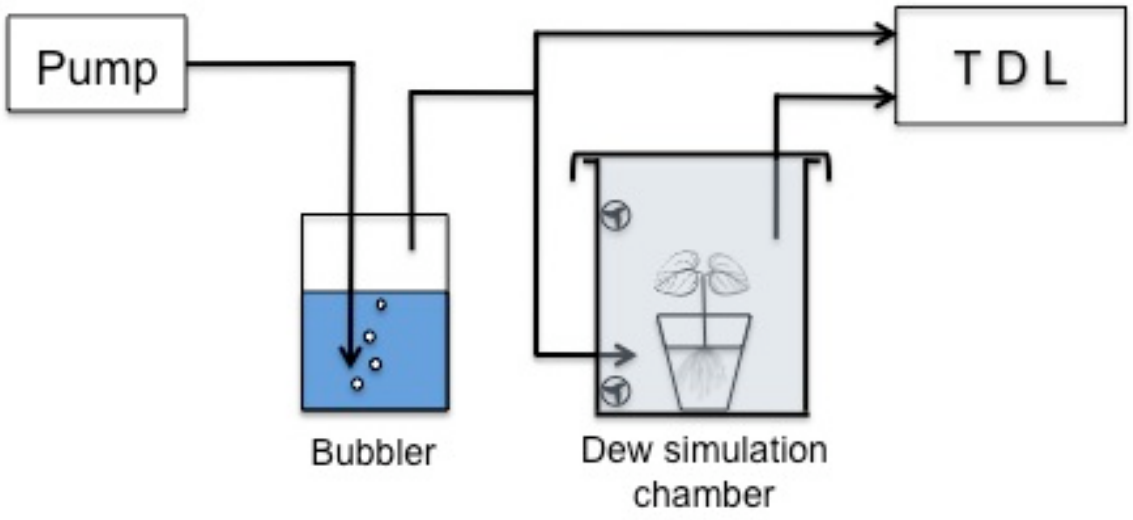

Figure 3.1. Schematic diagram of the dew simulation setup consisting of a bubbler, dew simulation/plant chamber, and a tunable diode laser analyzer (TDL) for measuring water vapor isotopes. Arrows indicate the direction of airflow.

The chamber was fed with water vapor generated by a bubbler filled with water of known isotope ratios at an airflow rate of 3.5 L min^{-1}. As room air entered the bubbler reservoir, bubbles rose from an aquarium air stone at the end of air inlet near the bottom of the reservoir and produced a moist air stream. Because the moist air stream was saturated with respect to the reservoir temperature, its isotopic compositions could be predicted from the equilibrium fractionation factors, the reservoir temperature and its isotopic compositions (Majoube, 1971). In the first dew experiment (Wheat 1), the predicted values were -21.4 and -156.4‰ for $^{18}O/^{16}O$ and D/H respectively. The vapor was gradually enriched as the experiments continued so that the predicted values in the last experiment (Sorghum 3) were -14.7 and -108.6‰ for $^{18}O/^{16}O$ and D/H, respectively. The bubbler vapor stream was split into two, 3.25 L min^{-1} being sent to the plant chamber and a small portion (0.25 L min^{-1}) to a tunable diode laser (TDL) analyzer (TGA 100, Campbell Scientific, Inc., Logan, UT, USA; Lee *et al*., 2005). The bubbler temperature was always set higher than the chamber temperature, ensuring dew formation inside the chamber. The vapor delivery tubing (Dekabon Type 1300, ¼ in OD $\times$ 0.040 in wall, Dekoron, Aurora, Ohio, USA) was heated in order to prevent condensation inside.

The TDL analyzer monitored, in real-time, the isotopic compositions of the bubbler vapor (chamber inlet; δ_B) and the vapor inside the chamber (chamber outlet; δ_V). The air from the two intakes was mixed with dry air before entering the TDL sample cell to minimize instrument nonlinearity (Lee *et al*., 2005). Because of this dilution, the mixing ratio measured with the TDL does not represent the true mixing ratio of the inlet and outlet air; instead, these mixing ratios were determined from the saturation vapor pressure at the chamber and bubbler temperatures.

The temperature and humidity of the chamber air were monitored by a thermocouple and a humidity probe (HMP45C-L, Vaisala Inc., Woburn, MA) installed inside the chamber. Five plant species were chosen for consideration of morphological and physiological traits. Of these plants, three were monocots with parallel venation (corn, *Zea mays*; sorghum, *Sorghum bicolor* (L.) Moench; and wheat, *Triticum durum*) and two were dicots with netted venation (soybean, *Glycine max;* cotton, *Gossypium hirsutum*). They also presented two types of photosynthetic system: C_3 (soybean, cotton and wheat) and C_4 (corn and sorghum) system. The plants were grown hydroponically in a greenhouse prior to the dew experiments.

Twenty-four hours prior to each experiment, the hydroponic solution of the experimental plants was replaced by solution made of enriched water (0.4 to 6.0‰ for $^{18}O/^{16}O$ and -24.3 to 6.6‰ for D/H). This way, the plant xylem would have been fully flushed with the water of known isotope ratios by the time the experiment started. The experimental plants were exposed to full sunlight in the ambient environment for 3 h to produce enriched leaf water. After that, they were moved to the plant chamber which had been fed with the bubbler moisture for 48 h. The plant root system with the hydroponic solution was carefully sealed to avoid contamination of the chamber air from the evaporation of the solution. The isotopic ratio of the solution was measured at the beginning and the end of the experiment.

A total of ten sets of complete dew simulation experiments were performed. Each experiment lasted 48 h and was repeated twice on every plant species. Such long dew exposure does not occur in field conditions but it permitted more precise determination of the transient and steady-state behaviors of δ_L than shorter exposures.

Sampling of various water pools was conducted as the experiment progressed. Collection of leaf samples took place immediately before the plants were placed inside the chamber, and every 4 to 12 h afterwards until the end of the 48 h experimental period. Dew was first removed prior to leaf sampling using clean paper towels. Except for wheat, the main vein was removed before the leaf sample was archived for analysis because the vein contained unfractionated xylem water. The dew water was collected at the end of the experiment. Because of leaf sample collection, the leaf area inside the chamber was reduced gradually over time over the dew simulation; this change was accounted for in the isotopic mass balance calculations (Eq. 3.8).

The leaf water was extracted using the cryogenic vacuum extraction method. The water isotopic analyses were carried out on a Thermo Finnigan DeltaPlus XP with Gas Bench and Thermo Finnigan MAT 253 with H-device in Yale University.

3.2.2. Preliminary experiments

Prior to the dew simulation experiments described above, a pilot study was conducted with soybean and corn. During the pilot study, no measurement of δ_V was available. Two of the experiments were conducted in saturated conditions and another two under subsaturation (mean relative humidity inside the chamber = 89%). These experiments lasted 48 h. The goals of the pilot study were to test the experimental apparatus and logistics and to compare the leaf water turnover in saturated and unsaturated conditions.

3.2.3. Isotopic mass balance

The method I used to estimate stomatal conductance (g_S) was based on isotopic mass balance principles. First, I computed the net water flux of the chamber for the major and minor isotopologues. Then I estimated the stomatal conductance of the plants inside the chamber. The complication introduced to the system of equations by dew formation inside the chamber was constrained by the measurement of dew water isotopic compositions and by the well-established relations of equilibrium fractionation.

The net water vapor flux of the plant chamber (F, mol $m^{-2}s^{-1}$) consists of dew flux (F_d) and leaf flux (F_L) as

$$F = F_d + F_L \tag{3.1}$$

The molar ratio of the minor to major isotope species of the flux can be expressed as

$$R_F = \frac{F^i}{F} = \frac{F_d^i + F_L^i}{F_d + F_L} \tag{3.2}$$

where superscript i denotes the minor isotope species (^{18}O or D). At saturation and because the leaf and air temperature were identical, the leaf flux F_L would vanish as there was no gradient in the $H_2{}^{16}O$ vapor pressure between the sub-stomatal cavity and the chamber air. However, F^i_L was not zero because of the non-zero vapor pressure gradient of the minor isotopologue. Eq. 3.2 can be simplified as

$$R_F = \frac{F_d^i + F_L^i}{F_d} \tag{3.3}$$

and can be converted into the delta notation, as

$$\delta_F = \delta_d + (F_L^i / F_d) \times R_{std}^{-1} \times 10^3 \tag{3.4}$$

where δ_F and δ_d denote isotopic composition of chamber flux and dew condensation inside the chamber in per mil, respectively, and R_{std} is the standard VSMOW $^{18}O/^{16}O$ or D/H molar ratio.

Eq. 3.4 was used to determine F^i_L from the measurement of all the other terms. The term δ_F on the left side of Eq. 3.4 was determined from the vapor isotopic composition δ_V (outlet) and δ_B (inlet) and saturation vapor pressure of the outlet and inlet airstreams at the chamber and the bubbler temperature, $e_S(T_a)$ and $e_S(T_B)$, as

$$\delta_F = \frac{e_S(T_B)\ \delta_V - e_S(T_a)\ \delta_B}{e_S(T_B) - e_S(T_a)} \tag{3.5}$$

This equation is equivalent to the intercept of the linear relation between the vapor delta and the reciprocal of the saturation vapor pressure. The term δ_d on the right side of Eq. 3.4 was given by

$$\delta_d = \delta_V + \varepsilon_{eq}(T_a) \tag{3.6}$$

$$\varepsilon_{eq} = \left(1 - \alpha_{eq}^{-1}\right) \times 10^3 \left(‰\right) \tag{3.7}$$

where α_{eq} (>1) is the temperature-dependent equilibrium fractionation factor (Majoube, 1971) and ε_{eq} denotes the equilibrium fractionation factor in per mil. The equilibrium prediction of δ_d was used instead of the δ_d measured at the end of the experiment from the collected dew water because δ_d was variable during the 48 h experiment. The dew flux, F_d, the rate of dew formation inside the chamber, was computed from difference in the saturation vapor density (ρ_S) at the chamber (T_a) and the bubbler temperature (T_B) as

$$F_d = Q\ \frac{\rho_S(T_a) - \rho_S(T_B)}{S} \tag{3.8}$$

where S is leaf area (m^2) and Q is flow rate ($m^3\ s^{-1}$).

I note that $F_L^{\,i}$ (mol $m^{-2}s^{-1}$), the leaf flux of the minor isotopes, is related to the stomatal conductance as

$$g_S = \frac{F_L^i}{e_S^i(T_a) - e_a^i} \times p_a \tag{3.9}$$

where $e_a^{\,i}$, is the vapor pressure of the minor isotope inside the chamber and P_a is atmospheric pressure (101.3 kPa). Here $e_a^{\,i}$ was obtained from the TDL measurement of δ_V and the chamber air temperature,

$$e_a^i = e_S(T_a)\ R_{std} \left(\frac{\delta_V}{10^3} + 1 \right) \tag{3.10}$$

and $e_S^{\,i}$, the saturation vapor pressure of the minor isotope species at leaf temperature (T_a), is given by

$$e_S^i = \frac{e_S}{\alpha_{eq}} R_L \tag{3.11}$$

where R_L is the molar ratio of the minor to the major isotope in the leaf water.

The estimate of g_S using Eq. 3.9 includes both stomatal and cuticular conductance, the latter is usually less than 0.02 mol $m^{-2}s^{-1}$ (Caird *et al*., 2007a). I also note that the g_S value is for the minor isotopologue, which is slightly (3%) lower than the value for the major isotopologue.

3.2.4. Response of leaf water isotope ratio to step change

The stomatal conductance estimate was used to quantify the time evolution of the leaf water isotope ratio (δ_L) under dew influence. The transient response of δ_L to the step change in the external forcing, which occurred when the plants were moved from the ambient condition to the plant chamber, is controlled by the turnover time of leaf water (τ). The isotopic composition of leaf water at a given time step is the mixture of unfractionated xylem water (δ_X) and the existing leaf water at the previous time step. Dongmann *et al*. (1974) suggested that the response follows the time course of change as

$$\delta_L = (\delta_{L,0} - \delta_{L,SS})\exp\left(\frac{-\Delta t}{\tau}\right) + \delta_{L,SS} \tag{3.12}$$

where Δt is the time elapsed since the step change, subscripts 0 and *SS* denote the time of step change (t = 0) and steady state, respectively. In using Eq. 3.12 to predict δ_L, I assumed that the leaf water isotope ratios at the new steady-state ($\delta_{L,ss}$) was equal to the isotopic composition of dew water (δ_d) given by Eq. 3.6. The τ value was determined from

$$\tau = \frac{W}{g_S \omega_i} \tag{3.13}$$

where W represents leaf water content (mol m^{-2}) and ω_i is the mole fraction of water vapor in the intercellular space (Farquhar and Cernusak, 2005).

3.3 Results

Table 3.1 summarizes the results of the pilot study conducted on soybean and corn in the sub-saturation and saturation conditions. The isotopic composition of the initial leaf water ($\delta_{L,0}$) was highly enriched over the xylem water immediately after the full sunlight treatment (t = 0), decreased steadily in the plant chamber until a new steady state was reached. For the saturation experiments, the leaf water isotopic composition at steady state ($\delta_{L,SS}$) was closer to the isotopic composition of dew water (δ_d) than to the xylem delta (δ_X). Here the dew value was estimated from the equilibrium theory assuming that the vapor in the chamber was in equilibrium with the liquid reservoir of the bubbler at the bubbler temperature and that the dew water was in equilibrium with the water vapor at the chamber temperature. The relative role of the dew water can be quantified as a fractional contribution

$$f = \left(\delta_L - \delta_X\right)/\left(\delta_d - \delta_X\right) \tag{3.14}$$

This end member fraction f is defined such that f = 1 indicates that all the leaf water originates from dew and f = 0 from the xylem water. The f value at steady-state was 0.75 (soybean) and 0.81 (corn) according to the ^{18}O tracer and 0.89 (soybean) and 0.94 (corn) according to the D tracer.

For the sub-saturation experiments, the steady state value $\delta_{L,SS}$ was 6.5‰ more enriched in ^{18}O and 37.7‰ in D than that obtained in the saturation experiments.

Table 3.1. Summary of variables in the pilot study. Here $\delta_{L,0}$ and $\delta_{L,48}$ are the measured leaf water isotope ratios at t = 0 and t = 48 h, respectively. The steady state leaf water isotopic composition $\delta_{L,SS}$ was obtained by fitting Eq. 3.12 to the observed δ_L using a nonlinear least squares method. The end member fraction (f) at steady-state was computed with Eq. 3.14. δ_X is the xylem water isotopic composition and δ_d is the isotopic composition of the dew water estimated using the equilibrium theory for the liquid bubbler reservoir (δ_B).

	$\delta_{L,0}$ (‰)	$\delta_{L,48}$ (‰)	δ_X (‰)	δ_d (‰)	$\delta_{L,SS}$ (‰)	f
$^{18}O/^{16}O$						
Saturation						
Soybean	21.0	-7.2	2.6	-9.8	-7.3	0.75
Corn	24.9	-6.8	9.2	-10.4	-7.0	0.81
Sub-saturation						
Soybean	10.2	-1.5	1.7	n/a	-1.5	n/a
Corn	19.6	0.2	3.0	n/a	0.1	n/a
D/H						
Saturation						
Soybean	13.9	-64.8	-19.8	-69.6	-65.0	0.90
Corn	39.6	-66.4	15.1	-72.3	-67.6	0.93
Sub-saturation						
Soybean	0.4	-32.1	-16.7	n/a	-32.1	n/a
Corn	19.9	-24.7	-13.2	n/a	-25.2	n/a

Figure 3.2 shows the transition of δ_L to the newer steady-state during the pilot experiments. For convenience of comparison, δ_L was normalized as

$$\hat{\delta}_L = \left(\delta_L - \delta_{L,48}\right) / \left(\delta_{L,0} - \delta_{L,48}\right) \tag{3.15}$$

and the normalized δ_L values of the two isotopologues were averaged in Figure 3.2. Soybean showed faster transition to the steady state than corn in both saturation and subsaturation conditions. For example, under saturation, the soybean δ_L reached 80% of the full step change at 8 h, and at the same time, the corn δ_L approached about 60% of the full step change.

Figure 3.3 compares the predicted and the measured dew water isotopic composition for the ten dew simulation experiments. This comparison serves as a check of the system consistency. The δ_d prediction was made using Eq. 3.6 with the chamber temperature and the vapor isotopic composition inside the chamber measured over the last 2 h of each experiment. The predictions of the dew water isotope ratios are in excellent agreement with the measured values, with an average error of 0.29 and 3.0‰ for ^{18}O and D, respectively. The good agreement indicates that the TDL measurement was unbiased relative to the mass spectrometry results.

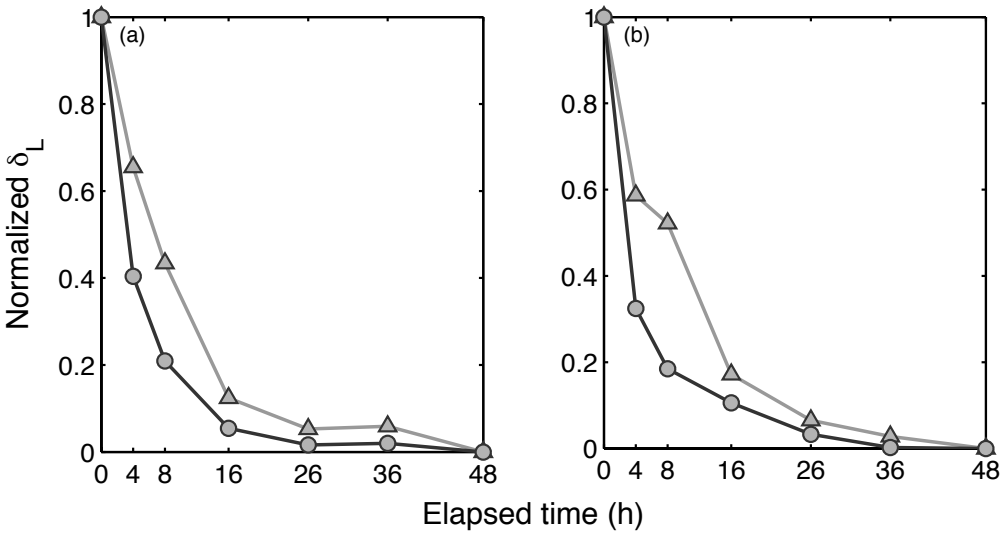

Figure 3.2. Normalized δ_L as a funciton of elasped time during the pilot study for corn (triangles) and soybean (circles): (a) left panel, saturation; (b) right panel, subsaturation. The normalized δ_L values were the averages of the two isotopologues.

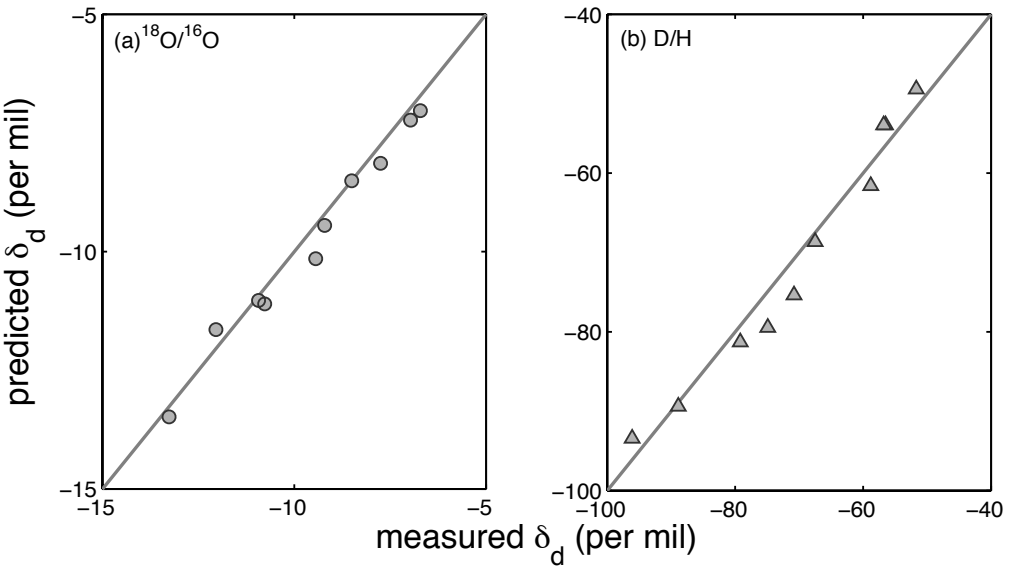

Figure 3.3. Comparison of the measured dew water isotopic composition and the equilbrium prediction according to Eq. 3.6. The solid lines represent a 1:1 relationship.

Figure 3.4 shows one example of the predicted δ_d and delta values of the measured water pools in one dew simulation experiment with corn. Table 3.2 lists the measurements of the water pools from all the 10 experiments reported as the average of two replicates for each species. The δ_d prediction (dashed line) was made using Eq. 3.6 with the δ_V measurement in reference to the chamber temperature. The predicted δ_d changed during the experiment in response to the changes in δ_V and approached the δ_d of the actual dew water collected at the end of the experiment (squares). This trend is seen in both $^{18}O/^{16}O$ and D/H. As in the pilot study, δ_L was highly enriched at $t = 0$ due to the full sunlight treatment, and slowly approached the new steady state. The observed δ_L did not return to isotopic composition of the plant source water at the new steady-state. The plant source water changed very little over time (Table 3.2), indicating a negligible loss of the reservoir water by evaporation. Also the bubbler maintained a supply of vapor stream with relatively constant isotope ratios.

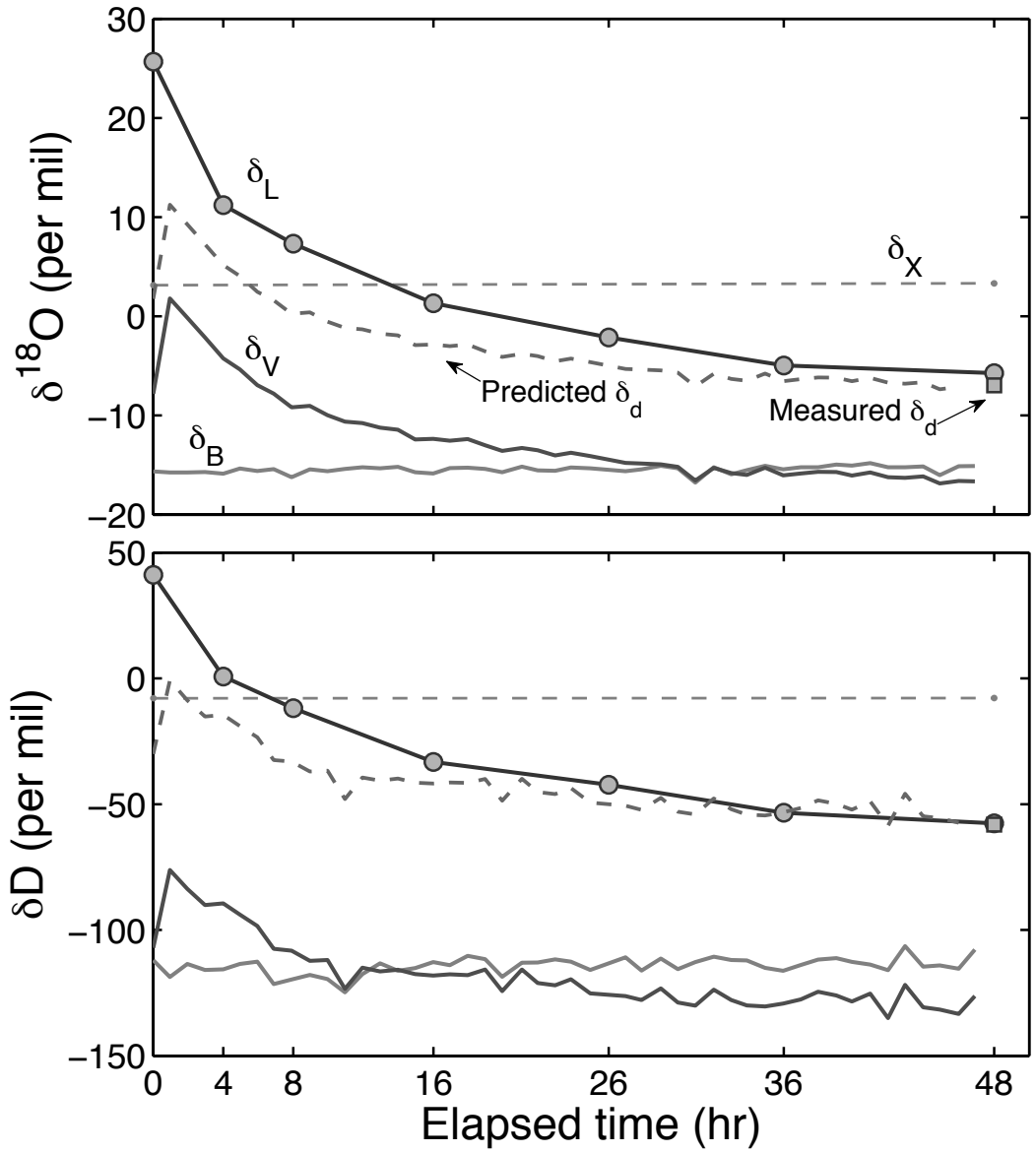

Figure 3.4. Time variations of the isotopic compositions of various water pools during a dew simulation experiment on a corn plant. The isotopic measurements of leaf water (δ_L, circles), dew water (δ_d, squares) and xylem water (δ_X, dots connected by dashed lines) were made with mass spectrometry. The measurements of the vapor in the chamber (δ_V) and the vapor generated by the bubbler (δ_B) were made with the TDL analyzer. The predicted dew delta value (δ_d, dashed) was obtained with the equilbrium relationship (Eq. 3.6).

Table 3.2. Isotopic compositions of leaf water (δ_L), plant source water (δ_X) and dew water collected at the end of the experiments (δ_d). The values are reported as the average of two replicates for each species.

	δ_L (‰)							δ_X (‰)		δ_d (‰)
Elapsed time (h)	0	4	8	16	26	38	48	0	48	48
$^{18}O/^{16}O$										
Corn	20.7	6.8	5.0	-1.6	-4.6	-6.7	-7.6	1.8	2.0	-8.9
Sorghum	17.5	6.5	1.0	-1.8	-4.0	-4.7	-5.6	5.4	5.4	-7.3
Wheat	14.1	2.1	-2.3	-5.2	-7.7	-8.6	-9.0	3.2	3.3	-10.9
Soybean	20.7	3.2	-1.9	-5.7	-7.6	-8.4	-8.6	2.4	2.5	-10.1
Cotton	18.4	2.4	-2.5	-6.6	-8.3	-9.2	-9.9	3.4	3.4	-10.7
D/H										
Corn	29.9	-15.3	-22.4	-45.9	-56.6	-67.2	-71.6	-16.1	-16.1	-71.5
Sorghum	25.3	-5.2	-27.4	-39.8	-48.0	-50.8	-53.5	4.6	4.1	-58.2
Wheat	13.7	-30.4	-49.0	-61.6	-72.5	-77.0	-80.1	-11.5	-10.7	-81.1
Soybean	26.0	-31.6	-49.5	-63.6	-72.8	-74.7	-78.5	-20.8	-20.9	-76.7
Cotton	18.5	-34.1	-51.4	-67.7	-78.0	-82.6	-87.2	-10.5	-10.0	-83.5

The chamber vapor delta was variable, but in a predicable way, over time. The δ_V spiked shortly after the experiment began and decreased continuously to a new steady-state. Neither the bubbler nor the chamber temperature changes could have caused the initial increase of δ_V. The bubbler temperature fluctuated within ±0.2ºC, which would produce a negligible change of 0.03 and 0.3‰ in the ^{18}O and D compositions, respectively, of the vapor entering the chamber. The chamber temperature immediately after the plants had entered showed an increase of 0.78 ± 0.28ºC and then stabilized from 3.3 h onwards. This initial increase was mainly caused by the heat released by the warm plants and the hydroponic solution brought in from the sunlight treatment. These temperature fluctuations produced a change of 0.06 and 0.75‰ in the isotopic equilibrium values for ^{18}O and D, respectively, not enough to explain the observed changes in δ_V. Instead, the change implies continued ^{18}O and D fluxes out of the leaves even under full saturation and the leaves being coated by dew water. This is because positive vapor pressure gradients of the minor isotopologues were maintained, by the highly enriched leaf water, between the substomatal cavity and the chamber air (e_S^i - e_a^i > 0 in Eq. 3.9). It is interesting to note that the trend of δ_V was almost identical to that of δ_L. In all the dew experiments, the flux of the minor isotopologues elevated the δ_V above the isotopic composition of the vapor entering the chamber (δ_B) for about 3 h after the onset of the experiment. Only towards the end of the experiments did δ_V become lower than δ_B. The results indicate that the leaves maintained partially open stomata in the presence of dew coating on their surface.

Figure 3.5 compares $\delta_{L,SS}$ to the dew water and xylem water isotope ratios, each data point representing one dew simulation experiment. Here $\delta_{L,SS}$ was determined by the

regression fit of Eq. 3.12 to the observed δ_L. In the δ_d - $\delta_{L,SS}$ plane (top x-axis and left y-axis, circles), $\delta_{L,SS}$ shows a strong linear relationship with δ_d that is parallel to the 1:1 line, indicating that δ_d played a significant role in determining $\delta_{L,SS}$ regardless of species or vein morphology. On the other hand, $\delta_{L,SS}$ shows much weaker correlation with δ_X (bottom x-axis and right y-axis, squares), indicating that the contribution of δ_X to $\delta_{L,SS}$ was minor.

Table 3.3 summarizes the results on the end member fraction f (Eq. 3.14) at 16 h of dew exposure using measured δ_L at t = 16 and sampled δ_d at t = 48. The τ values in Table 3.3 are the means of the first 16 h measurements according to Eq. 3.13. The isotopic turnover time varied with the isotopologue and the photosynthetic mode. In general, the C_3 plants and the D isotope showed more rapid changes than the C_4 plants and the ^{18}O isotope. For the C_3 plants, the mean values of the turnover time for the first 16 h were 1.5 and 1.0 h for ^{18}O and D, respectively. For the C_4 plants, these values were 3.0 and 2.4 h for ^{18}O and D, respectively. The mean τ values were significantly different between the C_3 the C_4 plants ($p < 0.001$). Because this experiments were conducted with a limited sample size, further investigation would be needed to answer the question as to whether this difference holds for other species.

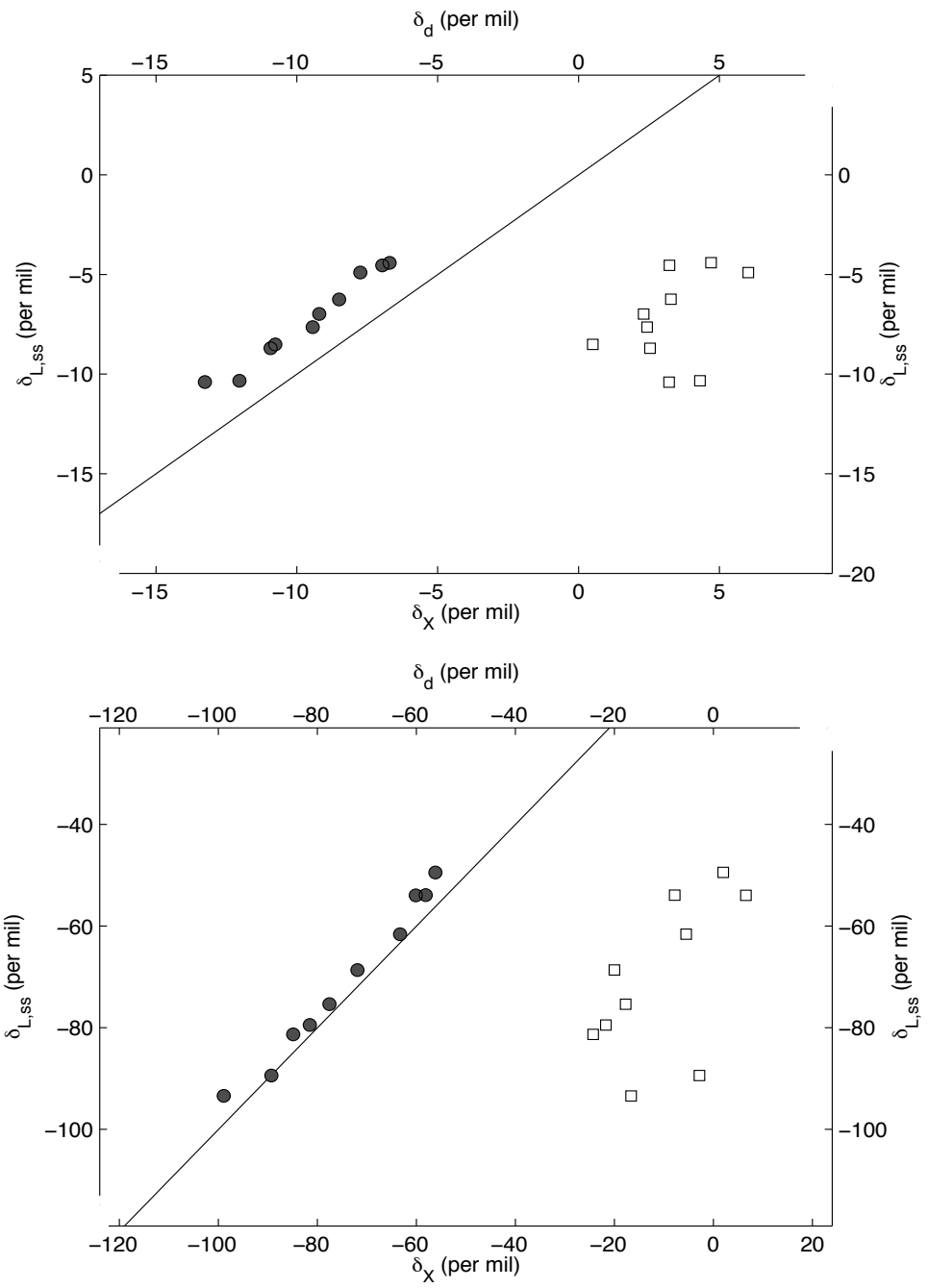

Figure 3.5. Comparisons of isotopic compositions of leaf water at steady state ($\delta_{L,SS}$, left y-axis) against that of the dew water collected at the end of each experiment (δ_d, closed circles; top x-axis) and $\delta_{L,SS}$ (right y-axis) against that of the xylem water (δ_X, bottom x-axis; open squares). The top panel is for $^{18}O/^{16}O$ and bottom for D/H. The solid lines represent a 1:1 relationship.

Table 3.3 indicates that the stomatal pathway played a large role in the temporal dynamics of δ_L in high humidity conditions at night. The average *f* value at 16 h indicates that the dew contribution to the leaf water was 56% (±17%) and 69% (±11%) according to the ^{18}O and D tracer, respectively. Some dependence on plant species and photosynthetic mode was suggested by the data in Table 3.3. For the C_3 plants, the *f* value ranged from 0.48 to 0.83 and from 0.62 to 0.86 according to the ^{18}O and D tracer, respectively. For the C_4 plants, the *f* values were smaller, ranging from 0.19 to 0.58 and 0.50 to 0.73 according to ^{18}O and D, respectively.

The 16 h dew duration represents the average value reported (Brewer and Smith, 1997; Dietz *et al*., 2007). In Figure 3.6, the fractional contributions are shown as functions of exposure time. The leaf water had reached a new steady state by 48 h, at which time the fractional contribution of dew water (*f*) was 0.89 ± 0.05 and 0.87 ± 0.01 according to the ^{18}O tracer and 1.02 ± 0.04 and 0.96 ± 0.05 according to the D tracer, for the C_3 and C_4 species, respectively. The mean *f* value of all the species was 0.89 ± 0.04 according to the ^{18}O tracer and 1.00 ± 0.05 according to the D tracer. Such long (48 h) dew events are not possible in field conditions. Nevertheless, the high *f* value points to the important role that the stomatal pathway played in the temporal dynamics of δ_L in the darkness and high humidity conditions.

Table 3.3. The end member fraction (f) at t = 16 and the leaf water turnover time (τ) using the ^{18}O and D tracers. Note that if f = 1, all the leaf water originates from the dew water.

	$^{18}O/^{16}O$		D/H	
	τ (h)	f	τ (h)	f
Corn	2.7	0.31	2.3	0.54
Sorghum	3.2	0.57	2.5	0.70
Wheat	1.2	0.58	0.9	0.71
Soybean	1.8	0.65	1.1	0.76
Cotton	1.4	0.69	1.0	0.77

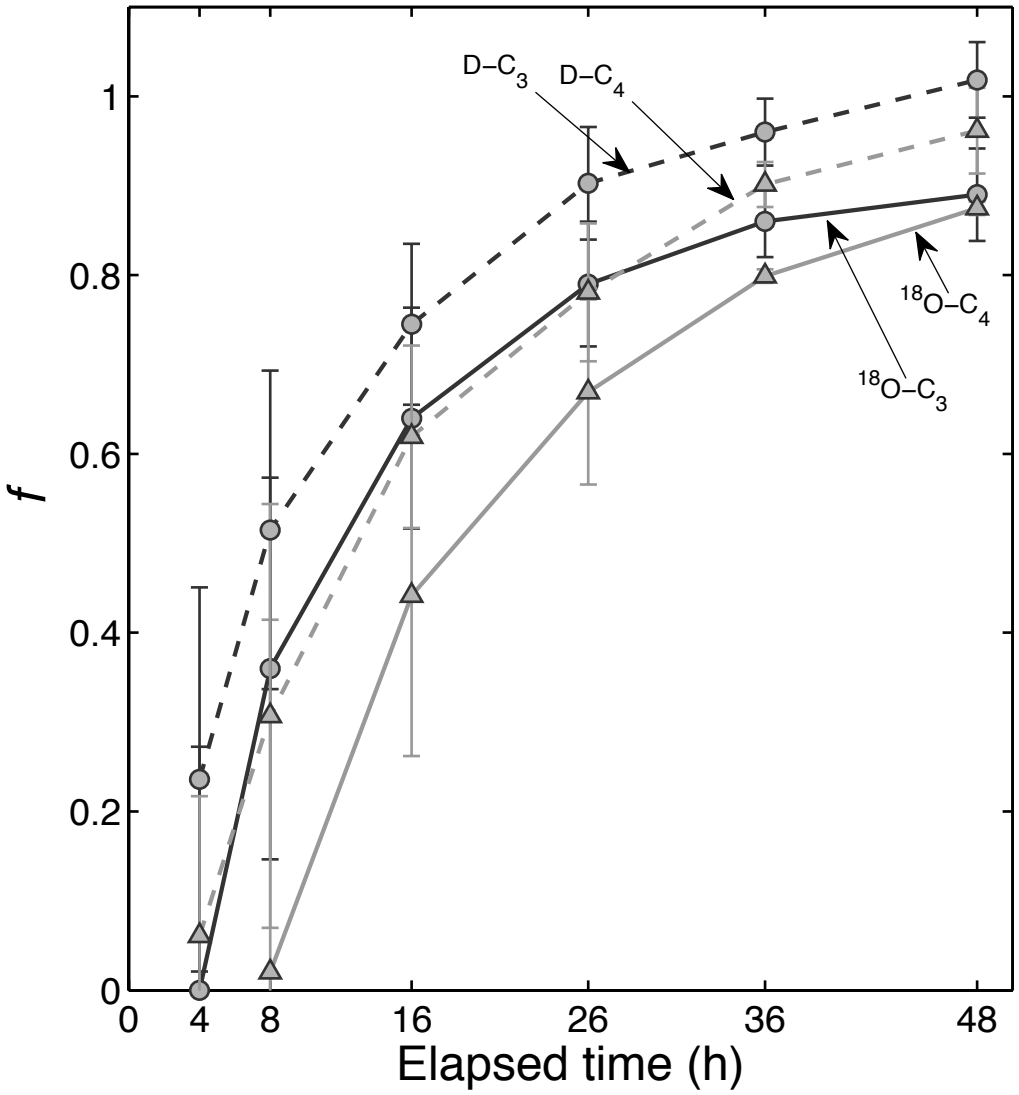

Figure 3.6. Fractional contribution of dew water to leaf water as a function of dew exposure time according to Eq. 3.14. Error bars indicate ± one standard deviation.

Figure 3.7 presents the stomatal conductance (g_S) estimated with the mass balance method at hourly intervals. According to the ^{18}O tracer, the estimated g_S was slightly lower than 0.02 mol $m^{-2}s^{-1}$, considered as a threshold cuticular conductance (Caird *et al*., 2007a), for soybean (Figure 3.7c) and sorghum (Figure 3.7e) at $t = 0$. At other times, g_S was greater than this threshold, indicating that the stomata were partially open in darkness. Use of the D tracer gave highly variable g_S values; occasionally g_S would be negative, which is not an acceptable result. In comparison, the result obtained with the ^{18}O tracer was much more robust. For all the species, the g_S value estimated with the ^{18}O tracer had a minimum at the beginning and showed a slight increase with duration of dew exposure. The mean g_S of all the experiments was 0.036 mol $m^{-2}s^{-1}$ at $t = 0$ and 0.087 mol $m^{-2}s^{-1}$ at 16 h. The increasing trend could be a result of increasing leaf water content and leaf water potential. In a separate experiment of corn plants growing in a well-watered field but exposed to ambient conditions, I found that the predawn leaf water potential was 0.33 MPa higher in the presence of dew than plants in dew exclusion treatment. (Dew exclusion was achieved by suspending a piece of plastic over the treatment plot at night (Appendix II).

Some variation of g_S among the plant species was suggested by the data in Figure 3.8. The estimated g_S for the C_3 plants (cotton, wheat and soybean) were greater than that of the C_4 plants (corn and sorghum). According to the ^{18}O mass balance method, the mean g_S of the C_3 plants was 0.067 mol $m^{-2}s^{-1}$ and that of the C_4 plants was 0.037 mol $m^{-2}s^{-1}$. Among the C_3 species, wheat showed larger values (mean 0.087 mol $m^{-2}s^{-1}$, ^{18}O tracer) than cotton (0.072 mol $m^{-2}s^{-1}$) and soybean (0.042 mol $m^{-2}s^{-1}$). The mean g_S of the C_4 plants was 0.040 mol $m^{-2}s^{-1}$ (corn) and 0.035 mol $m^{-2}s^{-1}$ (sorghum).

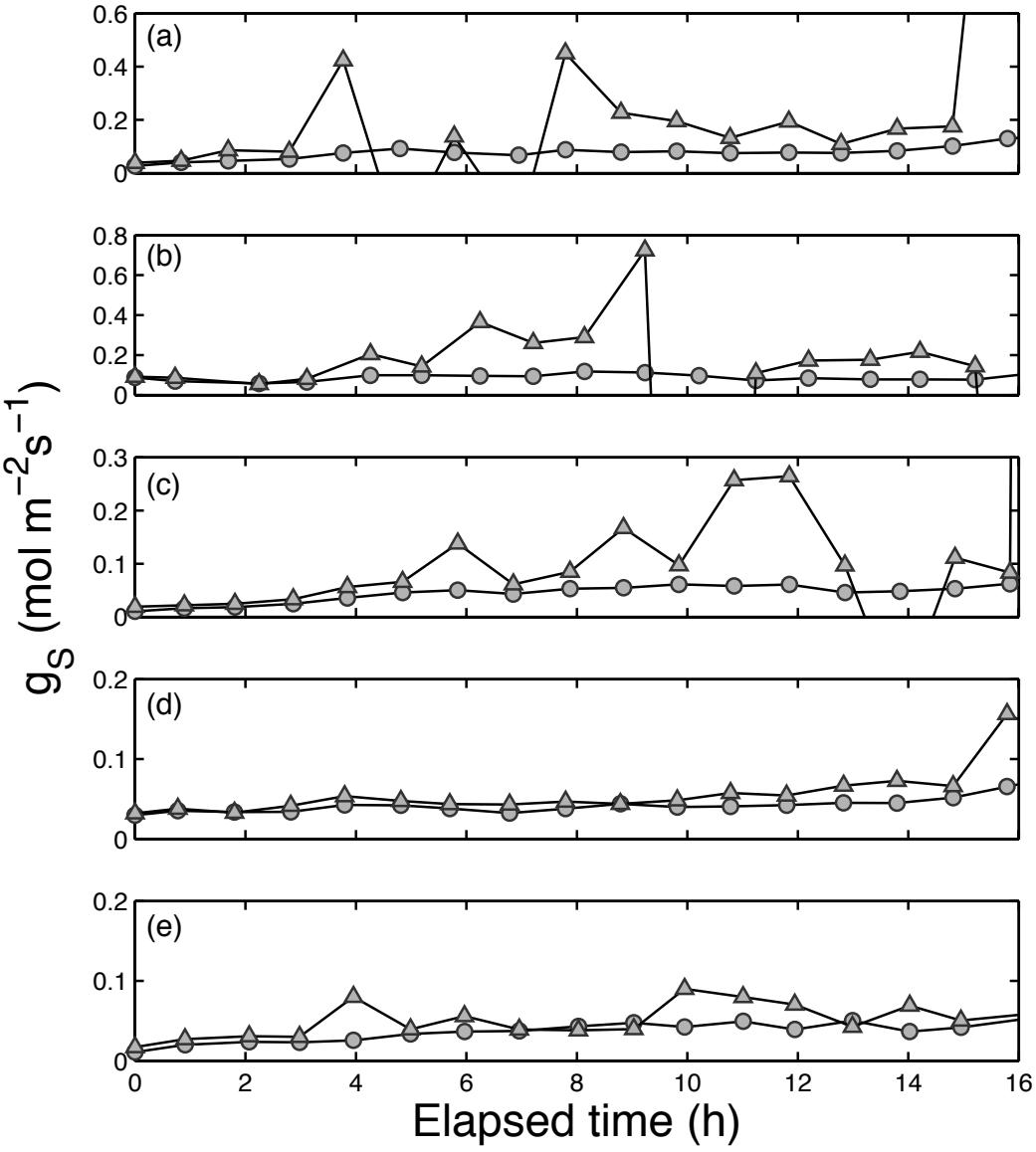

Figure 3.7. Stomatal conductance (g_S) determined with the $^{18}O/^{16}O$ (circles) and D/H (triangles) mass balance approach. Each data point represents average of two replicates for each species: (a) cotton, (b) wheat, (c) soybean, (d) corn and (e) sorghum. For reference, the threshold cuticular conductance is about 0.02 mol $m^{-2}s^{-1}$ (Caird *et al.*, 2007a).

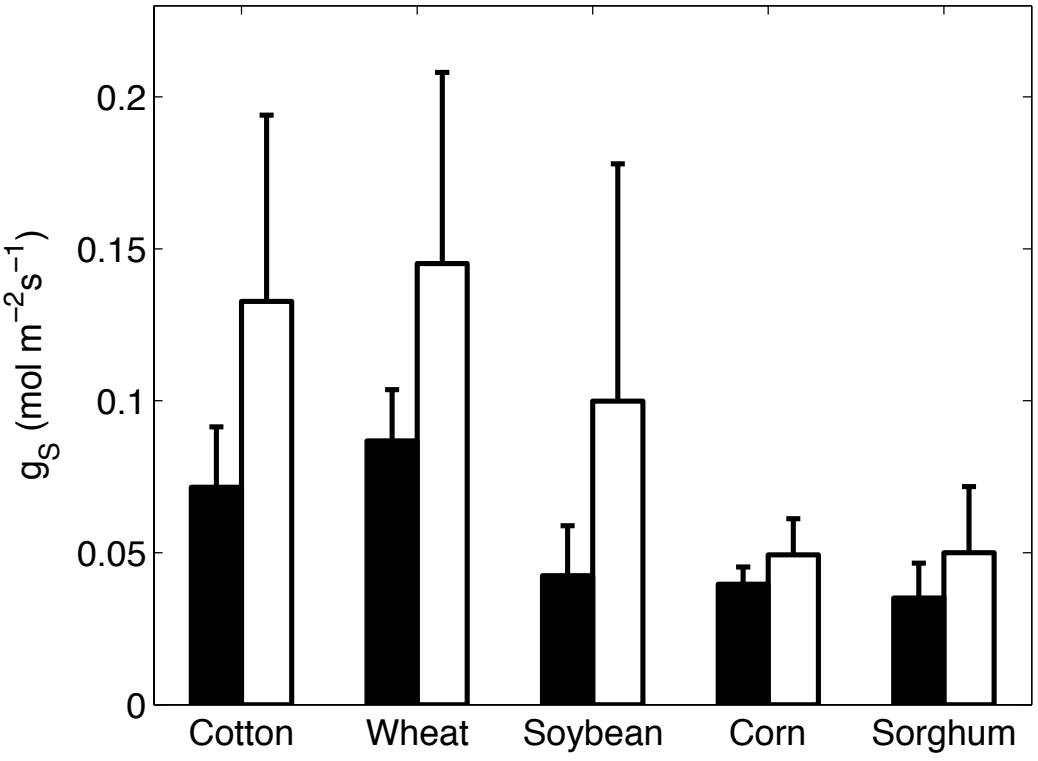

Figure 3.8. Comparison of the stomatal conductance determined with the $^{18}O/^{16}O$ (filled) and D/H (open) tracer. Error bars are standard deviations of the hourly values.

Figure 3.9 presents a comparison of the time variation of the measured δ_L with the predicted δ_L according to Eq. 3.12 for the same experiment described in Figure 3.4. The predicted δ_L shows excellent agreement with the measured δ_L during the first 4 h of the experiment. After then, the predicted δ_L values were lower than the measurements for both isotopologues. In the case of D, the δ_L prediction was made by excluding periods when the estimate g_S was unreasonable (negative or greater than 0.5 mol $m^{-2}s^{-1}$). Similar disagreement was also obtained during other dew experiments. An implicit assumption of Eq. 3.12 is that the δ_L asymptotic approach to a new steady state is caused by a step change in the external forcing. This assumption was not satisfied in this experiments. A sharp change to the driving variables of the plant gaseous exchange occurred when the plant was moved from sunlight to the dark enclosed chamber. However, the continued isotopic exchange through the partially open stomata modified the chamber vapor isotope ratios (δ_V) inside the chamber (Figure 3.4).

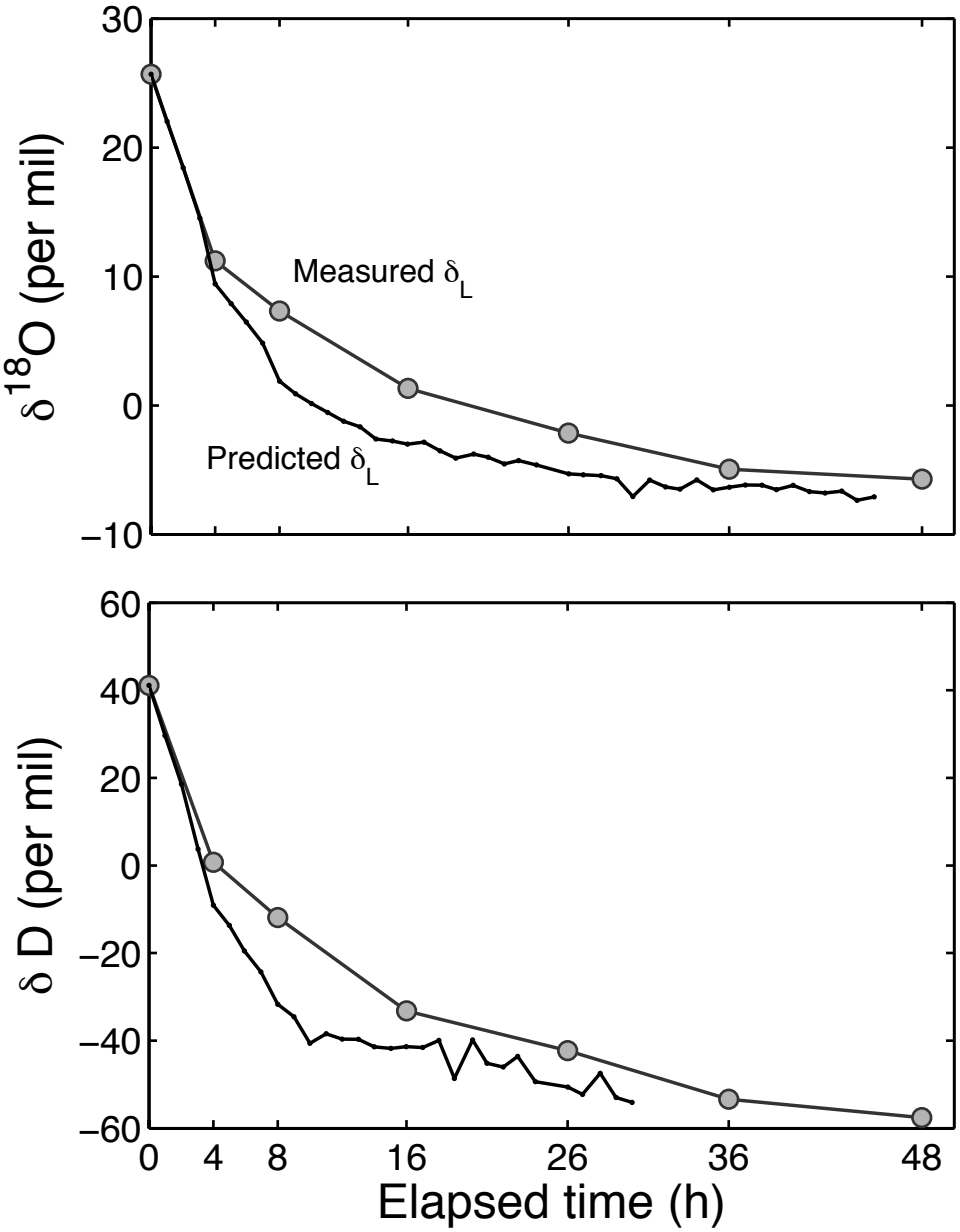

Figure 3.9. Comparison of the time variations in measured δ_L (gray dots) and predicted δ_L (black dotted lines, Eq. 3.12).

3.4 Discussion

3.4.1. Nocturnal isotope exchange at high humidity

The measurements of δ_V in this study reveal that a considerable degree of nighttime isotope exchange exists between the air and leaves even at extremely high humidity. In Figure 3.4, δ_V showed a steep increase immediately after the plant (corn) was placed in the chamber from full sunlight. The δ_V value inside the chamber was higher than δ_B for 30 h in the case of $^{18}O/^{16}O$ and 10 h in the case of D/H. For comparison, the turnover time of the chamber air was about 0.6 h. That $\delta_V - \delta_B$ was positive indicates a net flow of the $H_2{}^{18}O$ and HDO molecules from the leaf, whose water was enriched in ^{18}O and D, to the surrounding air whose vapor isotopic compositions were much lower. The positive gradient occurred in spite of dew formation which would make the vapor inside the chamber lighter than the vapor entering the chamber. It provides qualitative but direct evidence that the plants maintained partially open stomata in darkness and with the presence of dew water.

The complete absence of transpiration was observed at night in the presence of heavy fog (Burgess and Dawson, 2004) and at zero vapor pressure deficit (Daley and Phillips, 2006; Dawson *et al*., 2007). In the presence of dew water on the leaf surface, I also expect zero vapor pressure deficit and absence of transpiration. The results indicate that under these conditions the net flux of the minor isotopologues may not be zero. The theoretical analysis of Farquhar and Cernusak (2005) also shows that incomplete stomatal closure permits molecular diffusion exchange of the minor isotopes of the leaf water with atmospheric vapor while the net flux of $H_2{}^{16}O$ can be zero.

3.4.2. Implications of dew occurrence for leaf water delta

The data in this study show that the exchange of $H_2{}^{18}O$ and HDO in the leaf water with the vapor was not hampered by the dew presence on the leaf surface. Dew water is highly effective in coating plant tissues (Brewer and Smith, 1997; Burkhardt and Eiden, 1994; Washington *et al*., 1998). Because it spreads evenly on both the abaxial and adaxial sides of the leaf, dew water may interfere with stomatal gaseous exchange of both amphistomatous and hypostomatous plants. It is a common practice in leaf gas exchange studies to ignore diffusion through the stoma of wet leaves on the assumption that surface water films act as an impermeable barrier to gas diffusion (Wesely, 1989). The validity of the assumption remains unknown because conventional methods cannot measure the stomatal conductance of a wet leaf. The data show that the assumption is not valid for ^{18}O-H_2O and HDO diffusion.

The incomplete closure of stomata was observed for all the plant species investigated in this study. The high *f* value suggests that the stomatal pathway played a large role in the temporal dynamics of δ_L in the darkness and high humidity conditions. It is well established that evaporation through fully open stomata drives the isotopic enrichment of leaf water, resulting in maximum enrichment in the afternoon when transpiration is the highest diurnally. At night, the enriched leaf water is supposedly diluted by the unfractionated xylem water if leaves maintain complete closure of stomata. Because of long duration of this experiments, mixing with the xylem water would have caused δ_L to approach the xylem water isotope ratios. Instead, as a consequence of incomplete stomatal closure, the diffusion exchange with atmospheric vapor brought δ_L closer to δ_d or roughly the value in equilibrium with atmospheric vapor. Evidence of atmospheric

control of δ_L has been documented for dew events in natural field conditions (Hartard *et al*., 2009; Helliker and Griffiths, 2007; Reyes-Garcia *et al*., 2008; Welp *et al*., 2008; Wen *et al*. 2011).

In dew events, the δ_L temporal dynamics are unlikely a consequence of direct infiltration of dew water into the partially open stomata. This is because of the high surface tension of liquid water and the geometry of stoma (Schonher and Bukovac, 1972). Instead, I suggest that the role of dew is that of an intermediary. Dew preserves the influence of atmospheric vapor by maintaining an isotopic equilibrium state with the latter. Diffusion of the $H_2{}^{18}O$ and HDO molecules takes place in the gaseous phase through the stomatal opening that connects the dew water to the internal leaf water pool. Thus, although the transpiration flux vanishes in leaves covered by dew, the flux of the minor isotopes is potentially large. In fact, the isotopic flux has been shown to cause detectable changes in the isotopic content of atmospheric vapor (Welp *et al*. 2008).

According to the ^{18}O tracer, the fractional contribution of dew water to the leaf water did not reach unity at steady state (Table 3.3, Figure 3.6), indicating some diffusive exchange of the leaf water with the xylem water. As plants usually undergo water stress during the daytime, sap flow at night exists in order to recharge water storage in leaves (Daley and Phillips, 2006; Barbour *et al*., 2005; Caird *et al*., 2007b). In this experiments, the plants did not have water stress even after high transpiration demands during the full sunlight treatment because they were grown in the hydroponic system. The fractional contribution of the xylem water varied from 0.06 to 0.20 among the experiments.

The *f* value at 16 h was on average 16% lower for $^{18}O/^{16}O$ than that for D/H at steady-state except corn (Tables 3.3, Figure 3.6). In other words, the fractional contribution of the xylem water to the leaf water ^{18}O pool was 16% higher than to the D pool. This was largely a result of difference in the efficiency of molecular diffusion in liquid water as diffusion should be a main driving factor to govern the movement of the minor isotopologues because of the elimination of the flux of the major isotope species in this experiment. In liquid water, HDO diffuses 14% more slowly than $H_2{}^{18}O$ at 25°C (Wang *et al*., 1953). Although mixing of the leaf and xylem water existed, the large *f* value shows that this mixing mechanism was not as efficient as the exchange with atmospheric vapor.

3.4.3. Stomatal conductance of wet foliage

It is not possible to measure the stomatal conductance of wet foliage with conventional leaf chambers due to the difficulty in measuring water vapor exchange in high humidity conditions. In this research, I have demonstrated that the stable isotopes of water provide a unique way to overcome this difficulty. This is possible because the exchange of the minor isotopes continues to occur with wet foliage. In these experiments, I deliberately used heavier water as the plant source water and lighter water to generate water vapor. The large isotopic difference between these two water pools helped to break the net isotopic flux into the two component fluxes, the downward exchange with dew water and the upward xylem water flow. Exposure to sunlight, together with the heavy xylem water, produced highly enriched leaf water relative to the vapor fed into the chamber at the beginning of the experiment. The large vapor pressure gradient of the minor

isotopologues between the leaf and the air (Eq. 3.9) produced measureable isotopic flux signals, which then permitted the determination of the stomatal conductance.

In principle, the isotopic mass balance method can also be applied in field conditions, regardless of the leaf wetness status. It is now feasible to measure the isotopic fluxes with micrometeorological methods. The isotopic fluxes can be used with measurements of the leaf, vapor and dew water isotopic compositions, to determine the canopy conductance, in a similar manner to the laboratory setup in this study described in Section 3.2.1. One challenge is that the measurements of evapotranspiration isotope flux tend to be noisier at night than in the daytime (Griffis *et al*., 2010; Lee *et al*., 2007; Welp *et al*., 2008). Furthermore, in field conditions, the xylem and dew water isotopic compositions are often indistinguishable.

The results add to a growing amount of evidence suggesting that incomplete stomatal closure is common in darkness for both C_3 and C_4 species (Barbour *et al*., 2005; Caird *et al*., 2007b). Across the species, the estimated conductance values (0.035 to 0.15 mol $m^{-2}s^{-1}$) fall in the range of the nighttime conductance values previously reported for herbaceous annual species (Barbour *et al*., 2007; Caird *et al*., 2007a; Caird *et al*., 2007b; Easlon and Richards, 2009; Snyder *et al*., 2003). The C_4 plants (corn and sorghum) had smaller conductance than the C_3 plants (cotton, wheat and soybean), implying that the C_4 plants may have developed a conservative stomatal behavior by minimizing the nighttime stomatal opening even at saturation humidity (Figure 3.8). Among the C_3 species, wheat showed the largest values of g_S. It is not known whether the large g_S of wheat was related to its parallel vein structure. According to the ^{18}O tracer mass balance method, the C_4 species had mean stomatal conductance values of 0.040 mol $m^{-2}s^{-1}$ (corn) and 0.035 mol

$m^{-2}s^{-1}$ (sorghum). The occurrence of non-zero nighttime conductance of C_4 plants is not accepted widely, because the adaptation of the C_4 photosynthetic pathway to the environments with low water availability would mean the development of complete stomatal closure to avoid unnecessary water loss. That corn and sorghum maintained partially open stomata in darkness may have been a result of lack of water stress in this experiment. Corn and sorghum are two widely cultivated C_4 species for energy industry and for food supply. In field conditions, dew formulation can also relieve the physiological drought stress by increasing the leaf water potential (Appendix II), which may induce stomata to open.

3.5 Conclusions

This dew simulation experiments showed that leaf water continued to exchange the ^{18}O-H_2O and HDO molecules with atmospheric vapor in saturation humidity conditions when there was no net transpiration. The role of dew appeared to be one of an intermediary: It preserved the influence of atmospheric vapor by maintaining an isotopic equilibrium state with the latter. Diffusion of the $H_2{}^{18}O$ and HDO molecules took place in the gaseous phase through the partially open stomata that connected the dew water to the internal leaf water pool. In dew events, both dew water and xylem water contributed to the leaf water in darkness. The fractional contribution (f) of dew water to the leaf water at steady state was 0.89 ± 0.05 and 1.02 ± 0.04 for the C_3 plants and 0.87 ± 0.01 and 0.96 ± 0.05 for the C_4 plants, according to the $^{18}O/^{16}O$ and D/H tracer, respectively. These high f values indicate that the exchange with atmospheric vapor was the dominant process controlling δ_L at saturation air humidity. These values likely represent an upper limit for natural

ecosystems because natural dew events are much shorter than 48 h (Figure 3.6). The lower *f* values for ^{18}O than for D indicated a more efficient diffusive exchange of ^{18}O between the leaf water and the xylem water. The average isotopic turnover time fell in the range of 0.9 to 1.8 h for the C_3 plants and 2.3 to 3.2 h for the C_4 plants.

I used the mass balance approach to determine the stomatal conductance of the wet foliage. According to the ^{18}O isotopic mass balance method, the stomatal conductance varied from 0.035 to 0.087 mol $m^{-2}s^{-1}$ among the five species; these values fell in the range of the values of the nighttime stomatal conductance reported in the literature. Prolonging the exposure to dew caused g_S to increase slightly, suggesting that dew water may have increased the leaf water potential. (The D isotopic mass balance method was less reliable as the estimated g_S was very noisy and occasionally negative). Of the species used in this study, the C_4 stomatal conductance was lower than the C_3 conductance.

Acknowledgments

This work was supported by the U. S. National Science Foundation through grants DEB-0514904 and ATM-0914473 and by a Yale University Fellowship (to Kyounghee Kim).

3.6 References

Barbour, M.M. and Buckley, T.N., 2007. The stomatal response to evaporative demand persists at night in Ricinus communis plants with high nocturnal conductance. Plant Cell and Environment, 30(6): 711-721.

Barbour, M.M., Cernusak, L.A., WHitehead, D., Griffin, K.L., Matthew, H., Tissue, D.T. and Farquhar, G.D. 2005. Nocturnal stomatal conductance and implications for modelling delta O-18 of leaf-respired CO2 in temperate tree species. Functional Plant Biology, 32(12): 1107-1121.

Barbour, M.M., Farquhar, G.D., Hanson, D.T., Bickford, C.P., Powers, H. and McDowell, N.G. 2007. A new measurement technique reveals temporal variation in delta O-18 of leaf-respired CO2. Plant Cell and Environment, 30(4): 456-468.

Brewer, C.A. and Smith, W.K., 1997. Patterns of leaf surface wetness for montane and subalpine plants. Plant Cell and Environment, 20(1): 1-11.

Burgess, S.S.O. and Dawson, T.E., 2004. The contribution of fog to the water relations of Sequoia sempervirens (D. Don): foliar uptake and prevention of dehydration. Plant Cell and Environment, 27(8): 1023-1034.

Burkhardt, J. and Eiden, R., 1994. Thin water films on coniferous needles. Atmospheric Environment, 28(12): 2001-2011.

Caird, M.A., Richards, J.H. and Donovan, L.A., 2007a. Nighttime stomatal conductance and transpiration in C-3 and C-4 plants. Plant Physiology, 143(1): 4-10.

Caird, M.A., Richards, J.H. and Hsiao, T.C., 2007b. Significant transpirational water loss occurs throughout the night in field-grown tomato. Functional Plant Biology, 34(3): 172-177.

Cernusak, L.A., Farquhar, G.D., Wong, S.C. and Stuart-Williams, H., 2004. Measurement and interpretation of the oxygen isotope composition of carbon dioxide respired by leaves in the dark. Plant Physiology, 136(2): 3350-3363.

Cernusak, L.A., Pate, J.S. and Farquhar, G.D., 2002. Diurnal variation in the stable isotope composition of water and dry matter in fruiting Lupinus angustifolius under field conditions. Plant Cell and Environment, 25(7): 893-907.

Ciais, P., Denning, A.S., Tans, P.P., Berry, J.A., Randall, D.A., Collatz, G.J., Sellers, P.J., White, J.W.C., Trolier, M., Meijer, H.A., Francey, R.J., Monfray, P. and Heimann, M.1997. A three-dimensional synthesis study of delta O-18 in atmospheric CO2 .1. Surface fluxes. Journal of Geophysical Research-Atmospheres, 102(D5): 5857-5872.

Daley, M.J. and Phillips, N.G., 2006. Interspecific variation in nighttime transpiration and stomatal conductance in a mixed New England deciduous forest. Tree Physiology, 26(4): 411-419.

Dawson, T.E., Burgess, S.S.O., Tu, K.P., Oliveira, R.S., Santiago, L.S., Fisher, J.B., Simonin, K.A. and Ambrose, A.R. 2007. Nighttime transpiration in woody plants from contrasting ecosystems. Tree Physiology, 27(4): 561-575.

Dietz, J., Leuschner, C., Holscher, D. and Kreilein, H., 2007. Vertical patterns and duration of surface wetness in an old-growth tropical montane forest, Indonesia. Flora, 202(2): 111-117.

Easlon, H.M. and Richards, J.H., 2009. Photosynthesis affects following night leaf conductance in Vicia faba. Plant Cell and Environment, 32(1): 58-63.

Farquhar, G.D. and Cernusak, L.A., 2005. On the isotopic composition of leaf water in the non-steady state. Functional Plant Biology, 32(4): 293-303.

Farquhar, G.D. and Lloyd, J., 1993. Carbon and oxygen isotope effects in the exchange of carbon dioxide between terrestrial plants and the atmosphere, Stable isotopes and plant carbon–water relations. Academic Press, San Diego, pp. 47–70.

Farquhar, G.D., Lloyd, J., Taylor, J.A., Flanagan, L.B., Syvertsen, J.P., Hubick, K.T., Wong, S.C. and Ehleringer, J.R. 1993. Vegetation effects on the isotope composition of oxygen in atmospheric CO2. Nature, 363(6428): 439-443.

Feild, T.S., Zwieniecki, M.A., Donoghue, M.J. and Holbrook, N.M., 1998. Stomatal plugs of Drimys winteri (Winteraceae) protect leaves from mist but not drought. Proceedings of the National Academy of Sciences of the United States of America, 95(24): 14256-14259.

Francey, R.J. and Tans, P.P., 1987. Latitudinal variation in O-18 of atmospheric CO2. Nature, 327(6122): 495-497.

Griffis, T.J., Sargent, S., Lee, X., Baker, J., Greene, J., Erickson, M., Zhang, X., Billmark, K., Schultz, N., Xiao, W. and Hu, N. 2010. Determining the oxygen isotope composition of evapotranspiration using eddy covariance. Boundary-Layer Meteorol. 137:307-326.

Hartard, B., Cuntz, M., Maguas, C. and Lakatos, M., 2009. Water isotopes in desiccating lichens. Planta, 231(1): 179-193.

Helliker, B.R. and Griffiths, H., 2007. Toward a plant-based proxy for the isotope ratio of atmospheric water vapor. Global Change Biology, 13(4): 723-733.

Jacobs, A.F.G., Heusinkveld, B.G., Kruit, R.J.W. and Berkowicz, S.M., 2006. Contribution of dew to the water budget of a grassland area in the Netherlands. Water Resources Research, 42(3). doi:10.1029/2005WR00405.

Lee, X., Kim, K. and Smith, R., 2007. Temporal variations of the O-18/O-16 signal of the whole-canopy transpiration in a temperate forest. Global Biogeochemical Cycles, 21(3): doi:10.1029/2006GB002871.

Lee, X., Sargent, S., Smith, R. and Tanner, B., 2005. In situ measurement of the water vapor O-18/O-16 isotope ratio for atmospheric and ecological applications. (vol 22, pg 555, 2005). Journal of Atmospheric and Oceanic Technology, 22(8): 1305-1305.

Ludwig, F., Jewitt, R.A. and Donovan, L.A., 2006. Nutrient and water addition effects on day- and night-time conductance and transpiration in a C-3 desert annual. Oecologia, 148(2): 219-225.

Majoube, M., 1971. Oxygen-18 and deuterium fractionation between water and steam. Journal de Chimie Physique et de Physico-Chimie Biologique, 68(10): 1423.

Malek, E., McCurdy, G. and Giles, B., 1999. Dew contribution to the annual water balances in semi-arid desert valleys. Journal of Arid Environments, 42(2): 71-80.

Munne-Bosch, S. and Alegre, L., 1999. Role of dew on the recovery of water-stressed Melissa officinalis L-plants. Journal of Plant Physiology, 154(5-6): 759-766.

Munne-Bosch, S., Nogues, S. and Alegre, L., 1999. Diurnal variations of photosynthesis and dew absorption by leaves in two evergreen shrubs growing in Mediterranean field conditions. New Phytologist, 144(1): 109-119.

Pitacco, A., Gallinaro, N. and Giulivo, C., 1992. Evaluation of actual evapotranspiration of a Quercus ilex L. stand by the Bowen Ratio-Energy Budget method. Vegetatio, 99-100: 163-168.

Reyes-Garcia, C., Mejia-Chang, M., Jones, G.D. and Griffiths, H., 2008. Water vapour isotopic exchange by epiphytic bromeliads in tropical dry forests reflects niche differentiation and climatic signals. Plant Cell and Environment, 31(6): 828-841.

Sauer, T.J., Singer, J.W., Prueger, J.H., DeSutter, T.M. and Hatfield, J.L., 2007. Radiation balance and evaporation partitioning in a narrow-row soybean canopy. Agricultural and Forest Meteorology, 145(3-4): 206-214.

Schonher, J. and Bukovac, M.J., 1972. Penetration of stomata by liquids - Dependence on surface tension, wettability, and stomatal morphology. Plant Physiology, 49(5): 813-819.

Seibt, U., Wingate, L. and Berry, J.A., 2007. Nocturnal stomatal conductance effects on the delta O-18 signatures of foliage gas exchange observed in two forest ecosystems. Tree Physiology, 27(4): 585-595.

Snyder, K.A., Richards, J.H. and Donovan, L.A., 2003. Night-time conductance in C-3 and C-4 species: do plants lose water at night? Journal of Experimental Botany, 54(383): 861-865.
Wang, J.H., Robinson, C.V. and Edelman, I.S., 1953. Self-diffusion and structure of liquid water. 3. Measurement of the self-diffusion of liquid water with H-2, H-3, AND O-18 as tracers. Journal of the American Chemical Society, 75(2): 466-470.
Washington, J.R., Cruz, J. and Fajardo, M., 1998. Detection of chlorothalonil in dew water following aerial spray application and its role in the control of black Sigatoka in banana. Plant Disease, 82(11): 1191-1198.
Weast, R.C., 1977. CRC handbook of chemistry and physics [electronic resource].
Wen, X. F., Lee, X., Sun, X. M., Wang, J. L., Li, S. G. and Yu, G. R. 2011. Dew water isotopic ratios and their relations to ecosystem water pools and fluxes in a cropland and a grassland in China. In review.
Welp, L. R., Lee, X., Kim, K., Griffis, T. J., Billmark, K. and Baker, J. M. 2008. $\delta^{18}O$ of water vapour, evapotranspiration and the sites of leaf water evaporation in a soybean canopy. Plant Cell and Environment, 31(9): 1214-1228.
Wesely, M.L., 1989. Parameterization of surface resistances to gaseous dry deposition in regional-scale numerical models. Atmospheric Environment, 23(6): 1293-1304.
West, J.B., Sobek, A. and Ehleringer, J.R., 2008. A Simplified GIS Approach to Modeling Global Leaf Water Isoscapes. Plos One, 3(6): e2447. doi:10.1371/journal.pone.0002447.

Chapter 4. Field observation of water isotopes in ecosystem water pools

Abstract

This chapter presents the field observations of $H_2{}^{18}O$ and HDO for both ambient vapor and liquid waters conducted over a full growing season of 2009 in a mixed temperate forest, Ontario, Canada. This study revealed dynamics of hydrologic processes in a forest. Evapotranspiration flux above the overstory canopy did not reach isotopic steady state with the plant source water. The seasonal variations of the xylem water for overstory species were tightly coupled with the changes of the soil water measured at 50cm depth. The vertical profile of soil water isotope ratios revealed that the processes of infiltration and mixing of precipitation with existing soil water were governed by soil moisture. Precipitation collected in the Borden site was not in equilibrium with vapor, indicating that secondary evaporation occurred at falling raindrops.

4.1 Introduction

Water isotopes are excellent tracers to investigate the hydrologic processes that are controlled by abiotic and biotic factors simultaneously. For example, isotopic fractionations through water cycles in a forest ecosystem provides insights into identifying redistribution of precipitation, which is a major water input in terrestrial ecosystems. Here isotopic fractionation occurs on different levels. Evaporation which occurs at top layers of soil can be differentiated from deeper soil layers in the result of mixing of newer precipitation with existing soil water (Allison *et al*., 1983). Variations in δ_X originate from different sources of water (Dawson and Ehleringer, 1991). Enrichment of δ_L is determined by stomatal conductance among sampled species (Dongmann *et al*., 1974; Farquhar and Lloyd, 1993).

In addition to liquid water pools, continuous measurements of vapor isotope ratios provide a necessary constraint for gas exchanges of water between ecosystem surfaces and the atmosphere. Continuous measurements of whole-canopy isotope fluxes made over a full growing season reveal temporal variations in evapotranspiration sources in a forest, partitioned into components fluxes (Lee *et al*., 2007). Measurements of both relatively abundant isotopologues, $H_2{}^{18}O$ and HDO, in atmospheric vapor carry unique information regarding dynamic of liquid-vapor phase changes, assuming that precipitation is isotopically in equilibrium with vapor (Wen *et al*., 2010). The conjunction of measurements of liquid water pools and continuous observations of vapor isotopes offers an integration of has been available in recent years (Griffis *et al*., 2010; Lee *et al*., 2007; Welp *et al*., 2008).

The objectives of this chapter is (1) to investigate what abiotic and biotic factors influence the temporal variation of whole-canopy evapotranspiration isotope ratios, (2) to verify isotopic steady-state assumption at a whole-canopy scale and (3) to study the temporal dynamics of forest water uses by integrating water dynamics at an individual components of a forest into such as soil, into a forest over the growing season in the processes of redistributing precipitation.

4.2 Experimental methods

4.2.1. Site

The experiment was conducted in a mixed hardwood and coniferous forest located at the Environment Canada tower station on Canadian Forces Base Borden in southern Ontario (44°19'N, 79°56'W, 120m above sea level) from June to late August 2009. This site is a long-term flux monitoring station and details of the site information are given by Teklemariam *et al*. (2009). The dominant species were red maple (*Acer rubrum* L., 52.2%), Eastern white pine (*Pinus strobes* L., 13.5%), Aspen (*Populus grandidentata* Michx, 7.7%), and Ash (*Fraxinus americana* L., 7.1%). Mean canopy height was 22m and mean leaf area index (LAI) was 4.6. Mean annual and growing season air temperature (June-September) were 6.4 and 17.6°C, respectively. The average annual and growing season soil temperatures were 7.9 and 16.0°C, respectively. Mean annual precipitation was 858 mm.

4.2.2. Measurements of water vapor and flux ratios

Atmospheric vapor isotope ratios were measured for $^{18}O/^{16}O$ and D/H by an *in situ* water vapor isotope measurement system at two heights, above and under the overstory canopy. The measurement heights were switched manually during the measurement period. The *in situ* system consisted of a tunable diode laser analyzer (TDL, model TGA-100A, Campbell Science Inc., Logan, Utah) and a dripper calibration system. Details of the operational principle were given in the previous chapters (section 2.3.1 and 3.2.1). During the field experiment of 2009, the dripper delivered calibration water of a known isotope content (-16.4‰ for $^{18}O/^{16}O$ and -123.5‰ for D/H) at a flow rate that was determined depending upon ambient vapor concentrations in a given day. This dynamic calibration system was deployed to minimize instrument nonlinearity. A more detailed discussion of the system nonlinearity can be found in Section 2.3.2 (chamber nonlinearity). Canopy flux isotope ratio measurements were made hourly and converted to delta notation in reference to VSMOW (per mil).

4.2.3. Isotope analysis of ecosystem water pools

$^{18}O/^{16}O$ and D/H measurements of ecosystem water pools were made on a regular or event basis. For the measurements of leaf and xylem water isotope ratios, adjacently located three overstory trees: ash, aspen and red maple, were chosen within 15 m radius. Deltas of leaf water and stem were measured simultaneously every 3 – 7 days depending on the wetness of tree surfaces in between rain events. For leaf water isotope analysis, 4 – 7 leaves were collected in glass vials immediately after the center vein was removed. For stem water, non-green twigs were collected at the mid-canopy. I also made weekly

measurements of soil water at three depths: 5, 10, and 50 cm. In August, auxiliary measurements of soybean leaf and stem water were made simultaneously with the tree leaf sampling after removal of main veins at a soybean farm located near the research site (44º19'N, 79º93'W). Plants and soil samples were sealed and were kept frozen until cryogenic vacuum extraction at Yale University. Groundwater was collected twice. Event-based precipitation sampling was made in a forest opening area near the flux tower. Water isotopic analyses were carried out on a Thermo Finnigan DeltaPlus XP with Gas Bench, Thermo Finnigan MAT 253 with a H-device and a Thermo Finnigan DeltaPlus XP with TC/EA at the Yale Isotope Laboratory.

4.3 Results and Discussion

4.3.1. Water balance during the experimental period in the Borden forest

Figure 4.1 shows the cumulative precipitation and evapotranspiration of the Borden forest during the experiment in 2009. The rain gauge readings were integrated in order to estimate the cumulative precipitation. The cumulative forest evapotranspiration was estimated from the eddy covariance measurements. During the experimental period, precipitation exceeded evapotranspiration from the beginning (since DOY 140; May 20) and there was no evidence of water shortage found for the rest of the season. There were severe rainstorm events multiple times especially at the end of the season. From DOY 204 to 207 (July 23 – 26) and 221 to 223 (August 9 – 11), there were two large storm events with 62.8 and 48.8 mm of precipitation, respectively. The amount of precipitation recorded during these two events was equivalent to 38% of total precipitation observed

during the experiment. On DOY 240 (August 28), the cumulative evapotranspiration and precipitation were 130.8 mm and 292.6 mm, respectively, that the forest evapotranspiration accounted for only 45% of precipitation input during the experimental period of 2009.

4.3.2. Seasonal variations in vapor isotope ratios

Figure 4.2 presents seasonal variability of the isotopic compositions of ambient vapor (δ_V) above the overstory canopy. Discontinuities in δ_V (top and middle panels) were due to the understory measurements mode. The daily mean δ_V varied by 15 and 133‰ for $^{18}O/^{16}O$ and D/H, respectively, occasionally exceeding 10‰ ($^{18}O/^{16}O$) and 90‰ (D/H) over just a few days. These rapid changes in δ_V were also observed in previous studies measured over a temperate forest of New England and a soybean field in Minnesota by our research group (Lee *et al*., 2006; Welp *et al*., 2008). The seasonal trends of δ_V appeared to be correlated with those of air temperature. This correlation became especially stronger at the end of the experiment (after DOY 210; end of July). The correlation coefficients between δ_V and the air temperature were 0.47 and 0.50 (n = 70) for $^{18}O/^{16}O$ and D/H, respectively, for the entire measurement period and they increased by 0.67 and 0.76 (n = 18) from DOY 210 by the end of the season.

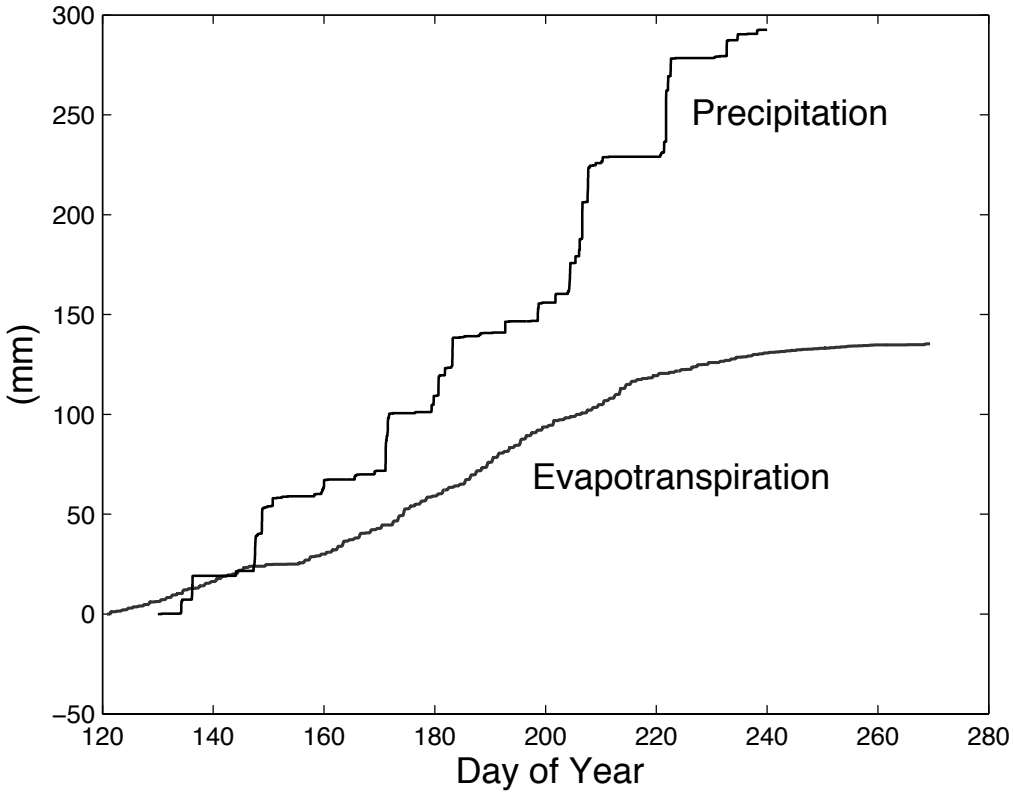

Figure 4.1. Cumulative precipitation and evapotranspiration above the overstory canopies in the Borden forest during the experimental period. The rain gauge was operated from DOY 130 to 240 (May 10 – August 28, 2009) and the eddy covariance dataset was available for a longer period from DOY 120 to 273 (April 30 – September 30, 2009).

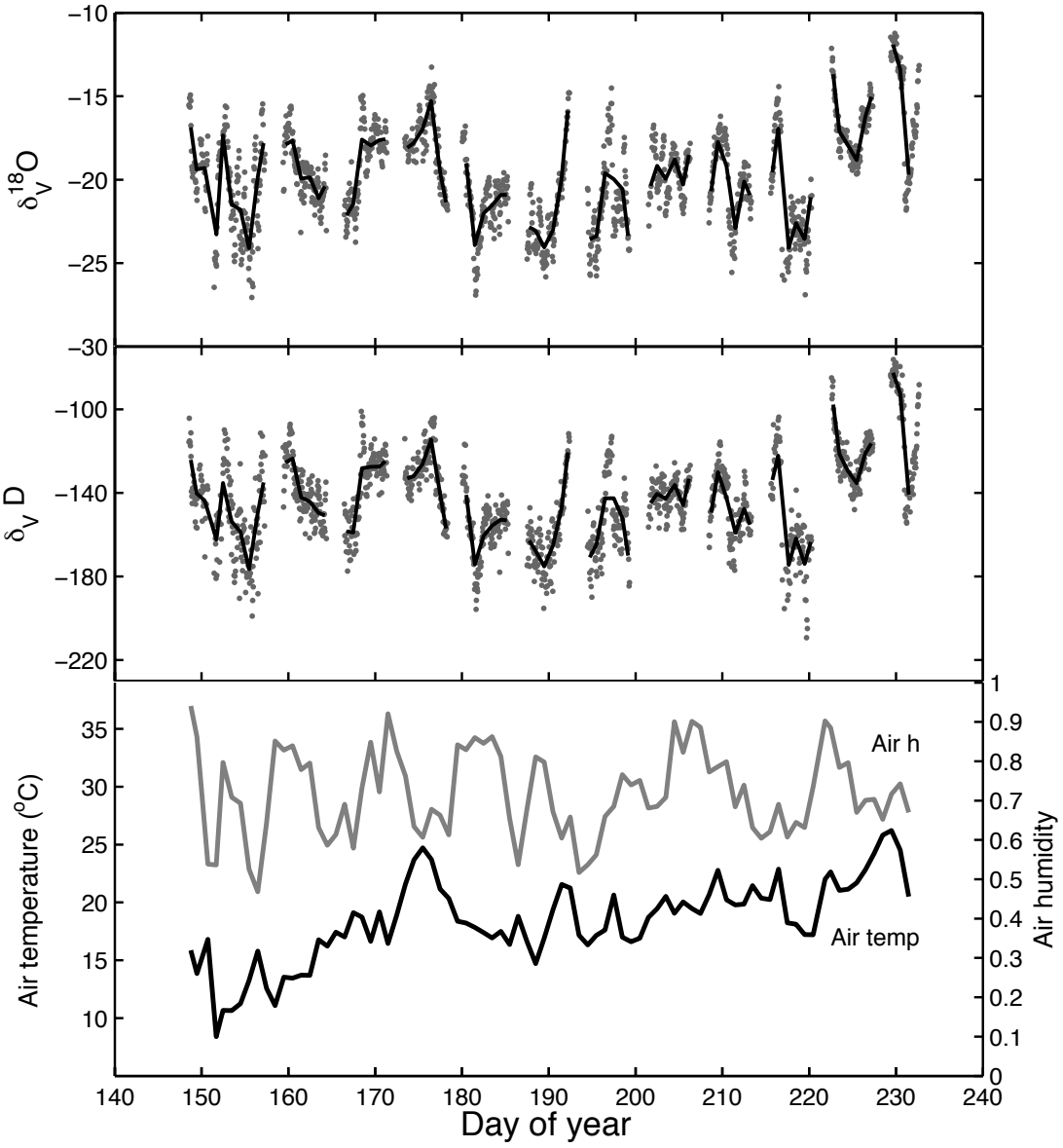

Figure 4.2. Hourly mean (gray dots) and daily mean ambient vapor measurements (black lines) for $^{18}O/^{16}O$ (top) and D/H (middle). Daily mean air temperature (bottom, black line) and humidity (bottom, gray line).

4.3.3. Liquid water isotopic compositions

Figure 4.3 presents the seasonal precipitation (δ_P), 5-day weighted average of δ_P ($\delta_{P\text{-}W}$), xylem (δ_X), three depths soil waters (δ_S) and groundwater isotope ratios (δ_G) measured at the Borden site during the experimental period in 2009. δ_P and $\delta_{P\text{-}W}$ varied and large variability was found on DOY 176 (June 25), 182 (July 1) and 208 (July 27). The deviation from the mean δ_P on these three days were ±7.1 and ±49.2‰ for $^{18}O/^{16}O$ and D/H, respectively. Except these three rain events, δ_P fell in the range between -12.2 and -4.8‰ for $^{18}O/^{16}O$ and -93.3 and -23.3‰ for D/H prior to DOY 210 (July 29). In the later season after DOY 210, δ_P increased, resulting in more enriched D- δ_P than the leaf water isotope rations (Figure 4.7).

Groundwater isotope ratios did not change over the season. δ_G was collected twice on DOY 196 (July 15) and 227 (August 15) from two walls drilled at the study site. The average of δ_G was -12.3 and -84.9‰ and the standard deviation was 0.21 and 1.34‰ for $^{18}O/^{16}O$ and D/H, respectively. For $^{18}O/^{16}O$, none of natural waters were more depleted than δ_G except δ_P on DOY 182 (July 1) and 208 (July 27), at which weighted δ_P were less depleted. For D/H, D- δ_S and D- δ_X approached to the value of δ_G at the end of the season mainly after DOY 200.

Xylem waters had little variability and were tightly coupled with the values of deep soil water at 50 cm. For both isotopologues, δ_X usually fell in the ranges of values of δ_S collected from three depths (5, 10, and 50 cm) except the end of the measurement periods. After DOY 217 (August 5), the δ_S values of 5 and 10 cm depth differentiated from δ_S at 50 cm, increasing by 3.6‰. The δ_X measurements, however, did not respond to

the changes in δ_S at the top two layers and remained close to the range of δ_S at 50 cm. There was species variability in the monthly means of δ_X (Table 4.1). The seasonal variability of the three species was 0.9 (maple), 1.2 (aspen) and 1.4‰ (ash) for $^{18}O/^{16}O$ and 5.5 (maple), 6.6 (ash) and 7.9‰ (aspen) for D/H. Of the three species, δ_X of maple showed the smallest variability.

Local meteoric water lines (LMWL) at the Borden site were plotted in Figure 4.4 in comparison to the regression of groundwater and global meteoric water line (GMWL). The regression line of precipitation was $\delta D = 7.6\delta^{18}O - 1.3$. The observed slope of 7.6 was slightly less than a slope of GMWL of 8, implying that the Borden site presents non-equilibrated meteoric conditions during the observation period. The regression line of groundwater was deviated from LMWL a $\delta D = 5.9\delta^{18}O - 11.7$. Assuming that precipitation is the ultimate water source of groundwater at the Borden site, the lower slope of the groundwater than the precipitation resulted from the secondary evaporation of precipitation during the recharging processes of groundwater.

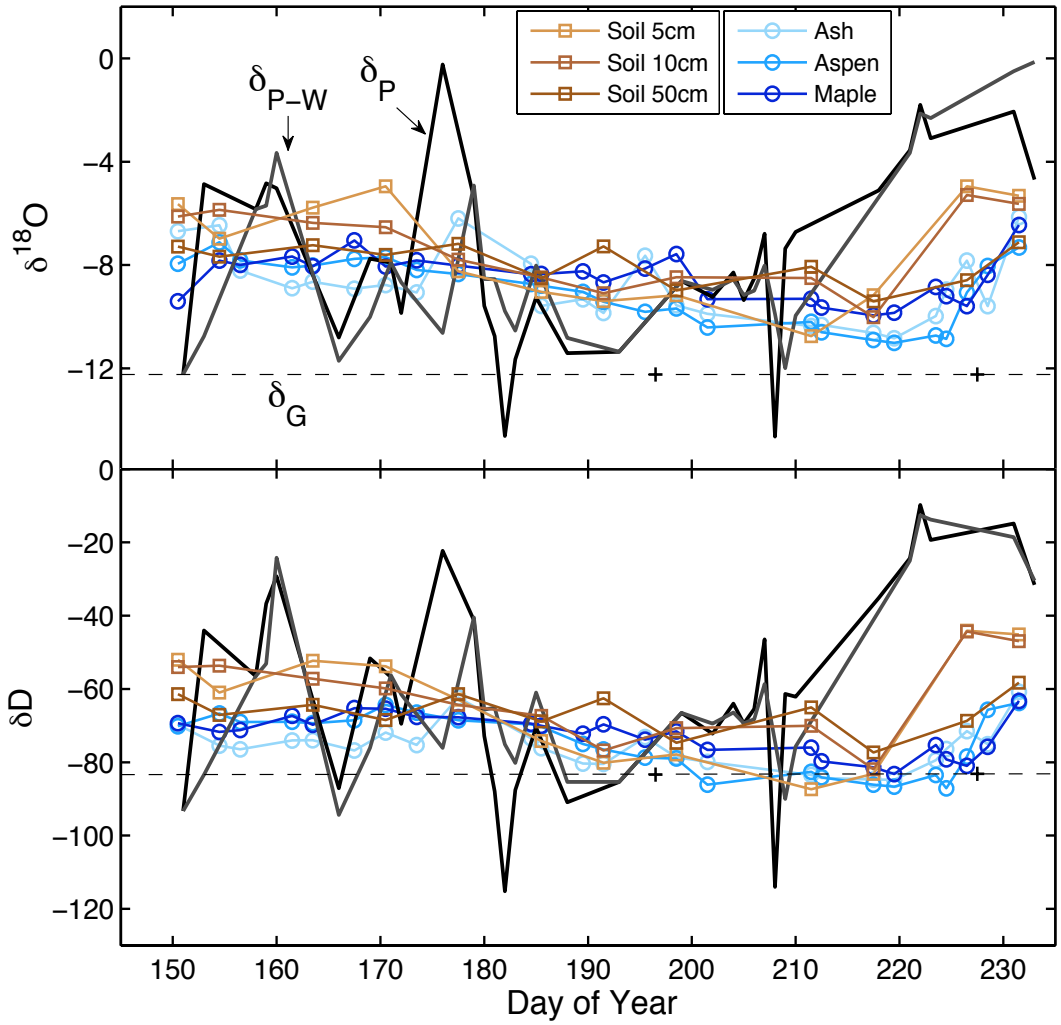

Figure 4.3. Seasonal variations in ecosystem water pools for $^{18}O/^{16}O$ (upper) and D/H (lower) in the Borden forest during the experimental period of 2009. Two measurements of groundwater (crosses, dashed lines), precipitation (black solid lines), 5-day weighted precipitation (gray solid lines), soil waters from three depths (open squares), and xylem waters (open circles).

Table 4.1. Monthly mean $\delta^{18}O$ and δD of liquid waters in per mil.

		$^{18}O/^{16}O$			D/H		
		June	July	August	June	July	August
Twig	Ash	-8.1	-9.4	-9.1	-73.3	-78.9	-76.1
	Aspen	-7.9	-9.6	-9.7	-67.7	-78.0	-78.8
	Maple	-7.8	-8.6	-8.9	-68.3	-73.2	-77.0
Leaf	Ash	8.2	3.4	4.8	-31.6	-53.6	-36.9
	Aspen	8.4	2.4	3.1	-29.1	-51.2	-41.7
	Maple	11.9	7.2	8.3	-26.7	-46.4	-35.8
Soil	5	-6.5	-9.6	-6.5	-57.5	-79.9	-57.5
	10	-6.6	-8.6	-7.0	-58.8	-71.2	-57.7
	50	-7.4	-8.2	-8.4	-65.3	-67.8	-68.1
Precipitation		-6.9	-9.8	-3.4	-54.7	-76.5	-22.5

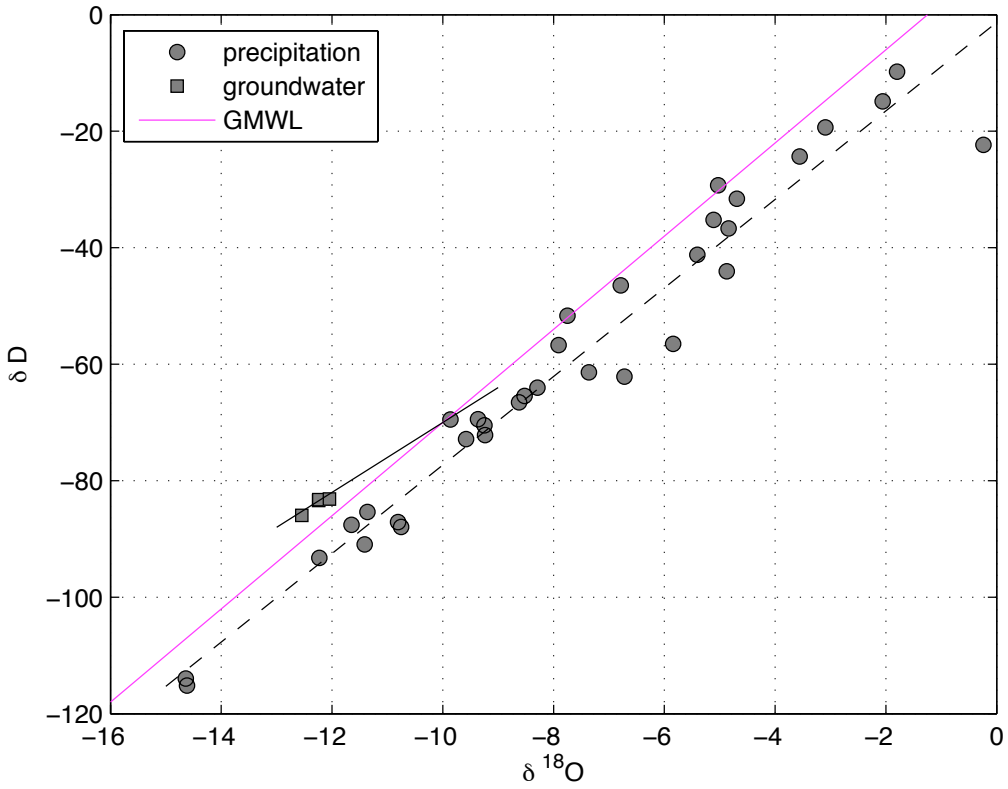

Figure 4.4. Local meteoric water line for precipitation (dots and dashed line), the regression of groundwater measurements (squares and gray solid line), and global meteoric water line (pink soil line) given by $\delta D = 8\delta^{18}O + 10$

Near-continuous δ_V observations provide us with a useful insight into the atmospheric transport processes of water vapor during phase changes. Figure 4.5 presents measured δ_P with the δ_V equilibrium values at air temperature (top and middle) and daily precipitation recorded in the rain gauge (bottom). According to Rayleigh's law, precipitation is assumed to be in equilibrium with vapor during condensation at a near-ground temperature (Dansgaard, 1964). At the Borden site, the δ_V measurements revealed that precipitation was isotopically near in equilibrium with vapor except a few periods in which the site was relatively dry in between rainstorms. As Wen *et al*. (2010) observed in Beijing, the disequilibrium at the Borden site was noticeable during and at the end of the dry periods. For example, large disequilibrium of measured δ_P with vapor was observed on DOY 176 June 25) and 218 - 221 (August 6 – 9) when precipitation did not occur for a while. It is noticeable that the measured δ_P values were more enriched than the equilibrium values at disequilibrium, indicating the kinetic effects at the failing rain drops. On the contrary, δ_P on DOY 193 (July 12) was more depleted than equilibrium, presumably implying a mechanism of rain produced by convective systems such as strong downdrafts (Gat, 1996).

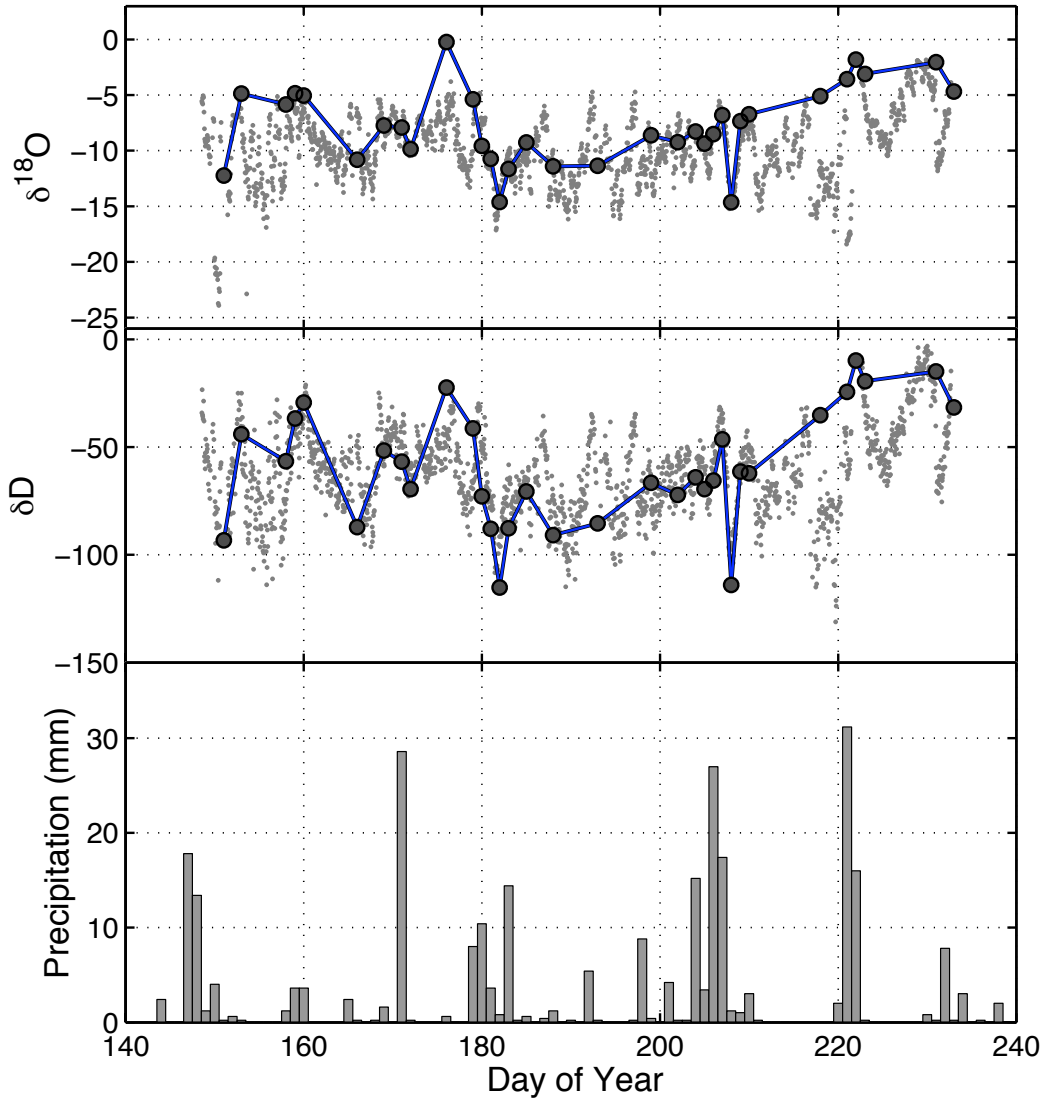

Figure 4.5. Comparison of δ_P (circles) in equilibrium with δ_V at air temperature (gray dots) for $^{18}O/^{16}O$ (top) and D/H (middle). Daily precipitation recorded in the rain gauge (bottom).

The effect of precipitation amount on soil water mixing varied with soil moisture conditions. Figure 4.6 shows the vertical profile of soil water isotope ratios. During the experiment in summer 2009, I had multiple strong rainstorms occurring in a short-period on DOY 170 (June 19; 28.6 mm), 179 – 183 (June 28 – July 2; 37.2 mm), 204 - 210 (July 23 – 29; 49.2 mm) and 220 (August 8; 49.2 mm). The maximum daily precipitation (31.2 mm) that was observed during these periods was equivalent to 17% of total rainfall recorded during the measurement period of 2009. After the first heavy rainstorm on DOY 170 (June 19), the vertical gradient of δ_S at three difference depths became small, less than 1‰ for $^{18}O/^{16}O$ and 7‰ for D/H and this well mixing soil waters lasted until the second rainstorm around DOY 180 (June 29). This was in result from the enhanced rainfall infiltration into a deeper layer at a dry soil.

A wet soil condition often limits infiltration of rainwater into deeper soil. After the second rainstorm, δ_S of top two layers (5 cm and 10 cm) were slightly more depleted than δ_S at 50 cm due to the negative δ_P (-14.6‰ for $^{18}O/^{16}O$ and -115.2‰ for D/H on DOY 182; July 1) because the mixing with a new rainfall occurred only at the top of the soil. The decoupling of top two layers from δ_S -50cm implied that mixing of new rainfall with existing soil water remained in the top layers. Poor mixing of soil water after large rainstorm explicitly indicated the effect of precipitation amount on the infiltration of rainfall into a deeper soil layer (Gazis and Feng, 2004).

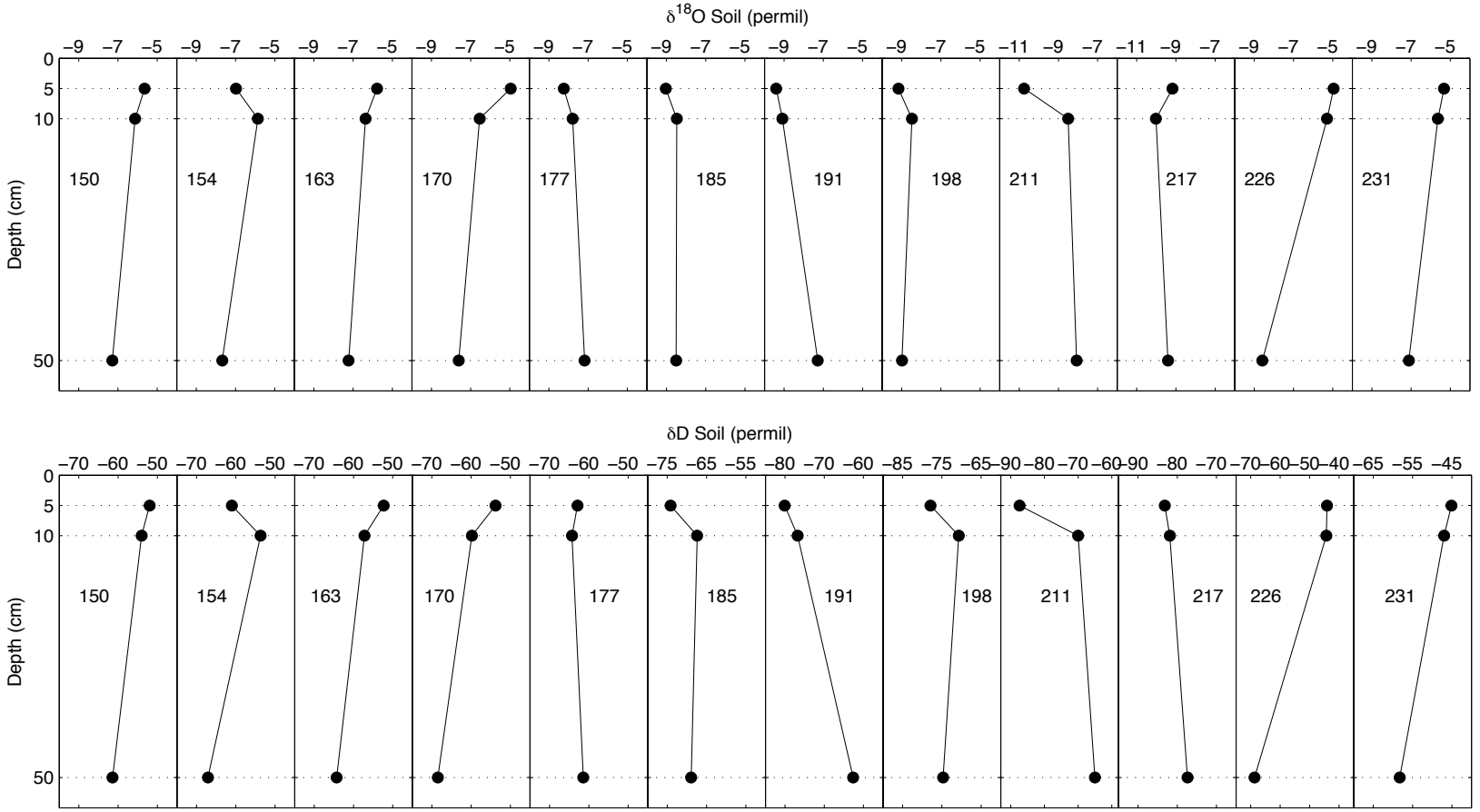

Figure 4.6. Vertical mixing of soil water for $^{18}O/^{16}O$ (upper) and D/H (bottom) at the Borden site. The measurements were made at three depths, 5, 10, and 50 cm.

Table 4.2 compares δ_X to the δ_X measurements after bark was peeled off that each measurement performed independently at the same day. The removal of bark has been recommended during twig sampling by previous studies (Barnard *et al*., 2007; Cernusak *et al*., 2008; Keitel *et al*., 2006; Tang and Feng, 2001) because bark could be in equilibrium with atmospheric vapor which tends to be isotopically depleted (Brunel *et al*., 1997). Practically, the bark removal, however, is intricate under field conditions and often can be very difficult in some species. Difficulty removing all bark can cause bias in δ_X measurements because of evaporation at bark-removed surfaces by exposure to the ambient air. The twig sampling in this study was conducted without the removal of bark throughout the experiment.

The removal of bark caused negligible differences in the δ_X measurements of ash and aspen but noticeable differences were found in red maple. δ_X was enriched when bark was removed than when bark was present in general. Except ash, bark-removed δ_X was always heavier than δ_X with bark present. For aspen, the differences were negligibly small, less than 0.4 ($^{18}O/^{16}O$) and 0.9‰ (D/H). For red maple, the δ_X differences of with and without bark increased that δ_X with bark present were 1 and 4‰ heavier than δ_X without bark for $^{18}O/^{16}O$ and D/H, respectively. These values were close to the standard deviation of the mean δ_X of the three species, 0.8‰ for $^{18}O/^{16}O$ and 4.0‰ for D/H. There was confounding by two sampling methods because samples with bark present could be depleted and samples with bark removal could be enriched. At this stage, it is not clear which sampling method cause more bias. Nonetheless, minimizing unexpected evaporation during sampling should be considered when designing field sampling in order to reduce a measurement error.

Table 4.2. Comparison of the effects of bark removal on the δ_X measurements.

		$^{18}O/^{16}O$		D/H	
Date	Species	Bark	Bark removal	Bark	Bark removal
July 14	Ash	-7.6	-7.9		
July 17	Aspen	-9.7	-9.3	-79.0	-78.1
July 20	Maple	-9.3	-8.4	-76.6	-73.4

The isotopic composition of leaf water (δ_L) varied with a similar trend observed in precipitation isotope ratios. The measured δ_L values showed much larger seasonal variability than xylem and soil waters, varying by 16‰ in $^{18}O/^{16}O$ and 34‰ in D/H. The changes in δ_L were observed approximately 1 to 6 days after the changes in δ_P. This time lag tended to be longer in the later part of the experimental period. For example, δ_L changed a day after δ_P had changed between DOY 180 to 190 (June 29 – July 9), then an increase of δ_L on DOY 228 (August 16) occurred 6 days after a sharp increase in δ_P on DOY 222 (August 10).

The δ_L measurements were more enriched than the δ_X measurements over the experimental period. Figure 4.7 exhibits the seasonal means and the standard deviations of δ_X, -8.8 ± 1.1‰ for $^{18}O/^{16}O$ and -74.4 ± 6.7‰ for D/H. The most extreme δ_L enrichments ($\Delta\delta_L = \delta_L - \delta_X$) were observed during the early part of the experiment, approximately 30‰ and 65‰ above δ_X for $^{18}O/^{16}O$ and D/H, respectively.

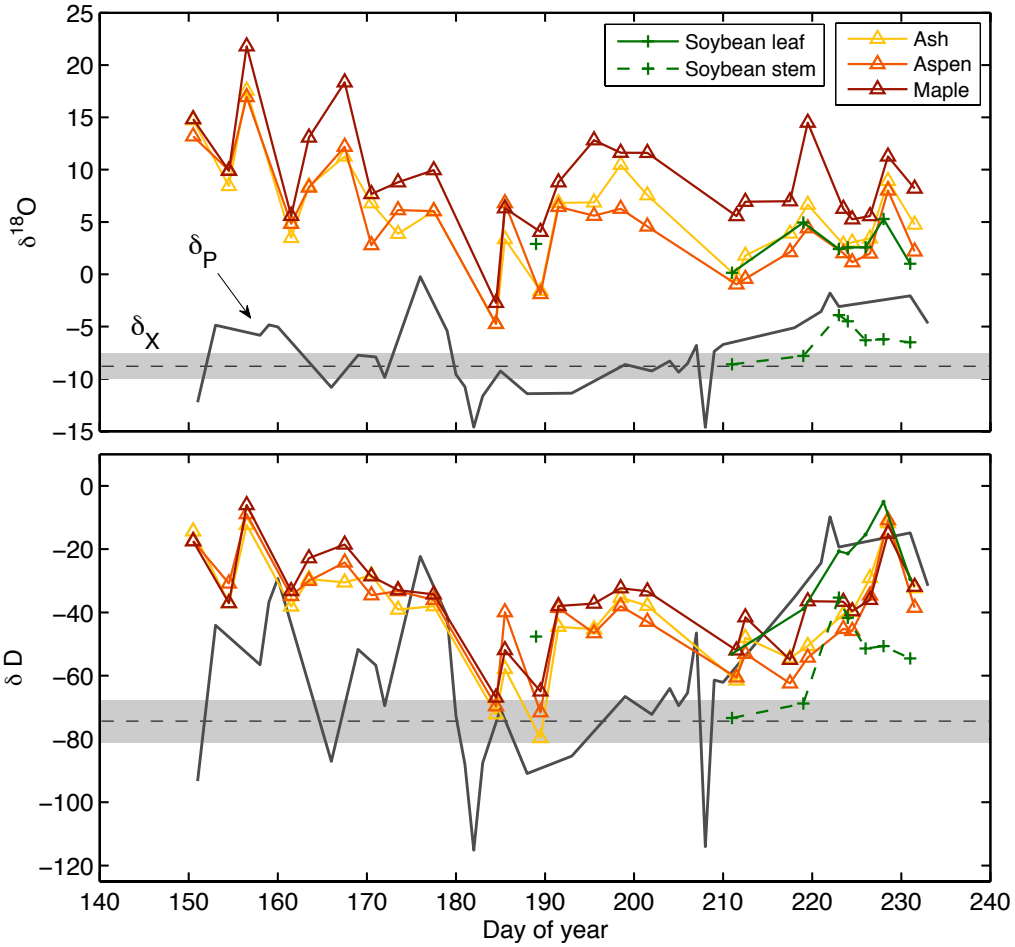

Figure 4.7. Seasonal variations in leaf water isotope ratios for three species, soybean leaf and stem isotope ratios for $^{18}O/^{16}O$ (upper) and D/H (lower). For detailed information about each species of δ_L, see the legend. For reference, precipitation (gray solid lines) and mean xylem isotope ratios ± standard deviations (dashed lines with shaded areas) were presented.

Leaf water enrichment is controlled by biotic and abiotic factors. Stomatal conductance is a biotic determinant of δ_L enrichment. Contrary to δ_X, large species variations were found in the δ_L measurements caused by the differences of stomatal conductance. Of the three species, the maximum stomatal conductance has been reported in red maple, ranged from 120 to 150 mol $m^{-2}s^{-1}$ (Auge *et al*., 2000; Daley and Phillips, 2006). The stomatal conductance of ash and aspen was in the range from 80 to 100 mol $m^{-2}s^{-1}$ (Abdul-Hamid and Mencuccini, 2009) and from 60 to 90 mol $m^{-2}s^{-1}$ (Ewers *et al*., 2005), respectively. For $^{18}O/^{16}O$, maple-δ_L was the most enriched among three species throughout the experimental period. The seasonal means of $\Delta\delta_L$ were 17.4, 14.3, and 13.8‰ for maple, ash, and aspen, respectively. For D/H, a similar trend was found in the δ_L measurements, in general. The seasonal means of $\Delta\delta_L$ were 35.6, 34.8, and 34.3‰ for maple, ash, and aspen, respectively.

Humidity acts as an abiotic constraint on leaf water enrichment. Figures 4.8 and 4.9 show the correlations between δ_L enrichment and atmospheric moisture conditions, relative humidity and vapor pressure deficit (vpd). For the correlation analyses, relative humidity and air temperature measured at the lower intake (33 m) during midday (12 - 3 pm) was averaged. The δ_L enrichment was a linear function of atmospheric moisture conditions: negatively correlated with relative humidity and positively with vpd, resulting from less δ_L enrichment at a high moisture condition. The linear least squares fit equation for ^{18}O-$\Delta\delta_L$ and humidity remained a strong correlation, with a R^2 value of 0.65 ($p < 0.0001$). With the humidity from 0.4 to 0.7 during the growing season, leaf water was enriched 10

to 20‰ and 20 to 45‰ above the xylem water for $^{18}O/^{16}O$ and D/H, respectively, in the overstory species.

Auxiliary measurements made on soybean leaves and stems suggested the stronger dependence of the source water of soybeans on precipitation than the overstory trees. The additional eight measurements of soybean were made in the later part of the growing season. The growth of soybean was delayed due to the unusually cold and wet summer in the study areas, so that a pair measurement of soybean leaves and stem was available after DOY 211 (July 30). Leaf sampling was made after the main vein was removed. The soybean stem fell between values of the top soil and the precipitation prior to DOY 226 (August 14). The reader is reminded that the use of δ_S should be limited to analogy to soil water isotope ratios of the soybean field only because the soybean field was located out of the Borden forest.

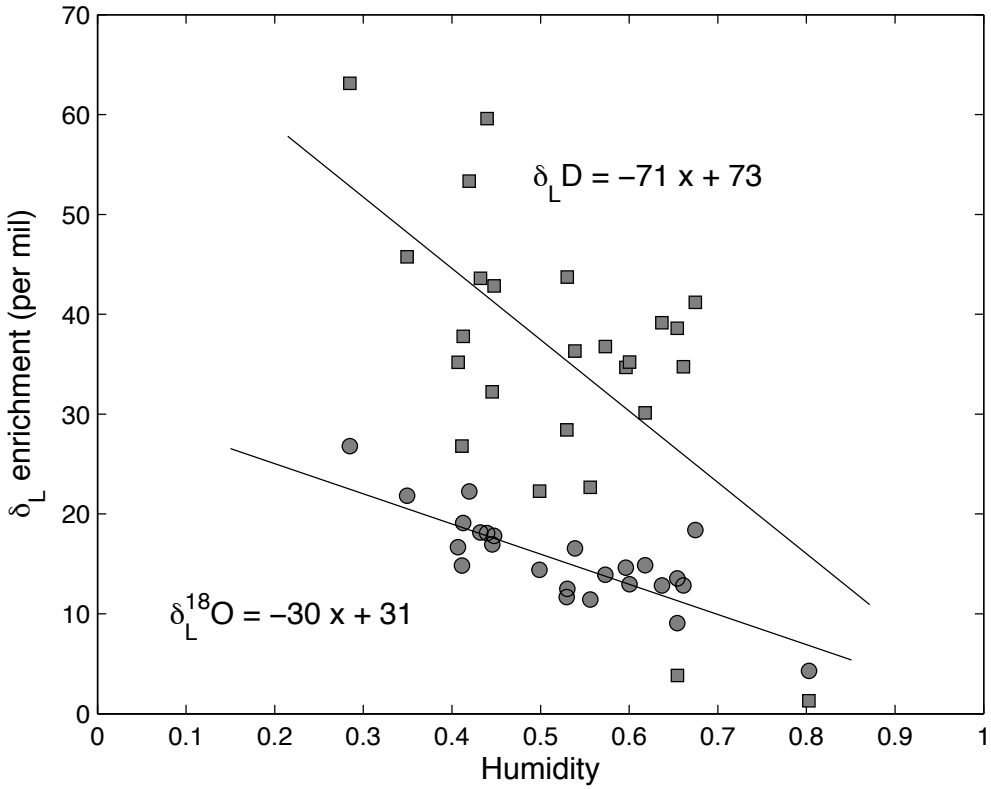

Figure 4.8. Correlations between leaf water enrichment (δ_L - δ_X) and relative humidity measured at lower intake (33m) for $^{18}O/^{16}O$ (circles) and D/H (squares). Linear least squares fit equations (solid lines) for $^{18}O/^{16}O$ and D/H are $y = -30x + 31$ ($R^2 = 0.65$) and $y = -71x + 73$ ($R^2 = 0.38$), respectively.

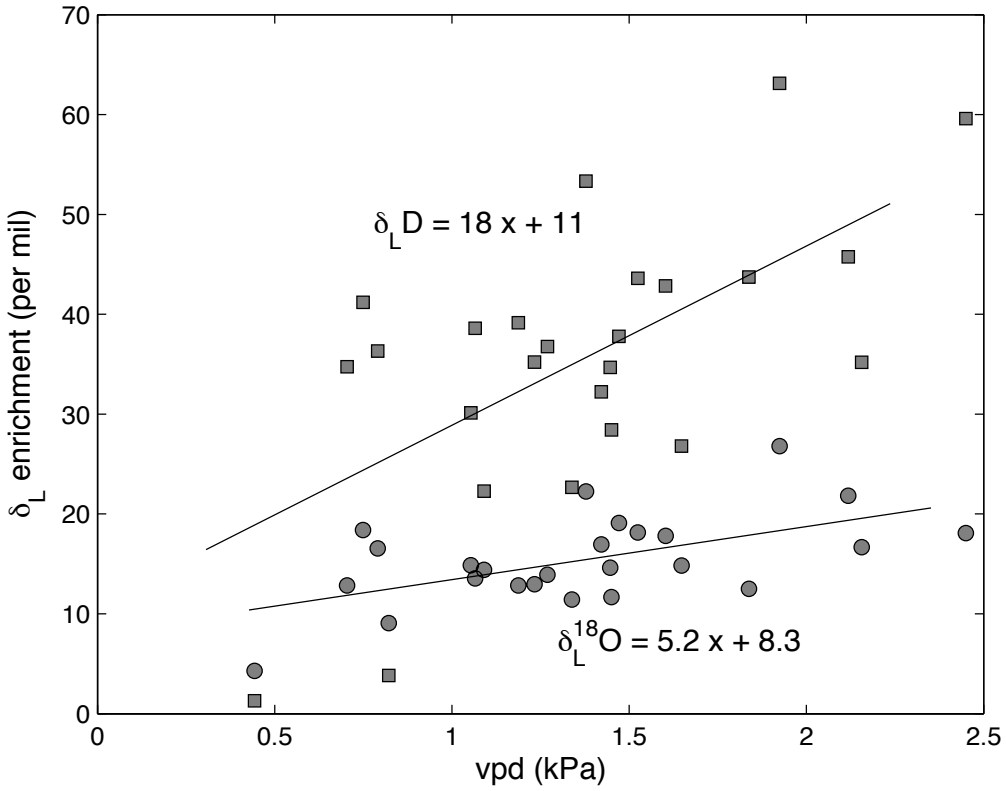

Figure 4.9. Correlations between leaf water enrichment (δ_L - δ_X) and vapor pressure deficit measured at the lower intake (33m) for $^{18}O/^{16}O$ (circles) and D/H (squares). Linear least squares fit equations (solid lines) for $^{18}O/^{16}O$ and D/H are $y = 5.2x + 8.3$ ($R^2 = 0.31$) and $y = 18x + 11$ ($R^2 = 0.39$), respectively.

4.3.4. Seasonal and diurnal variability of evapotranspiration flux

isotope ratios

Figure 4.10 presents evapotranspiration flux (δ_{ET}) of overstory (upper) and understory canopies (bottom) for $^{18}O/^{16}O$ and D/H, respectively, over the course of the experiment in 2009. The hourly means of δ_{ET} (dots) were very scattered so that the measurements had to be filtered ±50‰ for $^{18}O/^{16}O$ and ±500 ‰ for D/H in order for daily average estimates (black solid lines). In comparison to the daily δ_V measurements (gray lines), large variability was observed in the daily δ_{ET} values and there were no clear trends found over the measurement period. The variability of daily δ_{ET} ranged from -35 to 50‰ for $^{18}O/^{16}O$ and from -490 to 440‰ for D/H. The variations in δ_{ET} tended to decrease during relatively dry periods (i.e. around DOY 190 and 230; July 9 – August 18).

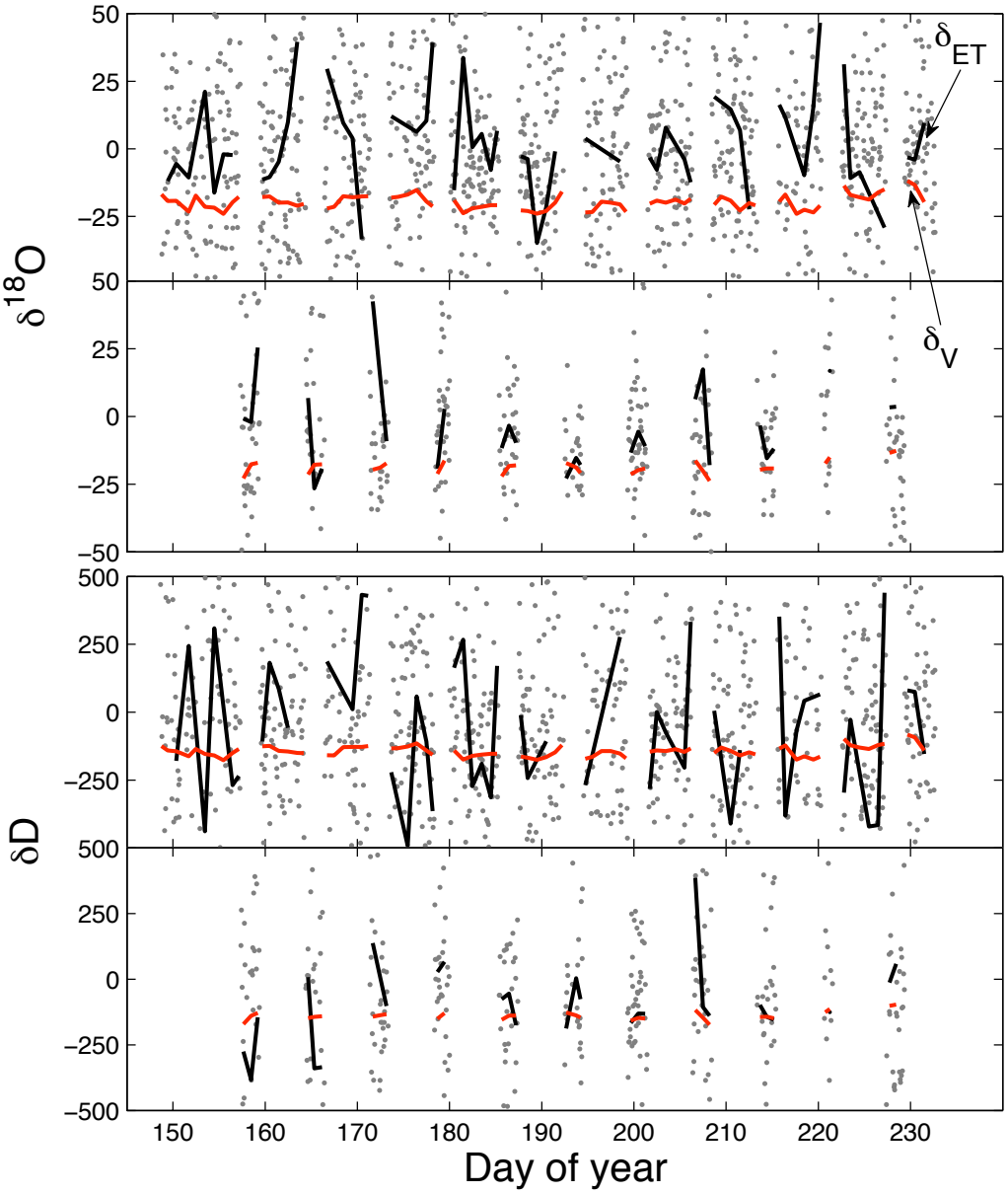

Figure 4.10. Seasonal variations in whole-canopy isotope fluxes for overstory (first and third panels) and understory canopy (second and fourth panels).

Figure 4.11 presents the diurnal composite of δ_{ET} measured at the overstory (gray lines) and understory canopy (black lines). Dashed lines are the seasonal means of δ_X with standard deviations presented in the shaded areas. The diurnal composite of δ_{ET} varied in less than 20 and 200‰ for $^{18}O/^{16}O$ and D/H, respectively. For $^{18}O/^{16}O$, understory δ_{ET} reached at δ_X rather than overstory δ_{ET} in the midday. For the understory canopy, δ_{ET} showed the least variability from the late morning hours until midday (10-1 pm), which reached to the steady state values. For the overstory canopy, δ_{ET} stayed relatively stable during the late afternoon hours (1–6 pm) with values that are 2.5 to 6‰ heavier than the steady-state values. The reader is reminded that the steady state value is the seasonal mean of δ_X measured in three of major overstory species at the Borden site. For D/H, the diurnal composites of δ_{ET} were much noisier than that of $^{18}O/^{16}O$. Neither the overstory nor the understory canopy was at steady state. For the overstory canopy, δ_{ET} stayed relatively stable between 12 to 3pm, more than 35‰ departure from the steady state value of -74.4 ± 6.7‰. For the understory canopy, the values of δ_{ET} showed fluctuations, which fell into the range between -150 and 31‰.

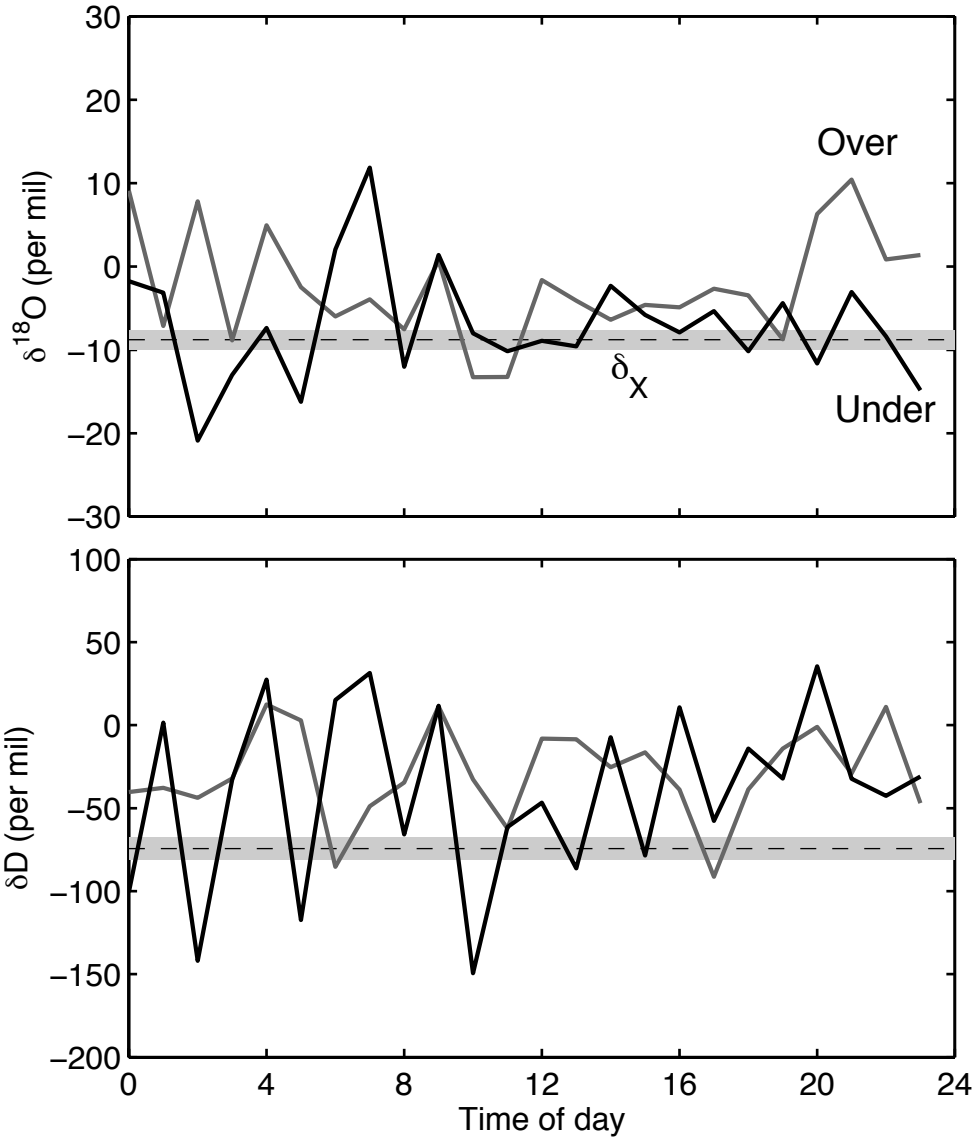

Figure 4.11. Ensemble mean diurnal cycles of δ_{ET} for overstory (gray solid lines) and understory canopy (black solid lines). Seasonal average of δ_X of three species (gray dashed lines) with +/- one standard deviation (shaded areas).

4.3.5. 5-day running average of overstory δ_{ET}

Figure 4.12 compares the 5-day running averages of δ_{ET} (δ_{ET5}) to xylem and precipitation isotope ratios. The use of δ_{ET5} is useful to scale up the measurements of δ_{ET} in comparison to δ_X, which features slower turnover time of the pools. For the running average calculation, overstory δ_{ET} were only considered and outliers (greater than 50 and 300‰ and less than -50 and -300‰ for $^{18}O/^{16}O$ and D/H, respectively) were removed prior to the calculations.

δ_{ET5} indicated that isotopic steady state was not achieved generally in the Borden forest except for three periods. On DOY 161 (June 10), 181 (June 30) and 196 (July 15), δ_{ET5} reached δ_X, however, the maximum duration of isotopic steady state was no more than three days (DOY 181~184; June 30 – July 3). Except during these three periods, δ_{ET5} was always more enriched than δ_X, and the departure from steady state ranged from 7.2 to 17.7‰ for $^{18}O/^{16}O$ and from -20.0 to 130.3‰ for D/H. This disagreement between δ_{ET5} and δ_X at the Borden site is smaller than that observed in Lee *et al*. (2007) because the use of δ_{ET5} dampened the fluctuations of δ_{ET} measurements.

The violation of steady state assumption under field conditions has been reported in recent studies (Harwood *et al*., 1999; Lee *et al*., 2007; Welp *et al*., 2008). The steady-state assumption (Craig and Gordon, 1965) has been criticized that $\delta_T = \delta_X$ is likely to happen only in the limited conditions of high transpiration usually at midday (Harwood *et al*., 1999). When transpiration flux and climatic variables are highly variable, the isotopic steady-state assumption was invalid and it led to the large disagreement between δ_T and

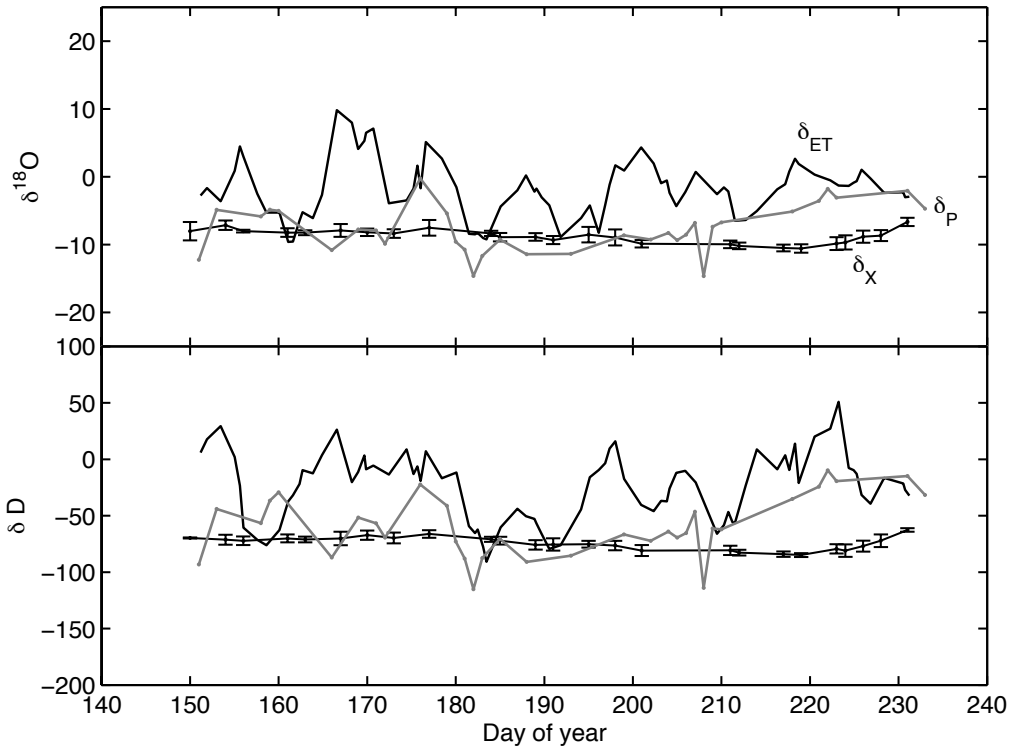

Figure 4.12. 5-day running average of δ_{ET} (black lines), δ_P (gray lines) and the means of δ_X (black lines) with one standard error (error bars).

δ_X (Lee *et al* 2007). The $\delta_T = \delta_X$ condition could be achieved in the case of integrating longer time scale than hourly observations (Harwood *et al*., 1999).

4.4 Conclusions

Continuous measurements of isotope ratios of water vapor and the evapotranspiration flux were made in a mixed temperate forest over a full growing season. Precipitation exceeded evapotranspiration at the Borden site during the measurement of 2009. The seasonal trends of δ_V appeared to be correlated with those of air temperature. This led to a reasonable agreement between measured and predicted precipitation in equilibrium with δ_V at air temperature and a disagreement happened in dry periods.

δ_X was closely coupled with δ_S at 50 cm depth and the species variations in the δ_X measurements were less than 1.1 and 6.7‰ for $^{18}O/^{16}O$ and D/H, respectively. The δ_X values after bark removal were slightly heavier than δ_X values without removal, indicating that bias could be caused during sampling procedures. The δ_L enrichment was affected by transpiration with a decrease of humidity in the air. Stomatal conductance was also a factor that maple with the highest stomatal conductance reported had the most enriched δ_L. The vertical profiles of δ_S were a good indicator of dynamics of soil water that infiltration of newer precipitation into a deep layer was enhanced at a dry condition. The diurnal composite of δ_{ET} varied in less than 20 and 200‰ for $^{18}O/^{16}O$ and D/H, respectively. In general, the variability of diurnal δ_{ET} tended to decrease in the daytime. The isotopic steady state assumption was invalid in the Borden site.

4.5 References

Abdul-Hamid, H. and Mencuccini, M., 2009. Age- and size-related changes in physiological characteristics and chemical composition of Acer pseudoplatanus and Fraxinus excelsior trees. Tree Physiology, 29(1): 27-38.

Allison, G.B., Barnes, C.J. and Hughes, M.W., 1983. The distribution of deuterium and 18O in dry soils 2. Experimental. Journal of Hydrology, 64(1-4): 377-397.

Auge, R.M. *et al*., 2000. Correlations of stomatal conductance with hydraulic and chemical factors in several deciduous tree species in a natural habitat. New Phytologist, 145(3): 483-500.

Barnard, R.L., Salmon, Y., Kodama, N., Sorgel, K., Holst, J., Rennenberg, H., Gessler, A. and Buchmann, N. 2007. Evaporative enrichment and time lags between delta O-18 of leaf water and organic pools in a pine stand. Plant Cell and Environment, 30(5): 539-550.

Brunel, J.P., Walker, G.R., Dighton, J.C. and Monteny, B., 1997. Use of stable isotopes of water to determine the origin of water used by the vegetation and to partition evapotranspiration. A case study from HAPEX-Sahel. Journal of Hydrology, 189(1-4): 466-481.

Cernusak, L.A., Mejia-Chang, M., Winter, K. and Griffiths, H., 2008. Oxygen isotope composition of CAM and C(3)Clusia species: non-steady-state dynamics control leaf water O-18 enrichment in succulent leaves. Plant Cell and Environment, 31(11): 1644-1662.

Craig, H. and Gordon, L.I., 1965. Deuterium and oxygen 18 variations in the ocean and the marine atmosphere. In: E. Tongiorgi (Editor), Stable Isotopes in Oceanographic Studies and Paleotemperatures, Lischi & Figli, Pisa, Italy, pp. 9-130.

Daley, M.J. and Phillips, N.G., 2006. Interspecific variation in nighttime transpiration and stomatal conductance in a mixed New England deciduous forest. Tree Physiology, 26(4): 411-419.

Dansgaard, W., 1964. Stable isotopes in precipitation. Tellus, 16(4): 436-468.

Dawson, T.E. and Ehleringer, J.R., 1991. Streamside trees that do not use stream water. Nature, 350(6316): 335-337.

Dongmann, G., Nurnberg, H.W., Forstel, H. and Wagener, K., 1974. On the enrichment of H218O in the leaves of transpiring plants. Radiation and Environmental Biophysics, 11(1): 41-52.

Ewers, B.E., Gower, S.T., Bond-Lamberty, B. and Wang, C.K., 2005. Effects of stand age and tree species on canopy transpiration and average stomatal conductance of boreal forests. Plant Cell and Environment, 28(5): 660-678.

Farquhar, G.D. and Lloyd, J., 1993. Carbon and oxygen isotope effects in the exchange of carbon dioxide between terrestrial plants and the atmosphere, Stable isotopes and plant carbon–water relations. Academic Press, San Diego, pp. 47–70.

Gat, J.R., 1996. Oxygen and hydrogen isotopes in the hydrologic cycle. Annual Review of Earth and Planetary Sciences, 24: 225-262.

Gazis, C. and Feng, X.H., 2004. A stable isotope study of soil water: evidence for mixing and preferential flow paths. Geoderma, 119(1-2): 97-111.

Griffis, T.J., Sargent, S., Lee, X., Baker, J., Greene, J., Erickson, M., Zhang, X., Billmark, K., Schultz, N., Xiao, W. and Hu, N. 2010. Determining the oxygen isotope composition of evapotranspiration using eddy covariance. Boundary-Layer Meteorol. 137:307-326

Harwood, K.G., Gillon, J.S., Roberts, A. and Griffiths, H., 1999. Determinants of isotopic coupling of CO2 and water vapour within a Quercus petraea forest canopy. Oecologia, 119(1): 109-119.

Keitel, C., Matzarakis, A., Rennenberg, H. and Gessler, A., 2006. Carbon isotopic composition and oxygen isotopic enrichment in phloem and total leaf organic matter of European

beech (Fagus sylvatica L.) along a climate gradient. Plant Cell and Environment, 29(8): 1492-1507.
Lee, H., Smith, R. and Williams, J., 2006. Water vapour O-18/O-16 isotope ratio in surface air in New England, USA. Tellus Series B-Chemical and Physical Meteorology, 58(4): 293-304.
Lee, X., Kim, K. and Smith, R., 2007. Temporal variations of the O-18/O-16 signal of the whole-canopy transpiration in a temperate forest. Global Biogeochemical Cycles, 21(3). doi:10.1029/2006GB002871.
Tang, K.L. and Feng, X.H., 2001. The effect of soil hydrology on the oxygen and hydrogen isotopic compositions of plants' source water. Earth and Planetary Science Letters, 185(3-4): 355-367.
Teklemariam, T., Staebler, R.M. and Barr, A.G., 2009. Eight years of carbon dioxide exchange above a mixed forest at Borden, Ontario. Agricultural and Forest Meteorology, 149(11): 2040-2053.
Welp, L.R., Lee, X., Kim, K., Griffis, T.J., Billmark, K., Baker, J.M. 2008. δ18O of water vapour, evapotranspiration and the sites of leaf water evaporation in a soybean canopy. Plant Cell and Environment, 31(9): 1214-1228.
Wen, X.F., Zhang, S.C., Sun, X.M., Yu, G.R. and Lee, X., 2010. Water vapor and precipitation isotope ratios in Beijing, China. Journal of Geophysical Research – Atmospheres 115: D01103, doi:10.1029/2009JD012408.

Chapter 5. Summary

This dissertation is concerned with experimental studies of stable water isotopes by extensively measuring $H_2{}^{18}O$ and HDO vapor. At the laboratory scale, the isotopic enrichment of surface water was investigated using an evaporation chamber. Emphasis was placed on investigating kinetic effects in determination of surface enrichment during evaporation. Fumigation experiments were carried out on five annual species of plants utilizing either C_3 or C_4 photosynthetic systems, with focus on dew effects on the equilibrium of leaf water with vapor at saturation through partially open stomata. At the ecosystem scale, field observations were made in a temperate mixed forest (Borden Forest, southern Ontario, Canada) during the summer of 2009.

A primary goal of the study is to verify surface enrichment at the evaporating surface and to investigate factors that influence kinetic effects. The concept of surface enrichment has been developed mostly in a theoretical perspective because accumulation of heavier isotopes at the evaporating surface is not amenable to direct observation. The most prominent factor is aerodynamic conditions at the evaporating surface, ranging from fully turbulent diffusion to fully molecular diffusion, which have not been verified by direct observations. The surface enrichment was substantial: on average, the surface water was 7.5 – 8.9‰ more enriched in ^{18}O and 12.6 – 16.5‰ in D than the bulk water, the exact value depending on the choice of the kinetic fractionation factor for evaporation. The aerodynamic conditions at the evaporating surface were dominated by molecular diffusion at the higher evaporation rates. Surface cooling was not a critical factor in the estimation of surface enrichment.

Another goal of this study was to investigate gas exchanges of water at leaf surfaces with the focus on dew effects on leaf water isotope ratios and nocturnal stomatal behaviors,

most importantly, estimating stomatal conductance at wet surfaces. Surface wetness has been considered an impermeable barrier to gas diffusion at plant surfaces (Wesely, 1989), but no such studies exist to validate the assumption of infinite resistance at wet foliage because direct measurement of stomatal conductance is impossible using conventional methods. Consequently, there is a limited understanding of how much and how dew water contributes to plant-water relations, possibly as a direct water input into vegetation. In this light, laboratory dew simulation experiment was conducted with development of a fumigation plant chamber system, which generated a vapor stream of known isotopes. In the experimental setup in which net water flux was zero, fluxes of minor isotopes presented that stomatal conductance existed at wet foliage with a similar degree of nocturnal conductance, ranged from 0.035 to 0.087 mol $m^{-2}s^{-1}$, reported elsewhere (Caird *et al*., 2007). The result has a great implication for setting deposition velocity at wet surfaces in air quality modeling studies.

The finding regarding incomplete stomatal closure has great implications in two ways: vapor equilibrium with leaf water and nighttime stomatal conductance. Diffusion of minor isotopologues took place in the gaseous phase through the partially open stomata. As an intermediary, dew presence at leaf surface played a role in interconnecting vapor to internal leaf water. By the end of the 48 h-long experiment, at least 90% of leaf water cam from dew. Dew-modified leaf water may be a dominant component in the measurements of evapotranspiration flux isotopes during early morning hours in field experiments.

In the condition of no drought stress, C_4 plants maintained partially open stomata in darkness. Cultivation of some of such plants, namely corn and sorghum, has been

intensified in recent year due to the increasing demands for biofuel production as well as food supply (Worldwatch institute, 2006). In agricultural, crops often cultivated with fully equipped irrigation systems. Partitioning components of evapotranspiration and regional water budget may change significantly in agriculture landscapes with maintenance of water loss by C_4 crops at night.

During the summer of 2009, an intensive field experiment of water isotope measurements, Chapter 4, was conducted to implement laboratory studies, Chapter 2 and 3, described in the previous paragraphs. Soil water mixing was affected by soil moisture conditions presented at the time of precipitation. Leaf water enrichment was controlled by both biotic and abiotic factors. Near-continuous measurements of evapotranspiration flux revealed that isotopic steady state was invalid at the study site. Tracing oxygen isotopes of water is of great interest in the global ^{18}O-CO_2 budget due to the exchanges of ^{18}O between CO_2 and water. These findings noticeably contribute to understanding of the dynamics of CO_2 in forest ecosystems.

References

Caird, M.A., Richards, J.H. and Donovan, L.A., 2007. Nighttime stomatal conductance and transpiration in C-3 and C-4 plants. Plant Physiology, 143(1): 4-10.

Wesely, M.L., 1989. Parameterization of surface resistances to gaseous dry deposition in regional-scale numerical models. Atmospheric Environment, 23(6): 1293-1304.

Worldwatch institute, 2006. Biofuels for transport: global potential and implications for sustainable agriculture and energy forthe 21st century. Worldwatch Institute, Washington, D.C., http://www.worldwatch.org/system/files/EBF008_1.pdf.

Appedix I. Ground-based remote sensing in relation to leaf water status on corn leaves

A1.1. Introduction

Leaf water status is a good indicator of plant physiological functions. It directly affects stomatal closure by releasing abscisic acid (ABA). By controlling stomatal closure, leaf water status physiologically regulates transpiration (Jones, 1978) and stomatal conductance (Saliendra *et al*., 1995). In terms of water isotope perspectives, the effects of leaf water on stomatal opening and transpiration are associated with the isotopic enrichment of leaf water. Determination of leaf water isotope ratios is sensitive to a turnover time of leaf water, which is a function of water contents in leaves (Chapter 3). Water stress in leaves causes an increase of leaf temperature that potentially affects the isotopic enrichment of leaf water at which two waters reaches isotopic equilibrium.

Construction of water contents in leaves has been a challenging task in many ecological studies. The changes in leaf water contents result from interplay between internal and external factors including soil water and humidity surrounding leaves (Gallego *et al*., 1994; Millar *et al*., 1971; Saranga *et al*., 1991; Smart and Barrs, 1973). Conventional methods of leaf water content measurement require laborious and destructive processes of a subject plant, which impede frequent data collection often with no less than a day interval. Use of ground-based remote sensing is an alternative to the estimation of leaf water status without damaging plants. Some studies have been reported using spectral reflectance measurement that the results might be limited to species-specific and weak correlations.

Three main purposes of this supportive study are (1) to explore the feasibility of developing a non-destructive leaf water estimation method using spectral reflectance measurements, (2) to provide supportive measurements for changes of leaf water for a

short-term scale and (3) to conduct preliminary investigation of nighttime stomatal conductance to support the dew experiment in Chapter 3.

A1.2. Experimental setup

Corn (*Zea mays*) was planted and grown in two plastic window boxes in the Greeley laboratory greenhouse (370 Prospect St. New Haven, Connecticut) with a daily temperature range of 18-42 ºC and mean relative humidity of 20% (12-45% range in May. The growth conditions including watering were controlled identically in the two groups of corn plants throughout the growth period. A week before the experiment, a new watering scheme was applied under which the two corn-planted pots were divided into two treatments, drought and control. For the drought treatment pot, water was completely withheld until the end of the experiment. Prior to the experiment, two pots were transported to the rooftop of the Environmental Science Center (ESC, 21 Sachem St., New Haven). At the end of the experiment, soil samples at 5 cm depth were collected from the two boxes and analyzed for water potential.

A1.3. Intensive measurements

For a period of 48 h from 18 to 20 September 2007, measurements of spectral reflectance, variables of plant water status and physiological variables at the leaf level were made every 4 h from potted corn plants at the rooftop of ESC. Spectral reflectance at the adaxial side was measured using a UNIspec Spectral analysis System (PP Systems, Haverhill, Massachusetts) over a full range of wavelength (310 – 1130 nm) with a 2.0

mm diameter foreoptic and an internal 6.8-watt halogen lamp. Detail of the system setup and standard control processes are provided elsewhere (Poulos *et al*., 2007; Richardson and Berlyn, 2002). Spectral reflectance scanned at three different points were randomly chosen at each experimental group and the three measurements of reflectance were averaged. This reflectance scanning was repeated in all four experimental groups (2 leaf segments × 2 drought treatments).

Three water band indices reported in previous studies and two indices modified based on the infrared spectrum measurements were tested. The water band index has been developed according to the different reflectance spectra of water absorption maxima throughout the infrared spectrum measured on leaf segments (Palmer and Williams, 1974). Using the reflectance ratio based on the difference of absorption at multiple wavelengths, water band index has been calculated (Penuelas *et al*., 1997), in reference to reflectance at 970 nm (R_{970}) as

$$WI_{970} = \frac{R_{900}}{R_{970}}$$

where R denotes reflectance ($0 < R < 1$) and the subscript denotes wavelength (nm), for example, R_{970} is a reflectance at 970 nm. This simple ratio was modified by Riedell and Blackmer (1999) as

$$WI_{970+} = \frac{R_{900} + \left(R_{900} - R_{830}\right)}{R_{970}}$$

Finally, Sims and Gamon (2003) suggested a water band index using reflectance ratio of 900 and 1180 nm. Because the maximum wavelength that could be measured using UNIspec is 1130 nm, I modified Sims and Gamon (2003) as

$$WI_{1130} = \frac{R_{900}}{R_{1130}}$$

In addition to three water band indices reported in previous studies, two modified indices were also tested. These modification were made because of species-specific feature of spectral reflectance properties (Sims and Gamon, 2003). In this study, the two reflectance minima occurred near 480 and 670 nm and the variations of the reflectance values in a given treatment were almost zero at 700 nm regardless of the measurements time steps (Figure A1.1). This trends were observed consistently throughout the experiment period. Therefore, two water band indices, WI_{970} and WI_{970+} have been modified as WI_{700} and WI_{700+} in reference to wavelength at 700 nm (R_{700}) as

$$WI_{700} = \frac{R_{900}}{R_{700}}$$

and

$$WI_{700+} = \frac{R_{900} + \left(R_{900} - R_{830}\right)}{R_{700}}$$

All five indices were estimated based on the measurements of spectra made on the corn plants during the experimental period and examined correlations with three leaf water variables measured during the experiment period simultaneously.

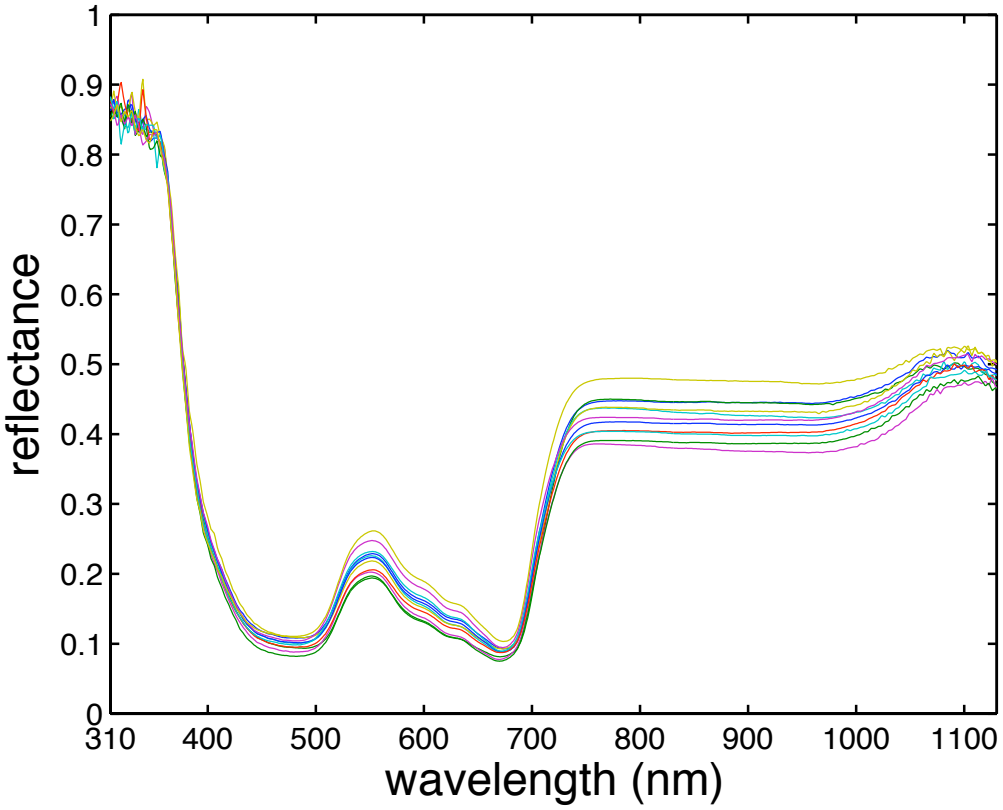

Figure A1.1. An example of infrared spectrum measurements made on the leaf base segment of corn plants using UNIspec at every 4 h during Sept 18 – 20, 2007. Each individual line represents the spectrum measured at each collection time step. Two measurements for drought and control treatments were averaged.

Every 4 h, corn leaves were collected for the measurements of leaf water potential (LWP, MPa), leaf water contents (LWC, g m^{-2}) and relative water contents (RWC, %). Leaves were sampled after the removal of veins for the determination of LWP using a Dewpoint PotentiaMeter (WP4, Decagon Devices, Inc., Pullman, Washington, USA). For the LWC measurements, leaves were stored in an airtight zipbag immediately after collection. After fresh weight (FW) was weighted, the collected leaf segments were photocopied for the later measurement of leaf areas using a leaf area meter (Li-Cor 3100 Area Meter, Li-Cor instruments, Lincoln, Nebraska, USA). The individual leaf segments were reweighted after oven dry at 70 ºC for several days and LWC was estimated as

$$LWC = \frac{FW - DW}{leaf\ area}$$

For the RWC measurements, leaf discs were cut and immersed in the distilled water for 24 h for turgid weight measurements (TW) immediately after fresh weight was measured. After TW was weighted, leaves were dried in a dry oven at 70 ºC for dry weight measurements (DW). Then, RWC was estimated as

$$RWC = \frac{FW - DW}{TW - DW} \times 100$$

In addition to the leaf water measurements, auxiliary measurements of leaf-level gas exchange were conducted including photosynthesis (A_n), transpiration (T) and stomatal conductance (g_S) using an open gas exchange system (LI-6400, Li-Cor, Lincoln, NE, USA). A mature leaf was chosen from each treatment and the same leaf was used for the repeated Licor measurements at each of the subsequent sampling intervals over the experiment period.

A1.4. Results

First, the effectiveness of the chosen factors in demonstrating plant water status in the experiment was statistically examined using a three-way ANOVA [2 levels of water stress: drought and control; by 6 levels of collection time: 12, 16, 20, 24, 4 8 am; by 2 levels of leaf segment: base and tip]. The analyses revealed that the drought treatment were statistically insignificant to manipulate water stress in the experimental plants. The measurements of soil water potential for the drought and watered treatment at the end of the experiment (midday) were -2.06 and -0.01 MPa, respectively. Such results were not expected on the basis of visually detected withered leaves in the drought plants observed during the experiment. At night, variations between the two treatments were narrowed, ranging from -0.71 to -1.07 MPa at 24 am, -0.83 to -1.06 MPa at 4 am on the second experiment day. Then the ranges of LWP increased at 12 pm, ranging from -0.67 to -1.11 MPa. Because dew formation was observed in both nights, I hypothesized that additional supply of dew water to leaf water relieved water stress at the leaf leave. Extra generalized linear model (GLM) analyses were conducted without nighttime measurements (24, 4, and 8 am), however, the filtering of nighttime measurements did not show statistically significance for any of the three variables ($p > 0.05$).

The ANOVAs (Table A1.1) revealed that the selection of the leaf segments and collection time were a significant factor in determining water status in leaves. However, the interaction effects of leaf segments and collection time on leaf water was not significant. Differences of the measured leaf water variables between the leaf segments were significant for LWP at $p < 0.05$ -level and for LWC and RWC according to a GLM

analysis ($p < 0.0001$). The analyses showed that the impact of intra-leaf variations of leaf water diminished when it examined the interaction effects of leaf segment x collection time. For examples, differences in the LWP measurements were significant with the leaf segment and collection time individually at the $p < 0.05$-level and $p < 0.0001$, respectively. However, differences in LWP did not show statistical significance with the interaction of the two factors. For LWP, the collection time was also a significant factor ($p < 0.0001$), however, other variables did not show significant differences in the measurements with respect to the changes of collection time of a day. This may be a result of the sensitivity of measuring LWP to diurnal plant water relations, indicating that the use of LWP would be the most useful method if understanding diurnal variation of leaf water is a subject of study.

Table A1.1. *P* values for effects included in the analysis of variance (ANOVA) conducted on LWP and a generalized linear model (GLM) analysis on LWC and RWC and Licor measurements (Photosynthesis and Conductance) on corn plants. Abbreviations: LWP = leaf water potential, LWC = leaf water contents, RWC = relative water contents, A_n = photosynthesis, T = transpiration and g_S = stomatal conductance.

Fixed factor	LWP	LWC	RWC	A_n	T	g_S
Treatment	0.915	0.465	0.785	0.318	0.796	0.938
Leaf segment	0.037	0.000	0.002	0.285	0.153	0.023
Collection time	0.000	0.279	0.070	0.000	0.000	0.000
Leaf × time	0.541	0.980	0.758	0.697	0.469	0.138

Figure A1.2 presents the measurements of leaf water variables made on two leaf segments in the corn crops for the 48 h period. Due to the statistical insignificance of the drought treatment (Table A1.1), the measurements of the two treatments were averaged and the maximum and minimum values were presented in the error bars. In general, the LWP measurements showed a diurnal pattern with a decrease of leaf water at midday and a recovery during nighttime (Figure A1.2, top). In comparison to the other variables, the diurnal pattern for LWP was the most obvious among three variables, with the minimum values of -1.61 (base) and -1.65 MPa (tip) during the daytime (12 – 4 pm) and the maximum values of -0.77 (base) and -0.98 MPa (tip) at night (24 – 4 am). In the segmental analysis, the LWP measurements at the base were always higher than that at the tip except the second measurements (16 pm, first day). The measurements from two leaf segments tended to be diverted by 0.48 MPa at the maximum (night), while LWP in the two segments was likely to be less varied at midday (12 - 4 pm) and during the recovering period (16 – 20 pm).

The LWC measurements (Figure A1.2, middle) showed the least diurnal variation among three variables, ranging from 0.014 to 0.019 g m^{-2} (base) and from 0.0095 to 0.013 g m^{-2} (tip), and a larger diurnal variation was found in the base (0.005 g m^{-2}) than in the tip 0.0035 g m^{-2}). In addition to the consistency over the 48 h period, the measurements made on the tip segment showed very small variations between two treatment groups. According to the definition of LWC, a measurement of LWC indicates the actual amount of water containing in a given leaf area, while LWP and RWC are a indicator of leaf water relative to saturation (LWP) or dry-full turgor weight. The very small changes of LWC observed in the diurnal cycle, therefore, may imply that the change of actual

amount of water in a short-term scale could be negligibly small in a single leaf of corn. Very few plant physiological studies were reported regarding leaf water measurements using the same LWC unit that I used at an hourly scale, so that it is unknown the impact of 0.005 g m^{-2} changes of leaf water occurred in a single leaf on plants. However, in micrometeorological perspectives, the assumption that vegetation could be considered as a consistent water pool and reach at steady state would be reasonable. This further implies that the location of LWC measurement in a given leaf is more important than the time of sampling. The use of a leaf disc with a known diameter is widely used in a field study, so that extra care should be exercised in designing a field experiment.

The measurements of RWC during the experimental period were unable to provide insight into a diurnal change of leaf water. The measured RWC tended to be consistent over the 48 h period within the range of 0.9 - 1.0 for both the base and tip segments except the last measurements made on the tip segment (0.87 MPa). In addition to the other variables, RWC at the base had less water stress than that at the tip, however, the mean difference was small (less than 5%).

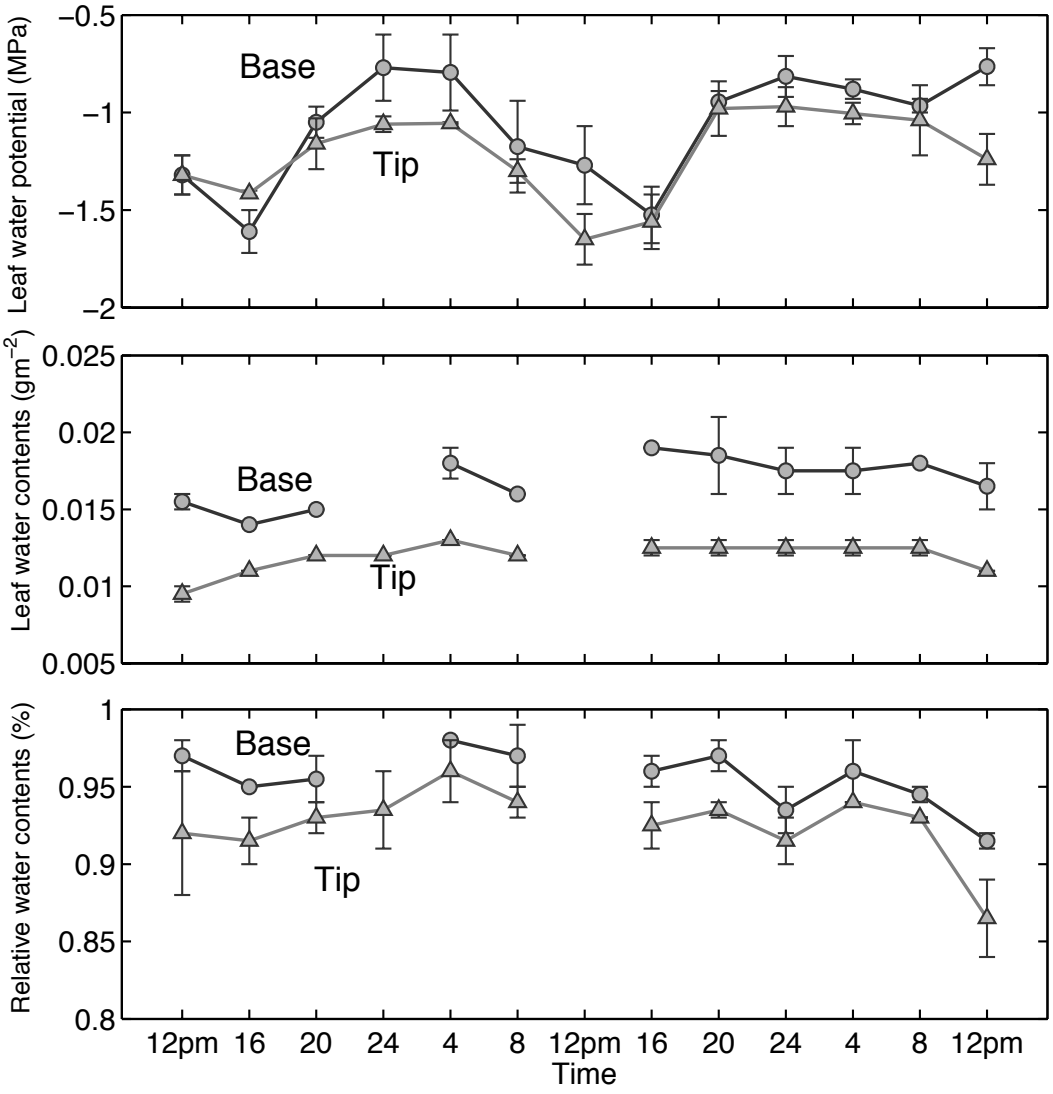

Figure A1.2. 48 h measurements of leaf water made on corn plants in three different variables: leaf water potential (top), leaf water contents (middle) and relative water contents (bottom). The measurements in the drought and control treatments were averaged.

Figure A1.3 presents the diurnal patterns of leaf gas exchange measurements for three variables for the 48 h period. For photosynthesis, maximum activity was observed at noon and no photosynthesis (negative values) was detected during the nighttime (20 – 4 am). The two measurements made on the tip and the base segments were very close, supporting the statistical analysis in Table A1.1. The mean photosynthesis for daytime (8 – 16 pm) was 3.3 ± 0.94 (s.d.) μ mol CO_2 $m^{-2}s^{-1}$. For conductance and transpiration, differences between the tip and the base segment became larger when the g_S/T values increased. The values of g_S/T at the tip segment tended to be higher than that at the base segment. In terms of diurnal patterns, the similar trend of diurnal cycle was observed in g_S and T, resulting in an increase of conductance and transpiration at daytime and a decrease at nighttime. In addition to the differentiation of values at the two segments, another difference from photosynthesis was that nighttime conductance and transpiration was detected and these values were significantly different from zero ($p < 0.0001$). The mean nighttime values (20 – 4am) were 0.023 ± 0.016 mol H_2O $m^{-2}s^{-1}$ and 0.25 ± 0.17 mmol H_2O $m^{-2}s^{-1}$ for stomatal conductance and transpiration, respectively. The mean daytime values were 0.043 ± 0.01 mol H_2O $m^{-2}s^{-1}$ and 0.65 ± 0.09 mmol H_2O $m^{-2}s^{-1}$ for stomatal conductance and transpiration, respectively.

Impacts of five water band indices (WIs) on the prediction of water contents in leaves were examined. Table A1.2 lists Pearson correlation coefficient (R) and p-values at 95% confidence intervals for correlation between the leaf water measurements and WIs corresponding to the leaf segments. For the base segment, LWC and LWP showed statistical significance over some of WIs. The LWC measurements were negatively correlated with WI_{970+}, WI_{700} and WI_{700+} at $p < 0.05$ and WI_{1130} at $p < 0.01$.

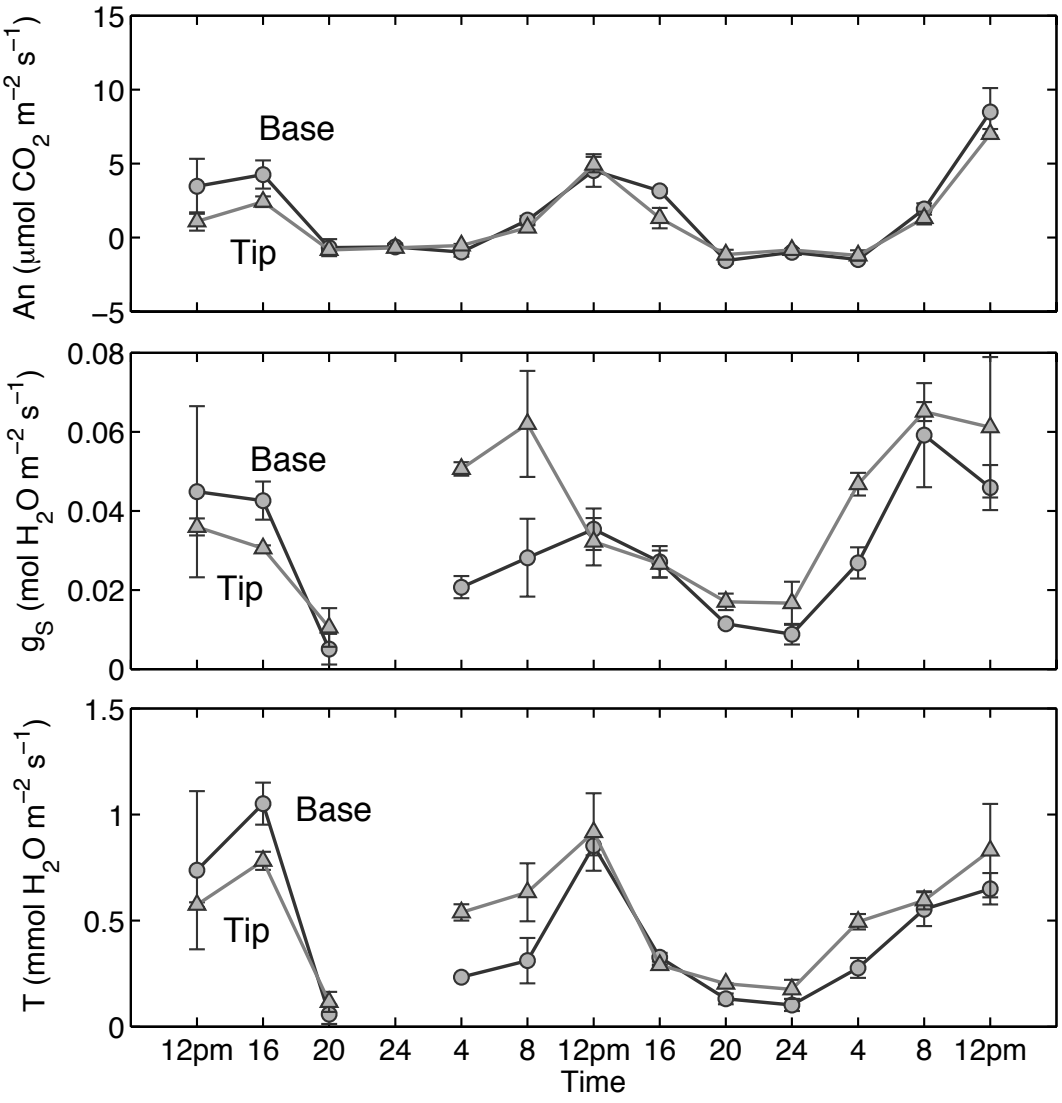

Figure A1.3. 48 h measurements of leaf-level gas exchanges made on corn plants: photosynthesis (top), stomatal conductance (middle) and transpiration (bottom). The measurements in the drought and control treatments were averaged.

The correlation coefficients were close to negative unity, with R values in the range of -0.69 to -0.77 in linear relationships. The *R* values for LWP were -0.61 and -0.62 for WI_{700+} and WI_{700} at $p < 0.05$ level, respectively. The analyses between WIs and RWC were found no significant correlation. The variation of measured RWC was limited to a narrow range from 0.9 to 0.98 for the base segment (Figure A1.2), resulting in no statistically significant correlation. In contrast to the base segment, no correlation coefficients between WIs and water contents were found statistically significant for the tip segment, indicating that spectral reflectance analysis could be biased depending on the choice of measurements portion in a single leaf.

The relative strength of correlations between WIs and different measurements of leaf water contents were changed if the analyses conducted on integrating two leaf segments.. For LWP, WI_{970+}, WI_{700} and WI_{700+} were linearly associated but the correlations for WI_{700} and WI_{700+}, for example, were weaker than that for the base only analyses. For LWC, the use of WI_{1130} only showed significant correlation among five indices with a weaker *R* value of -0.51 than that of -0.77 in the base segment. In contrast to other variables, adding measurements in the tip segment appeared to have effect on the correlations between RWC and indices and showed the significant correlations with WI_{970+} and WI_{1130}. In general, however, the correlations tended to be weaker in the analyses including both base and tip segments than in the base segment only presumably due to a poor relationship between the indices and water contents variables. This implies that reconstructing leaf water using remote sensing at a single-leaf level would be a challenge in a field practice since sampling of leaves for water content measurement is

Table A1.2. Pearson correlation coefficients (*R*) and *P*-values (95% CI) between the water index (WI_{XXX}) indices and leaf water measurements. The means of drought and control treatment in the measurements of spectral reflectance and leaf water variables were used. (*$p < 0.05$; ** $p < 0.01$)

	Base					Tip				
	WI_{970}	WI_{970+}	WI_{1130}	WI_{700}	WI_{700+}	WI_{970}	WI_{970+}	WI_{1130}	WI_{700}	WI_{700+}
LWP	0.034	-0.477	-0.350	-0.623*	-0.606*					
LWC	-0.469	-0.700*	-0.771**	-0.690*	-0.685*					
RWC	-0.142	-0.417	-0.549	0.160	0.174					
LWP						-0.223	-0.593	-0.284	-0.305	-0.278
LWC						-0.195	-0.591	-0.557	-0.241	-0.214
RWC						-0.131	-0.579	-0.600	0.198	0.222

	Base + Tip				
	WI_{970}	WI_{970+}	WI_{1130}	WI_{700}	WI_{700+}
LWP	-0.125	-0.514*	-0.352	-0.512*	-0.493*
LWC	-0.378	-0.348	-0.512*	-0.242	-0.247
RWC	-0.266	-0.458*	-0.610**	0.134	0.141

usually conducted over a whole leaf to avoid bias due to uneven water distribution in a leaf.

A1.5. Summary

The measurements of leaf water were made using three different methods. LWP showed the most obvious diurnal changes of leaf water among the three variables. The LWC measurements varied within 0.005 g m^{-2} and the mean difference of RWC were less than 5% during the 48 h period. The leaf segmental analyses showed an uneven distribution of leaf water so that the water contents at the base segment were always higher than that at the tip segments regardless of the choice of the leaf water variables. The drought treatment practiced in this study produced a statically insignificant effect.

Some of the water band indices were negatively correlated with leaf water variables depending on the leaf segment. In the leaf base segment, WI_{970+} and WI_{1130} were a negatively linear function of LWC. The empirically modified indices, WI_{700} and WI_{700+} showed a correlation with both LWP and LWC measurements. In the tip segment, none of the indices showed statistically significant correlations with leaf water measurements. A combination of the indices and the leaf water variables that were statistically significant appeared to have very little tendency to conclude, implying that prior research is necessary in the use of spectral reflectance indices for estimating leaf water.

A1.6. References

Gallego, H.A., Rico, M., Moreno, G. and Regina, I.S., 1994. Leaf Water Potential and Stomatal Conductance in Quercus-Pyrenaica Willd Forest - Vertical Gradients and Response to Environmental-Factors. Tree Physiology, 14(7-9): 1039-1047.

Jones, H.G., 1978. Modeling Diurnal Trends of Leaf Water Potential in Transpiring Wheat. Journal of Applied Ecology, 15(2): 613-626.

Millar, A.A., Jensen, R.E., Bauer, A. and Norum, E.B., 1971. Influence of Atmospheric and Soil Environmental Parameters on Diurnal Fluctuations of Leaf Water Status of Barley. Agricultural Meteorology, 8(2): 93-105.

Palmer, K.F. and Williams, D., 1974. Optical-properties of water in near-infrared. Journal of the Optical Society of America, 64(8): 1107-1110.

Penuelas, J., Pinol, J., Ogaya, R. and Filella, I., 1997. Estimation of plant water concentration by the reflectance water index WI (R900/R970). International Journal of Remote Sensing, 18(13): 2869-2875.

Poulos, H.M., Goodale, U.M. and Berlyn, G.P., 2007. Drought response of two Mexican oak species, Quercus laceyi and Q-sideroxyla (Fagaceae), in relation to elevational position. American Journal of Botany, 94(5): 809-818.

Richardson, A.D. and Berlyn, G.P., 2002. Spectral reflectance and photosynthetic properties of Betula papyrifera (Betulaceae) leaves along an elevational gradient on Mt. Mansfield, Vermont, USA. American Journal of Botany, 89(1): 88-94.

Riedell, W.E. and Blackmer, T.M., 1999. Leaf reflectance spectra of cereal aphid-damaged wheat. Crop Science, 39(6): 1835-1840.

Saliendra, N.Z., Sperry, J.S. and Comstock, J.P., 1995. Influence of Leaf Water Status on Stomatal Response to Humidity, Hydraulic Conductance, and Soil Drought in Betula-Occidentalis. Planta, 196(2): 357-366.

Saranga, Y., Rudich, J. and Marani, A., 1991. The Relations between Leaf Water Potential of Cotton Plants and Environmental and Plant Factors. Field Crops Research, 28(1-2): 39-46.

Sims, D.A. and Gamon, J.A., 2003. Estimation of vegetation water content and photosynthetic tissue area from spectral reflectance: a comparison of indices based on liquid water and chlorophyll absorption features. Remote Sensing of Environment, 84(4): 526-537.

Smart, R.E. and Barrs, H.D., 1973. Effect of Environment and Irrigation Interval on Leaf Water Potential of 4 Horticultural Species. Agricultural Meteorology, 12(3): 337-346.

Appedix II. Influences of dew on predawn leaf water potential in a corn canopy

A2.1. Introduction

The potential of dew presence on leaf surfaces as a hydrologic input was largely unexplored. Dew water at leaf surface has significant implications in many ecosystem studies as discussed in Chapter 3 was devoted to analysis of dew effects on leaf water for determining the potential of dew water in the ecosystems. However, very few studies have been conducted to report field observations of leaf water restoration under dew conditions (Munne-Bosch and Alegre, 1999; Munne-Bosch *et al*., 1999). The purpose of this field experiment was to provide the experimental evidence of the use of dew water by leaves in the field conditions by comparing predawn leaf water potential from the dew and dew-exclusion plots.

A2.2. Site description

The field sampling for predawn leaf water potential was made for three times on July 28, August 14 and August 15, 2010 at a corn field on the Lockwood Farm of the Connecticut Agricultural Experiment Station in Mount Carmel, Connecticut, United States (41º25' N, 72º55' W). More details of the site description can be found elsewhere (Aylor, 1993; He *et al*., 2003). The corn-planting section was situated at an open space near the center of the farm at which no structures were in close contact with corn crops to prevent interception of wind or radiation from the sky. Corn was planted in late May and reached maturity at the time of sampling collection.

A2.3. Experimental setup

Six plots, each with 5 rows and 5 m long were set up in the corn field, consisting of two types of treatments, dew and dew-exclusion plots. All six plots were adjacent to each other and the arrangements of plots are shown in Figure A2.1. For additional measurements of soil moisture, an access tube of a soil moisture probe (model PR1/2, Dynamax, Inc., Houston, TX, USA) was installed into soils at the center of Dry plot 2 in early July, so that soils around the tube could be stabilized. Due to the limited access to a deeper soil layer, the sensor rings on the access tube were able to detect soil moisture at the depths of 5, 15, and 25 cm (Figure A2.1).

A2.4. Field sampling and laboratory measurements

Prior to leaf sampling at sunrise, plastic films were covered over the dew-exclusion plots immediately after sunset on the night of the experiment in order to prevent dew formation at canopy surfaces (Photo A2.1). The plastic cover was carefully positioned right above the canopy because dew could be formed both side of the plastic films. In order to increase effectiveness of dew exclusion, thickness of a cover or types of cover material should be concerned, for example, a plastic cover lined with a piece of aluminum foil increased the effectiveness of dew exclusion (Photo A2.2 and see section A2.5).

The leaf sampling was conducted in the early morning between 6:30 and 7:15 am (Photo A2.3). Three plants in one plot were chosen for leaf sampling randomly but near at the center of each plot. Two leaves were sampled one at the top and another at the bottom of

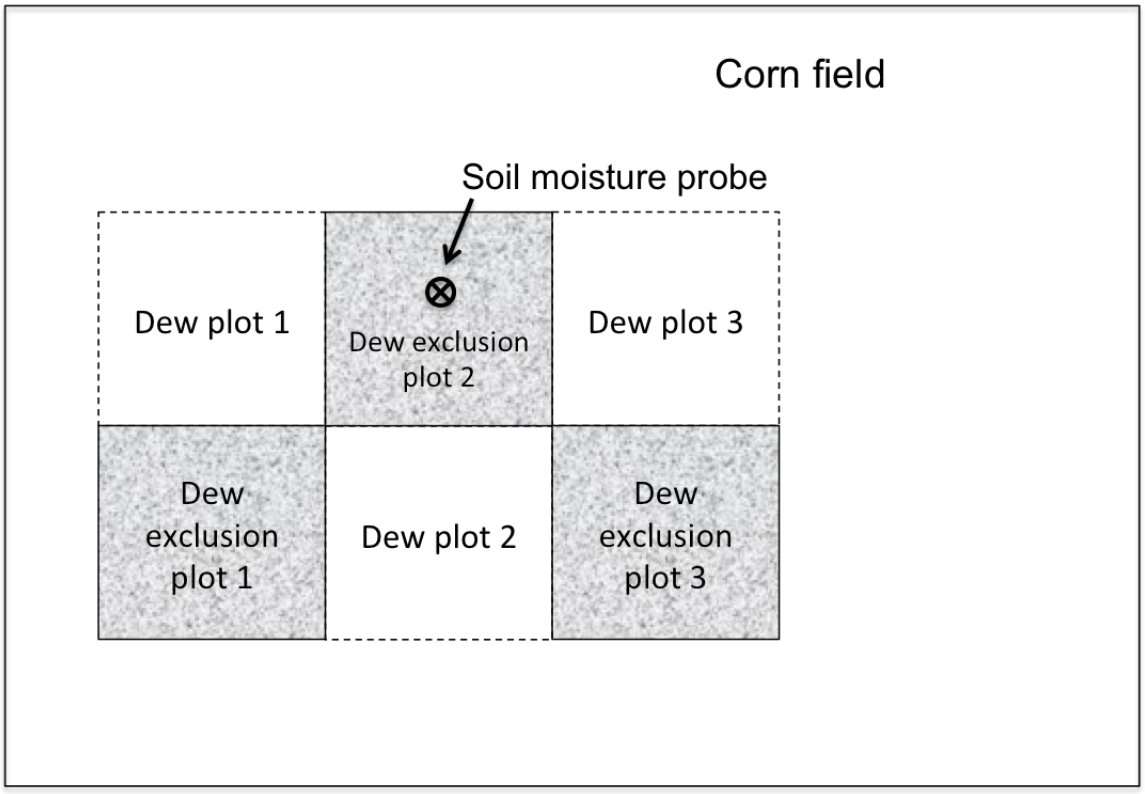

Figure A2.1. Sampling plot design in a corn field on the Lockwood Farm, Hamden, CT. Plastic films were covered over the dry plots to prevent dew formation.

a canopy in each plant. Multiple pieces of leaf samples were taken in the sampled leaf from a tip to a base because water contents could be varied depending on a location within a single leaf. For dew-wetted leaf sampling, dew was removed using paper towels. In addition, soil samples were collected at 15 cm depth near the plant that leaves were sampled. All leaf pieces and soils were stored and sealed in a plastic container and the measurements of water potential were made using a Dewpoint PotentiaMeter (WP4, Decagon Devices, Inc., Pullman, Washington, USA) in the ESC laboratory starting no later than an hour after the field collections were made. Three times of instrument reading were made and averaged.

A2. 4. Results

The measurements of leaf water potential (LWP) of top leaves showed clear dependence on the dew-dew exclusion plot treatment. The measurements of dew contact leaves showed higher values of water potential than that of dew-exclusion leaves. During the three day measurements, the means of top-dew were -0.77 (0.06 s.d.; July 28), -0.78 (0.05; August 14) and -0.76 MPa (0.2; August 15). At the same time, the means of top-dew-exclusion WP were -1.10 MPa (0.12 s.d.), -0.94 (0.17), and -1.34 MPa (0.2) (Table A2.1 and Figure A2.2, A2.3, and A2.4). The mean differences of the WP between the dew and the dew-exclusion plots were 0.33, 0.17 and 0.58 MPa, respectively, and these mean values were significantly different from zero ($p < 0.05$). The variation in the soil WP measurements between the two treatments was minor. The mean difference in the

Photo A2.1. Plots with the installation of plastic covers in the early evening 12 - 13 hours prior to leaf sampling.

Photo A2.2. A piece of aluminum foil lined at the bottom side of the plastic film cover..

Photo A2.3. Leaf sampling during the experiment.

three-day measurements of soil WP between the two treatments was 0.07 MPa (0.03, $p <$ 0.001).

Variations in the LWP showed statistically insignificant changes in the bottom leaves between the plot treatments during the measurements. The wetness on leaf surfaces varied depending on the canopy height so that the bottom leaves were almost dry at the moment of collection while the top leaves were heavily dampen. There were two reasons on creating the vertical gradient of leaf wetness in the canopy: first, temperature gradient between within and out of canopy and second, moisture filtering effects by top leaves. Both reasons resulted in the vertical gradient of leaf surface wetness in corn plants. The differences of the bottom LWP between two treatments for three measurements were 0.08, 0.07 and 0.14 MPa, respectively.

The vertical gradient of LWP in a plant was smaller in the dew-exclusion plots than in the dew plots. The means of the vertical LWP gradient were 0.44 MPa (0.21) for the dew plots and 0.17 MPa (0.12) for the dew-exclusion plots and the difference of the means were statistically significant (p = 0.006). Because the changes of LWP in between the treatments were smaller in the bottom leaves than that in the top leaves, the differences of the vertical LWP gradient provided the evidence of the extra supply of dew water for leaf water. Also, the smaller vertical gradient found in the dry plots indicates that the maturity of leaves was not a strong factor in determining leaf water status in a fully-grown corn plant.

Table A2.1. Predawn leaf water potential (MPa) measured in corn plants in the summer of 2010. All values listed in the table

	ID	Dew plots			ID	Dew exclusion plots		
		Top	Bottom	Soil		Top	Bottom	Soil
July 28	1	-0.75	-1.31	-0.65	1	-1.10	-1.11	-0.52
	2	-0.70	-1.18	-0.60	2	-1.20	-0.99	-0.59
	3	-0.82	-1.04	-0.62	3	-0.94	-1.17	-0.59
August 14	1	-0.80	-1.25	-1.25	1	-0.75	-1.07	-1.44
	2	-0.80	-0.84	-1.09	2	-1.05	-1.04	-1.05
	3	-0.72	-1.09	-0.78	3	-1.06	-0.94	-0.74
August 15	1	-1.04	-1.78	-1.53	1	-1.10	-1.17	-1.59
	2	-0.69	-1.14	-1.03	2	-1.45	-1.18	-0.90
	3	-0.56	-1.19	-1.02	3	-1.50	-1.25	-1.28

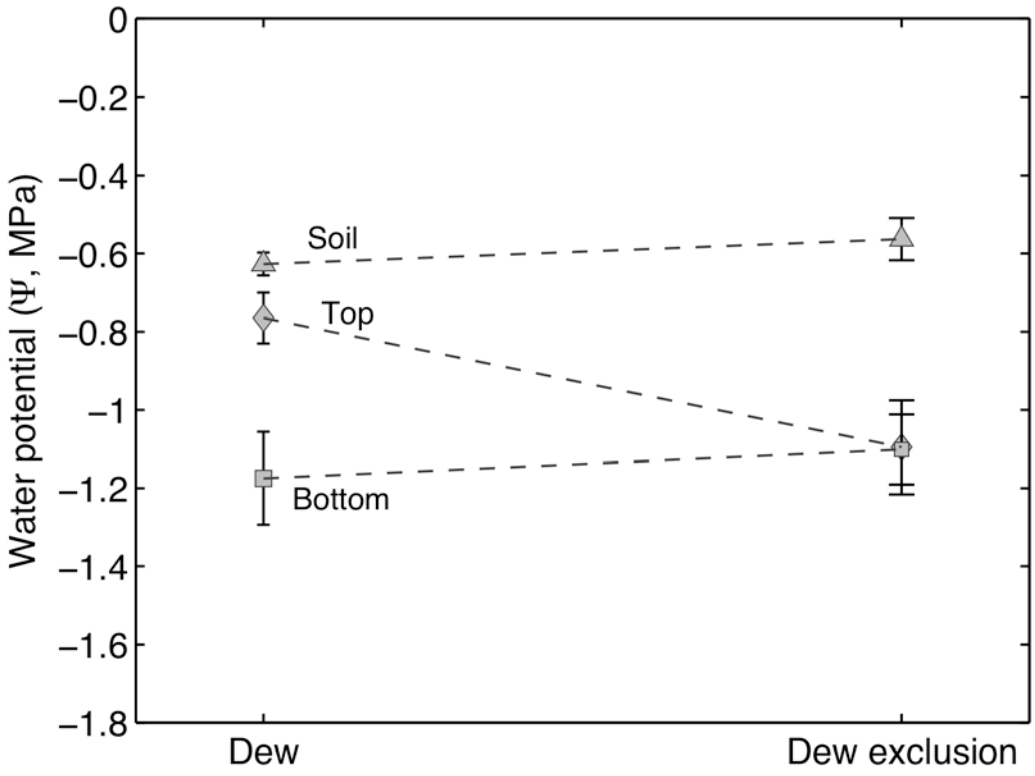

Figure A2.2. Water potential measurements of corn leaves and soil in the two treatment plots on July 28, 2010. The data points are the mean of three plots in each treatment. Each reading of water potential was made three times.

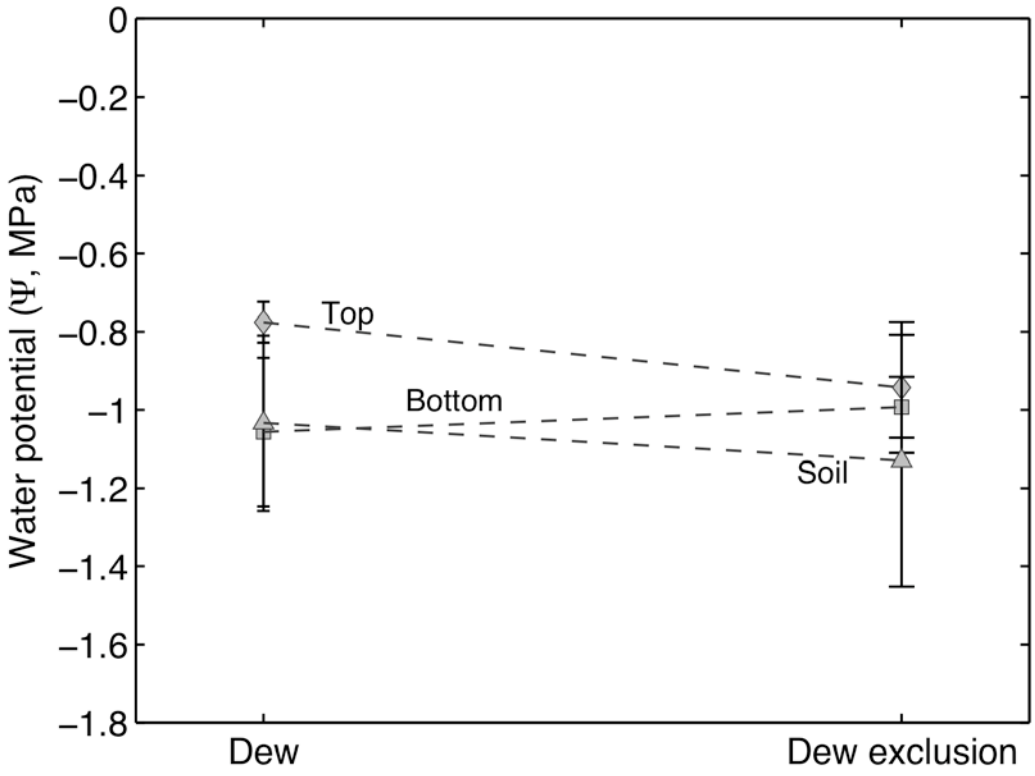

Figure A2.3. Water potential measurements of corn leaves and soil on August 14, 2010.

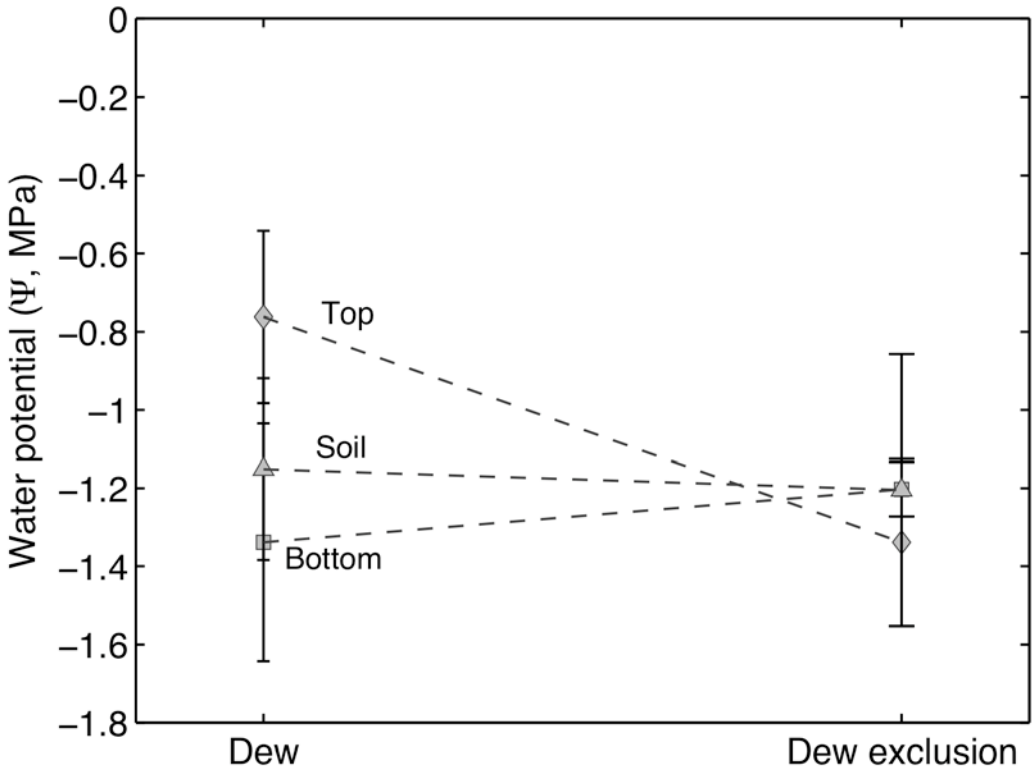

Figure A2.4. Water potential measurements of corn leaves and soil on August 15, 2010.

A2.5. Implications and field set-up improvement

The results of this field study present the importance of dew formation on leaf surface in ecological studies. The finding in this study provides the evidence of utilizing dew water at leaf surfaces, indicating that leaf water is determined by two end-members, xylem and dew, during nighttime and early morning hours.

For isotopic approach, considering dew water would be crucial when modeling leaf water isotopic enrichment. Furthermore, dew would play a significant role in the prediction of evapotranspiration isotope ratios during growing season. Further investigation would be needed to examine an sensitivity analysis of less enriched leaf water than prediction due to depleted dew water in comparison to current model predictions.

In order to obtain better quality measurement data regarding dew formation, the field set-up needs to be improved. First, the position of plastic canopy cover should be determined carefully without contacting canopy. If the canopy cover is in touch with canopy, dew cannot be controlled because dew could be formed on the both side of the canopy cover. Here I report the first measurements made on July 16, 2010, which failed to show dew effects on LWP due to the experimental fault (Figure A2.5). Also, the canopy cover should not intervene air flow in and out of canopy. Second, a choice of the type of material for a canopy cover could improve the control of dew in a dew-exclusion plot. A material with low emissivity may have better performance. For this experiment, HDPE film with emissivity is 0.91 was used. For better control of dew formation in the dew-exclusion plots, the patch of aluminum foil was layered on the surface of the canopy cover in the later experiment, which produced better dew control (Photo A2.2). The emissivity of aluminum foil is 0.04.

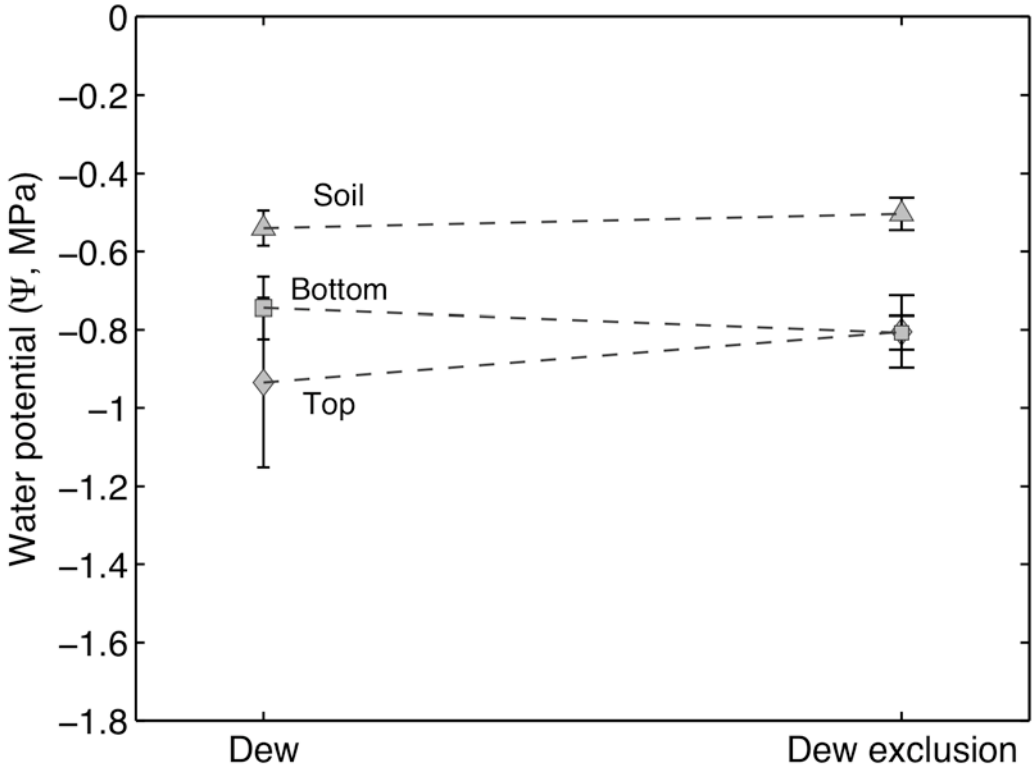

Figure A2.5. Water potential measurements made on July 16, 2010.

A2.6. References

Aylor, D.E., 1993. Relative collection efficiency of Rotorod and Burkard spore samplers for airborne *Venturia inaequalis* ascospores. Phytopathology, 83(10): 1116-1119.

He, H., Smith, R.B. and Aylor, D.E., 2003. Measurement of deuterium isotope flux ratio from an agricultural grassland. Journal of Geophysical Research-Atmospheres, 108(D9): 6. 4277. doi:10.1029/2002JD002491.

Munne-Bosch, S. and Alegre, L., 1999. Role of dew on the recovery of water-stressed Melissa officinalis L-plants. Journal of Plant Physiology, 154(5-6): 759-766.

Munne-Bosch, S., Nogues, S. and Alegre, L., 1999. Diurnal variations of photosynthesis and dew absorption by leaves in two evergreen shrubs growing in Mediterranean field conditions. New Phytologist, 144(1): 109-119.

Appedix III. Photos of field and laboratory experiment set-up

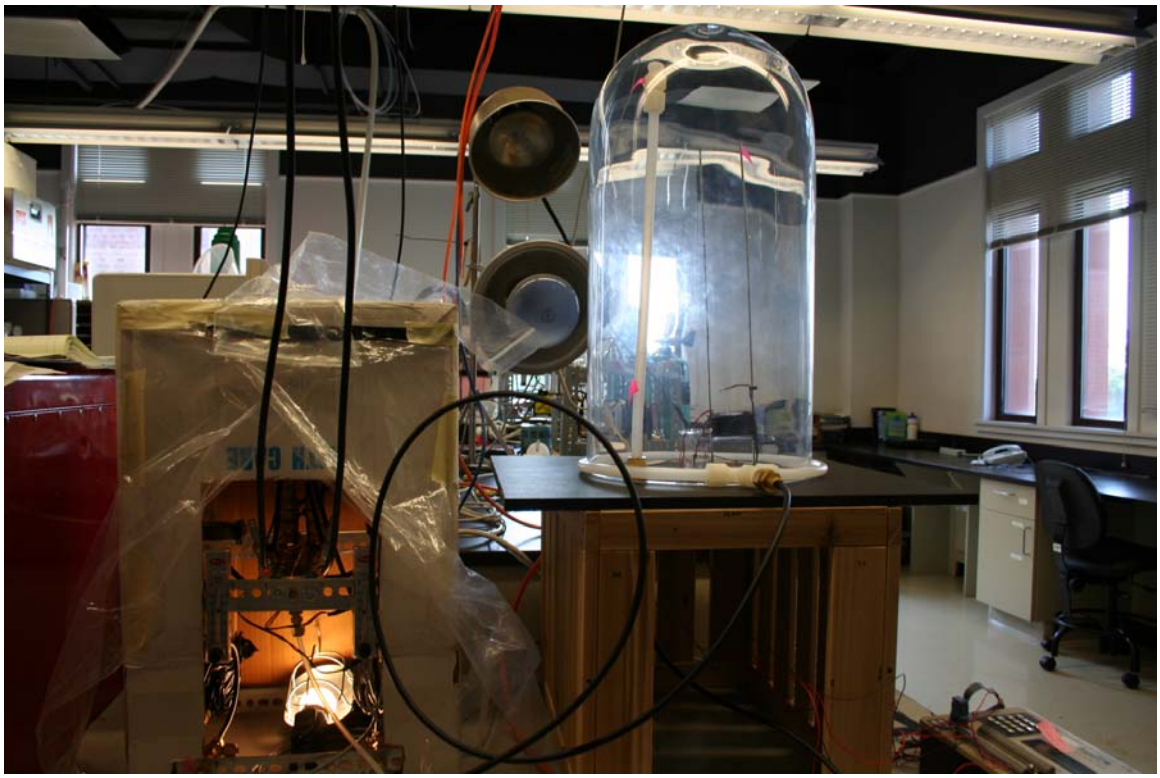

Photo A3.1. Laboratory set-up and measurements of evaporation isotope ratios (Chapter 2).

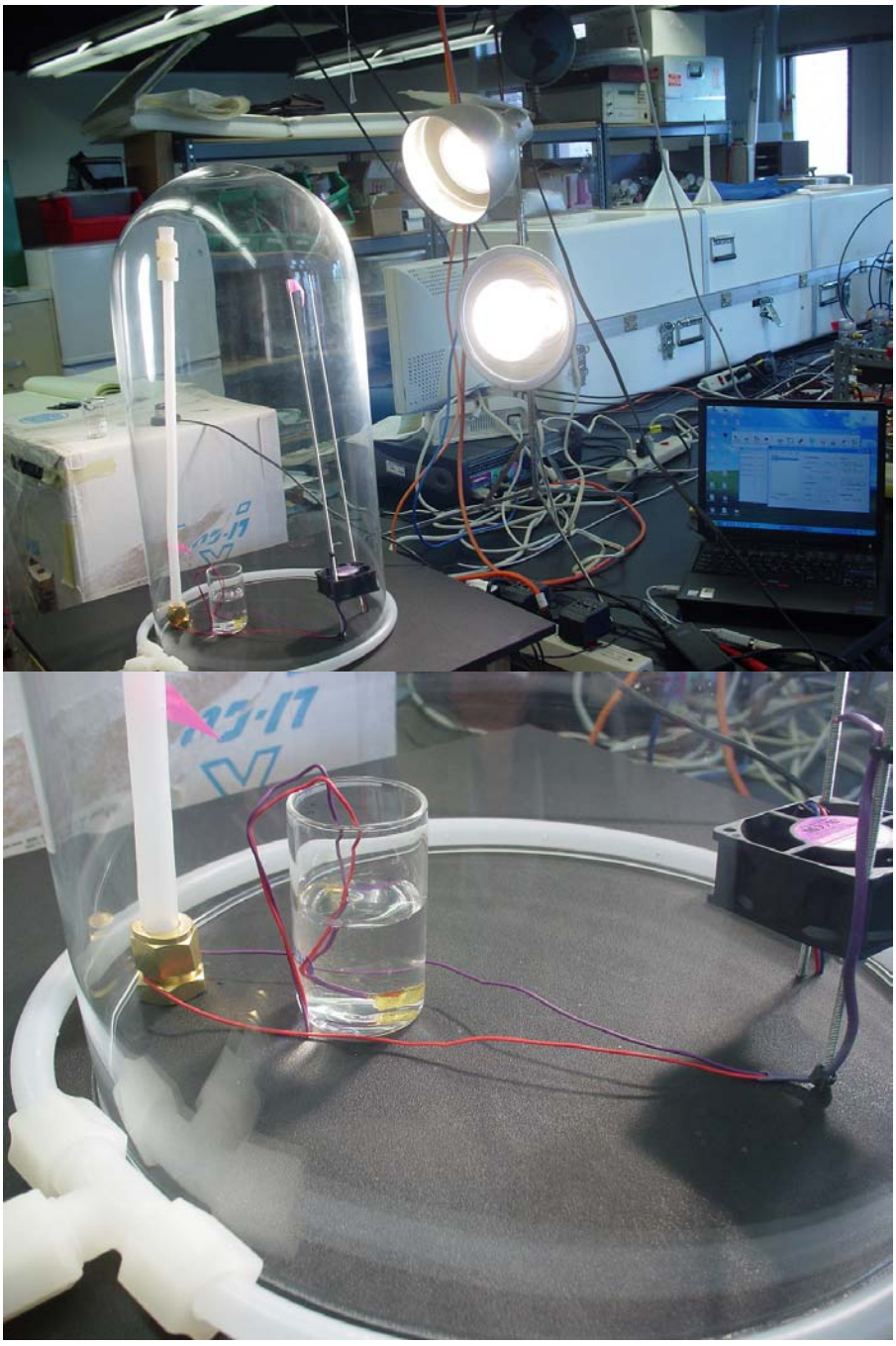

Photo A3.2. Laboratory set-up for the measurement of evaporation isotope ratios (Chapter 2). Set-up for the heated experiment (upper) and evaporating water inside the chamber with bulk water temperature measurements (bottom).

Photo A3.3. Hydroponically grown cotton and corn in the Greeley greenhouse (upper) and the full sunlight treatment at the rooftop of ESC prior to the 48 h-long fumigation experiment in Chapter 3 (bottom).

Photo A3.4. Plant source water was carefully sealed prior to the fumigation experiment (Chapter 3) in order to prevent from contaminating fumigation vapor.

Photo A3.5. Laboratory set-up for the fumigation experiment in Chapter 3. The bubbler (upper) and the plant chamber (bottom).

Photo A3.6. Field set-up at the Borden site, Ontario, Canada (Chapter 4). An intake of ambient air installed at a flux tower.

Photo A3.7. 48 h measurements of spectral reflectance in corn plants at the rooftop of ESC (Appendix I). Corn with the drought and control treatment (upper) and photocopied leaf segments for leaf water scanning (bottom).

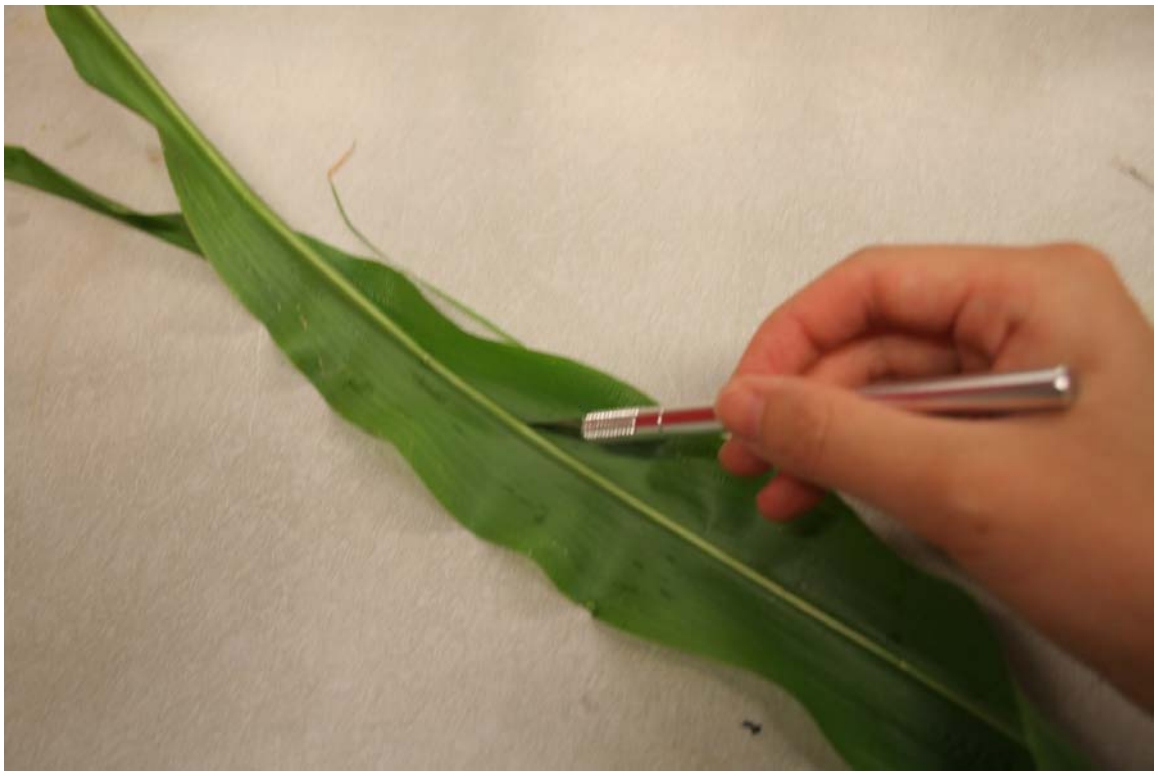

Photo A3.8. Leaf sampling after the removal of main vein for leaf water isotope analysis.